JOURNAL OF GEOPHYSICAL RESEARCH

The continuation of

TERRESTRIAL MAGNETISM AND ATMOSPHERIC ELECTRICITY
(1896-1948)

An International Quarterly

VOLUME 60 March, 1955 NUMBER 1

CONTENTS

(Contents concluded on outside back cover)

Published at

THE WILLIAM BYRD PRESS, INC.

P. O. BOX 2-W, SHERWOOD AVE. AND DURHAM ST.

RICHMOND 5, VIRGINIA

Address all correspondence to

JOURNAL OF GEOPHYSICAL RESEARCH

5241 BROAD BRANCH ROAD, NORTHWEST

WASHINGTON 15, D.C., U.S.A.

SIX DOLLARS A YEAR SINGLE NUMBERS, TWO DOLLARS

JOURNAL OF GEOPHYSICAL RESEARCH

The continuation of

Terrestrial Magnetism and Atmospheric Electricity (1896-1948)

An International Quarterly

Founded 1896 by L. A. BAUER *Continued 1928-1948 by* J. A. FLEMING

Editor: MERLE A. TUVE *Editorial Assistant:* WALTER E. SCOTT

Honorary Editor: J. A. FLEMING

Associate Editors

N. Arley, Polarvej 12, Hellerup, Denmark
J. Bartels, University of Göttingen, Göttengen, Germany
H. G. Booker, Cornell University, Ithaca, New York
B. C. Browne, Cambridge University, Cambridge, England
S. Chapman, Queen's College, Oxford, England
A. A. Giesecke, Jr., Instituto Geofisico, Huancayo, Peru
J. B. Hersey, Oceanographic Institution, Woods Hole, Massachusetts
D. F. Martyn, Commonwealth Observatory, Canberra, Australia
T. Nagata, Geophysical Inst., Tokyo Univ., Tokyo, Japan
M. Nicolet, Royal Meteorological Institute, Uccle, Belgium
M. N. Saha, University of Calcutta, Calcutta, India
B. F. J. Schonland, Atomic Energy Research Establishment, Harwell, England
M. S. Vallarta, C.I.C.I.C., Puente de Alvarado 71, Mexico, D. F.
J. T. Wilson, University of Toronto, Toronto 5, Canada

Fields of Interest

Terrestrial Magnetism
Atmospheric Electricity
The Ionosphere
Solar and Terrestrial Relationships
Aurora, Night Sky, and Zodiacal Light
The Ozone Layer
Meteorology of Highest Atmospheric Levels
The Constitution and Physical States of the Upper Atmosphere
Special Investigations of the Earth's Crust and Interior, including experimental seismic waves, physics of the deep ocean and ocean bottom, physics in geology
And similar topics

This Journal serves the interests of investigators concerned with terrestrial magnetism and electricity, the upper atmosphere, the earth's crust and interior by presenting papers of new analysis and interpretation or new experimental or observational approach, and contributions to international collaboration. It is not in a position to print, primarily for archive purposes, extensive tables of data from observatories or surveys, the significance of which has not been analyzed.

Forward *manuscripts* to one of the Associate Editors, or to the editorial office of the Journal at 5241 Broad Branch Road, Northwest, Washington 15, D. C., U. S. A. It is preferred that manuscripts be submitted in English, but communications in French, German, Italian, or Spanish are also acceptable. A brief abstract, preferably in English, must accompany each manuscript. A *publication charge* of $8 per page will be billed by the Editor to the institution which sponsors the work of any author; private individuals are not assessed page charges. Manuscripts from outside the United States are invited, and should not be withheld or delayed because of currency restrictions or other special difficulties relating to page charges. Costs of publication are roughly twice the total income from page charges and subscriptions, and are met by subsidies from the Carnegie Institution of Washington and international and private sources.

Back issues and *reprints* are handled by the Editorial Office, 5241 Broad Branch Road, N.W. Washington 15, D.C., U.S.A.

Subscriptions are handled by the Editorial Office, 5241 Broad Branch Road, N.W., Washington 15, D.C., U.S.A.

Entered as second-class matter at the Post Office at Richmond, Virginia, under the act of March 3, 1879

Journal of

GEOPHYSICAL RESEARCH

The continuation of

Terrestrial Magnetism and Atmospheric Electricity

VOLUME 60 MARCH, 1955 No. 1

INTERPRETATIONS OF RADIO REFLECTIONS FROM THE AURORA*

BY H. G. BOOKER, C. W. GARTLEIN, AND B. NICHOLS

Cornell University, Ithaca, N.Y.

(Received August 23, 1954)

*The research reported in this paper was performed under Signal Corps Project 26-182B.

ABSTRACT

Results obtained at Ithaca, N.Y., concerning radio reflections from the aurora by both pulse and continuous-wave transmissions are described. At 104 Mc/sec, radar reflections show the following properties: (*i*) They occur only during auroras having ray structure; (*ii*) the radar must be directed roughly normal to the rays; (*iii*) echoes are complex, indicating contributions from many scattering elements mutually interfering in more or less random phase. At various frequencies, from 2.4 to 144 Mc/sec, measurements of fading show that auroral reflections fade at a rate roughly proportional to frequency; rates are between one and two powers of ten faster than would be expected for a quiet ionosphere.

These observations are interpreted as indicating that radio reflections from auroras arise by scattering from numerous auroral columns of ionization, somewhat like meteor trails, having the magnetic zenith as radiant. The fading is principally due to a wind-like motion of the auroral columns, much faster than is customary for meteor trails, and apparently much faster than can actually be observed for meteor trails occurring during auroral disturbances. Visual observations of the fine structure of rays with high-power field-glasses and by photometric analysis show that rays often consist of a large number of fine streaks, each of which extends only part of the length of the ray and lasts only about a second. It is tempting to associate

these visual auroral streaks with the auroral ionization trails that are required to explain radio reflections from the aurora.

Alternative interpretations suggested by other workers are considered, especially that by Harang and Landmark [11]. Reasons are given for rejecting these interpretations in favor of that described above.

Although practically all of the auroral echoes observed at Ithaca are interpreted as coming from *E*-region levels, reasons are given why auroral echoes from *F*-region levels may be seen, especially by radars in lower latitudes.

1. *Introduction*

During the past 20 years, and more especially in the past five years, a ne means of investigating the aurora has become available. Whatever causes excitatio of the atoms and molecules during auroras also causes ionization, and the presenc of ionization can be detected using radio waves. The effect of the aurora on radi propagation was observed in 1933 by Sir Edward Appleton in an expedition t Tromsö, Norway, as part of the program for the Second International Pola Year [see 1 of "References" at end of paper]. Since then, phenomena believed to b associated with the aurora have frequently been observed using conventiona ionospheric radio sounders, particularly in Norway [2], in Germany [3], and i Canada [4]. It is, however, an unfortunate fact that, at the frequencies used i conventional ionospheric sounders (1 to 20 Mc/sec), one of the most strikin auroral phenomena is attenuation, frequently amounting to a complete black-ou of echoes. It is now known that, to obtain echoes from auroral ionization, it i in fact best to operate in the frequency range 20 to 150 Mc/sec. Below 20 Mc/se attenuation is troublesome, while above 150 Mc/sec, back-scattering is too weak

The fact that radio echoes from the aurora were possible was known befor World War II to radio amateurs operating on frequencies of 28, 50, and 144 Mc/se They obtained unusual, and often distorted, communication by pointing thei directional antennas northward instead of at each other [5]. Since then, use ha been made of radar methods at various frequencies between 30 and 100 Mc/se Auroral radar echoes in this frequency range were first obtained by Harang [6 at Tromsö, Norway. After World War II, they were obtained more or less acciden tally at Manchester, England [7], and Ottawa, Canada [8], by equipment erecte to examine echoes from meteor trails. Since then, auroral radars have been i use at a number of other locations (Kiruna, Sweden [9]; Saskatoon, Canada [10 Ithaca, New York; Oslo and Tromsö, Norway [11]; and Fairbanks, Alaska [12] At Cornell University, the results obtained by amateurs were first examined an verified [5], and the character of the striking fading of auroral reflections wa established [13]. Radar equipment operating on a frequency of about 100 Mc/se was established as soon as a suitable military radar could be procured [14]. Informa tion concerning the motions of the auroral ionization has been determined usin both radar and Doppler methods. The diurnal and seasonal variations of th phenomena have been ascertained [15].

The observations that have been made at Ithaca (76° west, 42° north; geomagnetic latitude 54° north; dip 74°) are described in Sections 2, 3, 4, and 5, and are compared with similar observations by other workers where available. Section 2 deals with pulse radar experiments, and Section 3 with observations of fading rate using continuous-wave transmissions. The aspect of the visual observations concerned with the fine structure of rays is described in Section 4. Section 5 is concerned with the diurnal and seasonal variation of the radio phenomena.

Agreement between observations made by various workers at different locations is, on the whole, good. In spite of this, however, there is no corresponding agreement concerning the interpretation of these observations. Harang and Landmark [11] even deny that the echoes concerned are genuine auroral echoes. Their view is that the echoes are from the surface of the earth seen by reflection in the ionosphere and that the function of the aurora is merely to provide the mirror. Another view is that auroral echoes are produced by partial reflection at a comparatively abrupt interface of ionization, formed perhaps by an auroral curtain, scattering from the different parts of the curtain being more or less coherent [7]. Yet another view is that the echoes are from more or less isotropic clouds of ionization that are so dense as to cause total reflection at sufficiently great heights in the lower ionosphere and total attenuation at sufficiently small heights even at the highest frequencies involved in auroral reflections [10]. The view favored by the authors is that the aurora with ray structure probably is associated with columns of ionization lying along the earth's magnetic field, and that echo-contributions from different columns combine in more or less random phase. This fits in with the calculations of Chapman [16]. It also agrees with the viewpoint of Aspinall and Hawkins [7], if the surface to which they refer in their Section 5 is intended to be the surface of a single auroral ray rather than that of an auroral curtain.

On the character of the motion in the aurora revealed by radar, Doppler, and visual investigations, there is likewise remarkable lack of agreement. One view is that, under auroral conditions, there are winds in the ionosphere as large as 1,000 m/sec [17]. Another view is that the motions are more akin to sound waves than winds. Perhaps the most reasonable suggestion is that they are due to motions in the source of excitation of the aurora. A further suggestion [18] is that the motions of the incoming particles along the lines of force of the earth's magnetic field could produce Doppler whistles akin to those produced by meteors. These disagreements are discussed in Section 6.

2. *Pulse Radar Experiments*

Pulse radar experiments at Ithaca, N.Y., have been carried out at 104 Mc/sec by Thayer [14] and at 2.4 Mc/sec by Flood [19]. In addition, a frequency-sweeping ionospheric sounder of lower sensitivity has been available. Phenomena on 104 Mc/sec are similar to those observed by workers at Saskatoon [10], and those on 2.4 Mc/sec are similar to those obtained before the war by German investigators [3].

Echoes at 104 Mc/sec are associated with auroras having ray structure and arrive from directions mainly within 30° of magnetic north. Ranges normally lie between 550 and 1,050 km. Assuming echoing at *E*-region heights, angles of elevation vary from 2° to 8°, which corresponds to the lowest lobe of the vertical

antenna pattern. On one occasion, an echo was obtained at a range of about 400 km, corresponding to the second lobe of the antenna pattern, which however is weak. No echoes have been obtained at angles of elevation above about 12°, although the antenna has good sensitivity for airplanes at angles from about 2° up to 75°, as shown in the computed curves of Figure 1. In this Figure, the upper

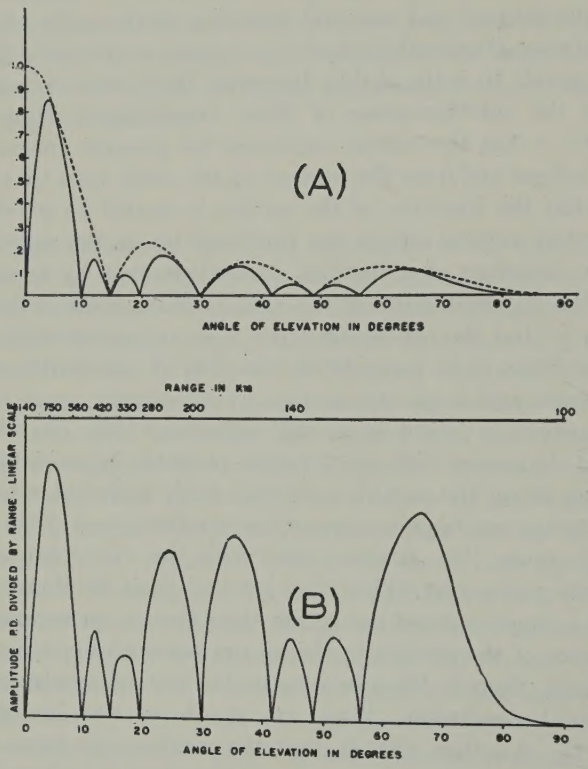

FIG. 1—(*A*) Vertical amplitude polar diagram for 100-Mc/sec radar antenna (dotted curve is for free space); (*B*) Vertical angular sensitivity of 100-Mc/sec radar to targets at 100-km height

diagram shows the amplitude polar diagram; in the lower diagram, the amplitude at each angle has been divided by the appropriate range to a target at a height of 100 km to give the angular sensitivity. Tipping the antenna up so as to fill the gaps in the vertical antenna pattern at the expense of low-angle coverage has never resulted in echoes at ranges less than 400 km, even when masses of visual rays were available at angles of elevation up to the zenith.

The comparative lack of short-range auroral echoes seems to be a feature observed by all workers, and this does not seem to arise from lack of auroral activity at short range. Bowles [12], at the invitation of the Geophysical Institute of Alaska, set up at Fairbanks, Alaska, a 106-Mc/sec radar, substantially identical with that used at Ithaca. Even in the midst of the auroral zone with auroral activity available almost anywhere in the sky, echoes were predominantly from the northern quadrant and occurred only at ranges in excess of about 400 km.

His results are shown in Figures 2 and 3. Similar results were obtained in Alaska by Dyce [12] at a frequency of 51.7 Mc/sec (see Figures 4 and 5).

Viewed on a range-amplitude scope, all auroral echoes observed at Ithaca are complex. They are like rainstorm echoes on an *S*-band radar rather than like an airplane echo. They are like spread-*F* echoes on an ionospheric recorder rather than like a regular echo from an undisturbed *F*-region. Pictures of typical echoes as seen on a range-amplitude display are shown in Figure 6. Outlines of the

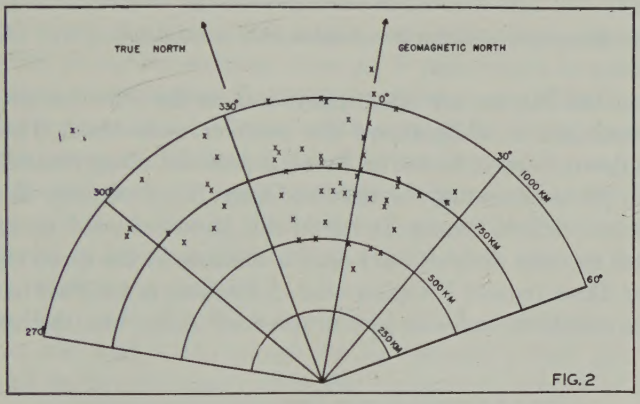

FIG. 2—Variation of range and azimuth of 106-Mc/sec radar echoes from aurora, College, Alaska, Aug.-Sept., 1953 (after Bowles)

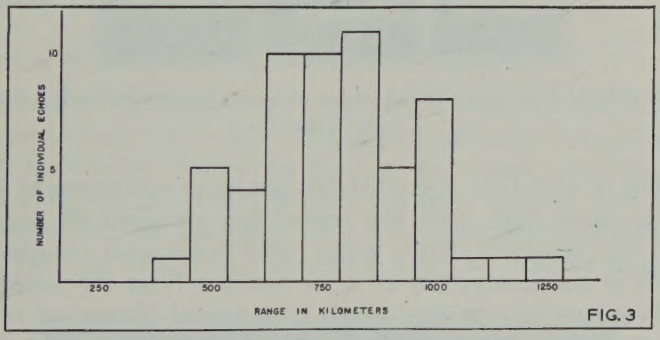

FIG. 3—Frequency of occurrence at various ranges of 106-Mc/sec radar echoes from aurora, College, Alaska, Aug.-Sept., 1953 (after Bowles)

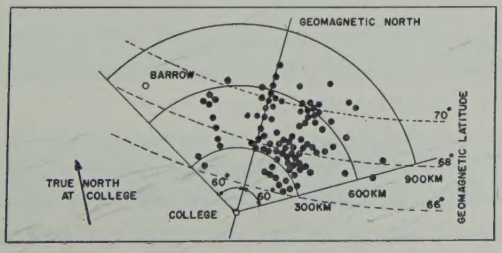

FIG. 4—Centers of 51.7-Mc/sec auroral echoes (after Dyce)

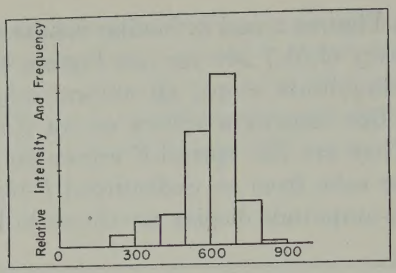

FIG. 5—Range probabilities of auroral echoes at frequency of 51.7 Mc/sec

auroral echoes at 104 Mc/sec are often spiky, and, as the echo dies away, one or two spikes may remain for a while above the receiver noise-level. These spikes still appear to fade down to zero, however. Some superficial disagreement with English [7] and Swedish [9] workers may be involved here. They classify their echoes into discrete echoes and diffuse echoes. It would not have occurred to us to make this distinction, since no echo that we have seen is discrete in the sense that it is like an airplane echo or like a regular *F*-region echo. All echoes are diffuse in the sense that they are like a rainstorm echo or like a spread-*F* echo, but the spread in range varies widely.

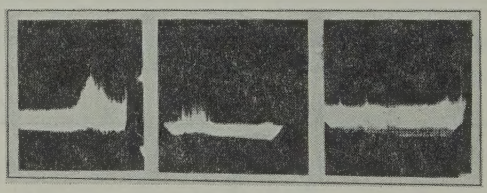

FIG. 6—The 104-Mc/sec radar auroral echoes on range-amplitude display, Ithaca, N.Y. (after Thayer)

In the course of operation of the 104-Mc/sec radar equipment at Ithaca during auroras, it was found that, with the transmitter switched off, increases in the noise-level on the range-amplitude scope were sometimes obtained on certain azimuths. This is not interpreted as noise emitted from the aurora. There are several FM broadcasting stations within a thousand kilometers of Ithaca that use a frequency close to 104 Mc/sec. These illuminate the auroral ionization and some energy is scattered toward the radar receiver. The transmission seems noisy because of the high fading rate imposed on the modulation and because of the substantial degree of multipath involved. It is thus useless to look for noise emitted from the aurora except under circumstances where it is certain that there is no other transmission on approximately the same frequency within a thousand miles of the auroral activity under investigation.

In the presence of auroral ionization, it should be possible to obtain auroral echoes not only at VHF, but also at HF, except in so far as the higher absorption may interfere. HF echoes from auroral ionization having the same range as those observed at VHF would appear on an ionospheric recorder at virtual heights exceeding normal *F*-region heights. During auroral activity, two types of echo at

these heights are seen at 2.4 Mc/sec. Both are complex echoes and have high fading rates. One appears at a range approaching 1,000 km early on certain auroral nights. The range decreases to that of the *F* region, with which it appears to combine to form spread *F*. This coincidence appears to argue in favor of an advancing front of irregularities moving southward in the *F* region at a speed usually of the order of 1,000 km/hr, but sometimes as slow as 100 km/hr [19]. This echo only appears in the early stages of an auroral night and then only if the night has been immediately preceded by non-auroral nights. It has not always been seen even on initial auroral nights, but might well have been missed. Subsequent nights of a period of auroral activity have an *F* echo which is spread from sunset onward. However, after spread-*F* echoes have been established, a second weak echo sometimes appears at 2.4 Mc/sec, with a range exceeding that of the *F* echo. Its range varies between 400 and 1,000 km, but not continuously. It may fade out at one range and then appear at another. It is not *G* scatter [20], which has never been recognized at Ithaca. The echoes may well be the counterpart at 2.4 Mc/sec of auroral reflections obtained at 104 Mc/sec, but we have not so far established this with any certainty.

Apart from this possibility, there seems to be little positive correlation between observations on HF and VHF, except for an unusually high rate of fading. At 2.4 Mc/sec, and on the frequency-sweeping equipment, echoes of the sporadic-*E* type occur at various stages during auroral activity, ranges varying from 100 to 250 km [19]. HF black-outs also occur, and may occur even when VHF reflections are present. There is some evidence suggesting that strong VHF echoes are associated with weak HF echoes and *vice versa*.

3. *Observations of Fading Rate*

A striking feature of auroral radio propagation at all HF and VHF frequencies is the high rate at which signals fade. The associated flutter that garbles modulated signals is well known [5]. During the heart of an auroral disturbance, all echoes received at 2.4 Mc/sec have fading rates between one and two powers of ten greater than occur at this frequency for a quiet ionosphere. Reception of WWV (Washington, D.C.) at Ithaca on 5 Mc/sec acquires at an early stage in an aurora

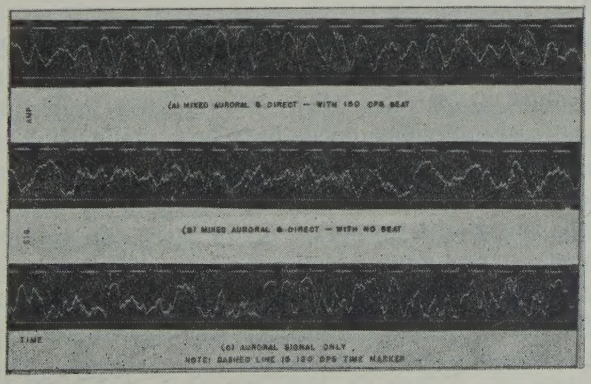

FIG. 7—Examples of auroral fading, 50 Mc, Ithaca, N.Y., April 1952 (after Bowles)

a fading rate of 2 to 5 cycles/sec, between one and two powers of ten greater than normal, and so high that an Esterline-Angus recorder does not follow it. Bowles [13] has measured the fading spectrum of amateur transmissions at about 50 Mc/sec during auroral propagation and found that the fading spectrum extends to 200 cycles/sec or more. At times there are higher frequency components (up to 2,000 cycles/sec) superimposed on the normal spectrum. These measurements have been verified, using an amateur station located 30 km from Ithaca under the operator's own control [21]. Examples of the fading of this continuous 50-Mc/sec carrier are shown in Figure 7. Figures 7(*A*) and 7(*B*) show the result of adding a signal received directly, by ground-wave, to the auroral signal. The mean frequency shift in the auroral signal is demonstrated by the beat frequency seen in Figure 7(*A*). In Figure 7(*C*), the antenna has been turned so that the direct signal has been reduced to negligible amplitude. Similar experiments at 144 Mc/sec gave fading spectra extending to 600 cycles/sec or more. The table of Figure 8 shows

OPERATING FREQUENCY Mc/sec	NUMBER OF RUNS	AVERAGE FADING RATE Cycle/sec	SPREAD IN FADING RATE Cycle/sec
50	20	101	43-190
145	5	434	250-610

FIG. 8—Auroral fading rates (after Bowles)

the average values of fading rates measured at 50 and 145 Mc/sec. Fading has not been recorded on the 104-Mc/sec radar because the repetition rate of the radar is less than the fading rate. Fading rate increases with operating frequency over the wide range 2.4 to 144 Mc/sec in such a way as to suggest that the fading arises from Doppler frequency-shifts associated with some velocity involved in the aurora.

The high fading rates observed under auroral conditions for radio waves of terrestrial origin returned by the ionosphere fit in with the high twinkling rates observed by Little and Maxwell [22] for extraterrestrial radio waves transmitted through an aurorally disturbed ionosphere.

4. *Visual Fine Structure of Rays*

During auroras, visual, photographic, photoelectric, and spectroscopic observations are made at Ithaca, and, in collaboration with Colgate University, auroral heights are determined by parallax. Observations likely to be quite significant in connection with auroral radio phenomena have been made using seven-power field-glasses. It has already been reported by Gartlein [23] that rays frequently have a fine structure consisting of streaks of light or raylets. A particular raylet only extends part of the length of a ray, is as narrow as the glasses can determine (less than about 100 meters), and lasts only about a second. It is the unceasing creation and decay of these raylets throughout the ray that leads to the optical illusion of a smooth ray. The raylets are somewhat like visual meteor trails, except that each raylet appears to the eye to be created instantaneously, as a whole. Of course, if it were created like a meteor trail, but with the velocity of incoming aurora

particles, creation would appear instantaneous to the eye. Fine structure of this type in auroral rays, if not an illusion of some sort, presumably involves a corresponding ionization-phenomenon that would be of importance in interpreting radio echoes from auroral rays. Meinel [24], however, has looked for this fine structure and has been unable to see it.

In an attempt to establish the reality of the raylets, a number of photographic plates, taken with auroral cameras of 46-mm focal length, have been studied using a microphotometer. With the microphotometer, traces were made running at right-angles to the ray structure, using a slit about 0.6 mm in length along the ray and 0.02 mm in width across the ray. At the end of this trace, the microphotometer was reset and a second trace was run with a displacement along the rays of about 0.2 to 0.3 mm. Similarly a third trace was made. Figure 9 shows a plate to which

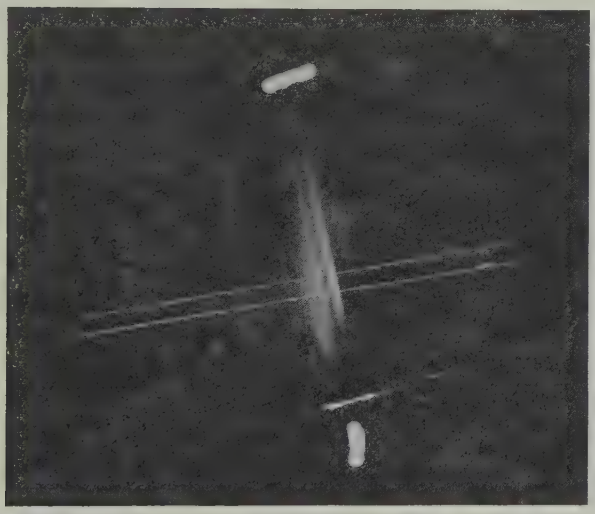

FIG. 9—Group of auroral rays photographed with 10 seconds exposure from Ithaca, N.Y., Sept. 19, 1941, 01:25 EST; the white lines define the region used for the photometric analysis shown in Fig. 10

this technique was applied after enlargement about 20 times, and Figure 10 shows the three microphotometer curves obtained therefrom. It will be seen that the curves show fine structure. Not only are there sharp changes in the intensity corresponding to the edges of rays, but there are irregularities within the rays, which in our opinion correspond to the raylets. It should be noted that the exposure-time for the plates is ten seconds, which is about ten times the duration of a raylet as seen by the eye. The photometer trace, therefore, presumably corresponds to quite a smoothed representation of the actual distribution of intensity across the rays. The scale of the fine structure illustrated in Figure 10, both at the edge and in the interior of the rays, corresponds in distance to about 100 meters.

Of course, it occurs to the mind that the irregularities within the rays shown in Figure 10 might in reality be due simply to the graininess of the photographic plate. This is why three traces were made at a separation large compared with

the grain size. If the irregularities in Figure 10 were due to photographic graininess, there would hardly be any correlation between the top and bottom curves in the diagram. But clearly there is a good correlation, showing that the irregularities are genuine irregularities in the intensity of the auroral light.

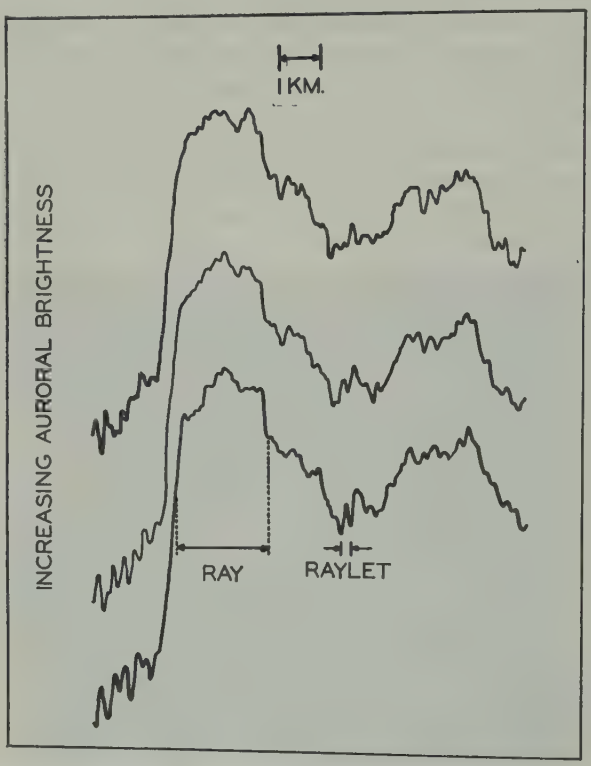

Fig. 10—Three partially overlapping photometric traces obtained from the plate used in Fig. 9; the horizontal scale is 20 times that of Fig. 9

We are, therefore, of the opinion that the raylets of which rays frequently seem to be constituted are a real phenomenon. In all probability, they are a normal feature of an aurora with ray structure, even though they cannot always be distinguished by eye.

5. *Diurnal and Seasonal Variations of Radio Reflections*

Most of the observations referred to above were made with equipment that was only in operation during a known aurora. In order to obtain more homogeneous data on the occurrence of radio reflections from the aurora, use was made of transmissions from high-power continuous-wave stations, operating at 49.6 and 49.8 Mc/sec, at Cedar Rapids, Iowa [25]. This station is always received at Ithaca weakly by ionospheric forward scatter-transmission. At times, it is also received strongly by reflections from the sporadic-*E* region. These transmissions arrive more or less from the west and have normal fading rates of several cycles/sec.

During periods of auroral activity, however, reception of the station is also obtained from a roughly northwesterly direction and has a greatly increased fading rate. This phenomenon is presumed to be due to scattering from auroral ionization over southern Ontario. The geometry is shown in Figure 11. Reflection from auroras

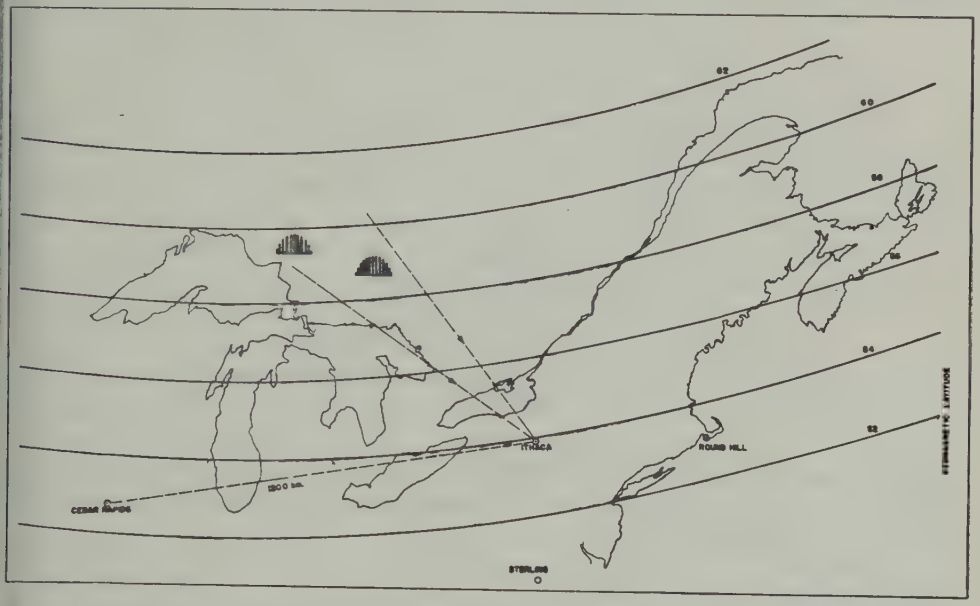

FIG. 11—Geometry of Cedar Rapids to Ithaca path, showing directions of reception of Cedar Rapids transmission at 49.6 and 49.8 Mc/sec

in this area, therefore, can be monitored by recording continuously, on an Esterline-Angus recorder, the field strength of the Cedar Rapids station and selecting the periods when propagation is of auroral type. This has been done for two years by R. Dyce [15]. The diurnal and seasonal variations are shown in Figures 12 and 13. Results show that auroral reflections are infrequent between sunrise and midday. They become more frequent as sunset is approached and are most frequent at

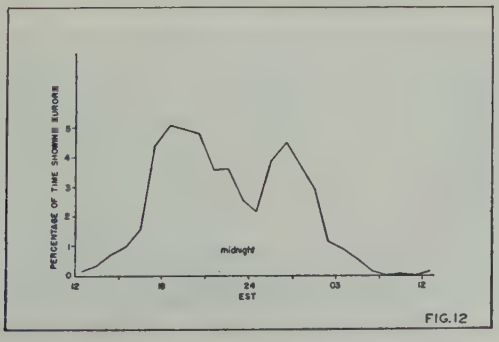

FIG. 12—Diurnal variation of Cedar Rapids signal propagated by aurora, Sept. 1952—May 1954 (after Dyce)

night, with maxima before and after midnight, separated by a subsidiary minimum. Seasonal variations show maxima at the equinoxes and minima at the solstices. Occurrence of auroral transmission from Cedar Rapids during the afternoon is usually the first warning at Ithaca of an aurorally disturbed night.

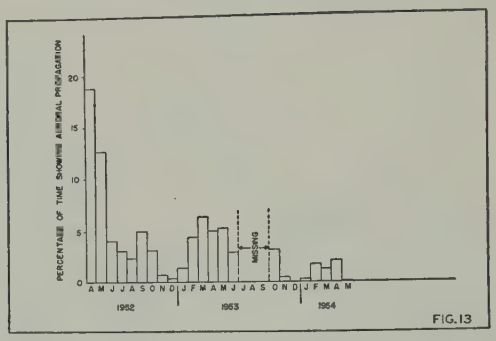

Fig. 13—Seasonal variation of Cedar Rapids signals propagated by aurora, April 1952—May 1954 (after Dyce)

These observations fit in with observations of the diurnal and seasonal variations of auroral echoes by radar, and in particular with the observations reported by Currie, Forsyth, and Vawter [10].

6. *Interpretation of Auroral Echoes*

It seems appropriate to initiate a discussion of the foregoing observations by considering the viewpoint of Harang and Landmark [11]. These authors deny that the observed echoes come directly from auroral ionization. They argue that the echoes in reality come from the rough surface of the earth seen by reflection in the ionosphere, and that the only function of the aurora is to provide an auroral *E* region to act as a horizontal mirror. Ground returns mirrored in a regular ionospheric layer, and even in the sporadic-*E* region, are well known at lower frequencies, and it is the suggestion of Harang and Landmark that this is what is occurring at frequencies up to 100 Mc/sec or more during auroral activity. The present authors find it difficult to accept this explanation.

Harang and Landmark conducted pulse observations on frequencies of 35 and 74 Mc/sec. They state in their paper that their antennas on these frequencies were specially designed so as to cover the same part of the sky. In spite of this, they found that the ranges from which echoes were obtained were appreciably less at 35 Mc/sec than at 74 Mc/sec, and it is upon this point that their interpretation rests to a considerable extent. However, these echoes were obtained, not with the antennas pointed upward at an angle of elevation exceeding the beamwidth, but with the antennas directed horizontally. With the antennas directed horizontally, the interference-patterns produced by ground-reflection have a vital influence on the angle of elevation at which transmission and reception are maxima. Harang and Landmark undoubtedly designed their antennas to cover the same part of the sky in the absence of the ground. But in the presence of the

ground, they should have placed them at the same number of wavelengths above ground, whereas in fact they placed them at the same absolute height above ground. The consequence is that their 35-Mc/sec antenna had an angle of elevation for maximum transmission and reception roughly double that for the 74-Mc/sec antenna. It is not surprising, therefore, that echoes from *E*-region scatterers occurred at a lower range at 35 Mc/sec than at 74 Mc/sec.

Of course, it is true that, at 35 Mc/sec but not at 74 Mc/sec, echoes from the ground mirrored in a sporadic-*E* region should be observable from time to time. It may be that the multiple echoes to which Harang and Landmark refer are such that the lower-range echo arises by back-scattering from irregularities in the *E* region and the longer-range echo arises by ground-scatter mirrored in the *E* region. However, the phenomena of "multiple" echoes do not appear to be common, nor does the multiple range-relation appear to be precise. It is perhaps equally likely that auroral activity at two different ranges, possibly in somewhat different directions, could explain these observations.

Furthermore, the interpretation of Harang and Landmark appears to be contradicted by a number of aspects of the observations at Cornell and elsewhere, including some of Harang and Landmark's own observations. All the observations at Ithaca and at College, Alaska, show that auroral echoes are obtained almost entirely from the northern quadrant. They are never received from the south, even when there is visible aurora to the south. A few instances of echoes to the south have been reported from Saskatoon, but these may be meteor echoes as observed in the course of the Alaska observations. Harang and Landmark themselves agree that echoes come from the northern quadrant, not only at Kjeller in southern Norway, but also at Tromsö in northern Norway, where many auroras occur to the south. There is nothing about the explanation of Harang and Landmark that would account for the remarkable directional features of auroral echoes.

Moreover, in the transmissions from Cedar Rapids to Ithaca, described in Section 5 of this paper, the following two phenomena are observed:

(*i*) Large increases in received power, particularly around the summer solstice, with no obvious change in fading rate or systematic change in direction of arrival. This phenomenon we interpret as arising from non-auroral sporadic *E* having no relation to auroral activity. A typical example is shown in Figure 14.

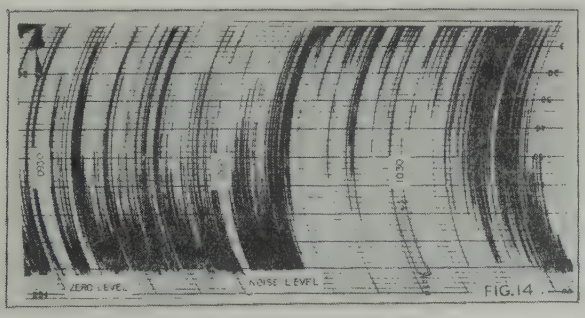

FIG. 14—Typical response of Esterline-Angus recorder to sporadic-*E* signal on 49.6 Mc. June 21, 1952

(*ii*) Small increases in received power, particularly around the equinoxes, with a substantial increase of fading rate and a marked systematic change in the direction of arrival towards the north. A typical example is shown in Figure 15. (The response of the recorder is linear in field strength to about two-thirds of full scale and somewhat non-linear above.) This phenomenon we interpret as arising

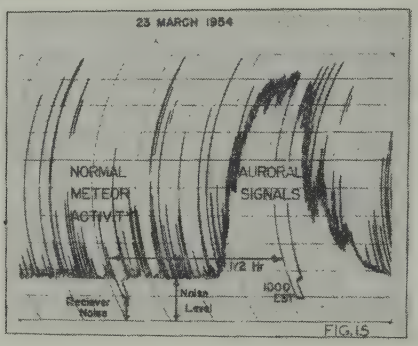

FIG. 15—Esterline-Angus record on 49.8 Mc from Cedar Rapids

from auroral scattering and might be associated with what is frequently called auroral sporadic *E*. It is closely associated with auroral activity. Even if it is appropriate to think of phenomenon (*ii*) as indicating the presence of a mirror in the ionosphere, it is unquestionably a much worse mirror than that associated with phenomenon (*i*). Yet the auroral echoes at 100 Mc/sec occur in association with phenomenon (*ii*), but have not been observed in association with phenomenon (*i*). On Harang's interpretation, therefore, it would be necessary to explain why the echoes occur in the presence of a poor mirror but fail to occur in the presence of a better mirror.

We proceed to consider the hypothesis that auroral echoes could be due to coherent reflection from an auroral surface or curtain. This view has been advanced by Herlofson [28], and appears to have been in the minds of other authors as well. Coherent reflection from a surface involves an isolated bounce-point at the foot of a perpendicular from the radar, with Fresnel zones around it. The auroral surface need not necessarily involve a discontinuity of ionization. The transition in the ionization-density could be continuous, and reflection could be either partial or total.

Any mechanism involving completely coherent reflection from auroral ionization does not seem consistent with the character of the observed fading. Bowles [21] frequently finds that the statistical distribution in the amplitude of auroral reflections is Rayleigh in type. Although departures from a Rayleigh distribution do occur, they are not usually of the type that favor a coherent reflection theory. If fading were frequently such that the fading range were small compared with the mean amplitude, with the statistical distribution of amplitudes about the mean being normal, coherent reflection from an auroral surface would be indicated, with some incoherent scattering due to irregularities superimposed. It is quite unusual to observe fading with properties approximating to this. Fading is nearly

lways Rayleigh, or roughly Rayleigh, in type, and this implies many contributions nterfering in roughly random phase. This could perhaps arise from a twisted uroral surface having many perpendiculars from the radar, the lengths of which ere varying with time. However, the long range and comparative narrow angular pread of the echoes militate against this explanation. Moreover, we would have hought that there would be many occasions on which the echo would be primarily ssociated with a single perpendicular.

Of course, if the "discrete" echoes observed by Aspinall and Hawkins [7] t 72 Mc/sec were airplane-type echoes, it would be entirely appropriate to inter- ret these in terms of coherent reflection from an auroral surface. But such echoes ave not been seen at Ithaca, and it may be suspected that those who have used he expression "discrete" merely meant that the echoes had a narrow range-spread nd did not intend to imply that they were unlike rainstorm echoes.

Harang and Landmark [11] described in some detail the fading of the auroral choes that they obtained. At 74 Mc/sec, the echoes were of the rainstorm type nd fit in with the fading observations described in this paper. At 35 Mc/sec, the ame appears to have been true on most occasions. But cases are described in hich airplane-type echoes did occur at 35 Mc/sec. Thus, coherent auroral echoes re possible at 35 Mc/sec, but there is no evidence for their occurrence at any igher frequency. It seems legitimate to deduce that the ionization extending hrough a considerable volume of an aurora may occasionally be overdense at a requency of 35 Mc/sec, but not at a higher frequency, such as 50 Mc/sec. This ould put the order of magnitude of the mean E-region ionization-density in an urora at not more than 10^7 electrons/cc, irregularities in this ionization leading, owever, to scattering of radio waves at frequencies up to perhaps 150 Mc/sec.

Except occasionally at the bottom end of the VHF band, the hypothesis of ompletely coherent reflection from auroral ionization seems, therefore, to be ntenable. Moreover, we interpret the Rayleigh, or nearly Rayleigh, character f the fading as indicating scattering from a distribution of ionization involving rregularities in space and time. It is not unreasonable to think of a relation between he distribution of ionization in an aurora and the distribution of luminosity. ince radio echoes from auroras are associated with displays showing ray structure, he distribution of luminosity in such an aurora might be a reasonable starting oint in picturing the distribution of ionization. The auroral ray thus becomes a ypical auroral scattering unit, as suggested by Aspinall and Hawkins [7], and s assumed by Chapman [16]. But in practice, many auroral rays are involved in orming auroral echoes and these interfere with each other in more or less random hase, leading to fading of roughly Rayleigh type.

Let us now give further attention to one of the most striking features of auroral choes, namely, that they seem to come only from low angles of elevation in the orthern quadrant. At Ithaca, on 104 Mc/sec, only one auroral echo has been een at a range of less than 550 km. Ithaca is, of course, over 1,000 km south of he conventional center of the auroral zone. For this reason alone, many auroral choes would come from low angles of elevation in the north. While this explains hy many auroral echoes are seen at ranges in excess of 550 km, it does not explain he almost complete absence of echoes at shorter ranges. There are many individual

auroral displays that extend southward as far as Ithaca and even farther. Even during these auroral displays, echoes are only received in the northern quadrant at ranges of many hundreds of kilometers. At Fairbanks, Alaska, Bowles working on 106 Mc/sec and Dyce on 51.7 Mc/sec have obtained similar results. A VHF radar in the middle of the conventional auroral zone obtains its auroral echoes predominantly from displays near the polar edge of the zone.

It was suggested by R. K. Moore [18] that the Ithaca observations on 104 Mc/sec, as well as similar observations at Saskatoon [10], indicate a striking aspect sensitivity in auroral scatterers, and that the aspect sensitivity is of the type that would be expected for columns of ionization lying along the earth's magnetic field. If the ionization were distributed uniformly along a column, reflection from the column would come predominantly from the neighborhood of the foot of the perpendicular from the radar. In the case where the radar and the column are in the same magnetic meridian, R. K. Moore worked out an appropriate formula for the length of the perpendicular from a radar onto a line of force of the earth's magnetic field. A more accurate and complete calculation of the same type has been carried out by Chapman [16], who considered also the case where the column and the radar are not in the same magnetic meridian. The results of these calculations for a radar located at Ithaca are shown in Figure 16. It will be

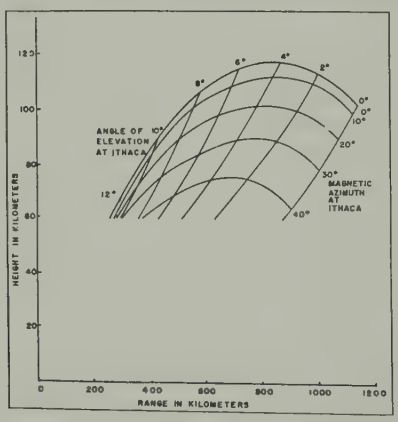

FIG. 16—Locus of feet of perpendiculars from Ithaca, N.Y., onto lines of earth's magnetic field

seen that the foot of the perpendicular never occurs at a height greater than 120 km. Moreover, if it is assumed that columns do not extend to heights below 80 km, the lengths of the perpendicular vary from 400 to 1,150 km. This agrees quite well with the ranges at which auroral echoes have been observed at Ithaca on 104 Mc/sec.

It should be said that, while the agreement between the Chapman calculations and the Ithaca observations at 104 Mc/sec is very good, the agreement is not quite so good with the Saskatoon [10] observations at substantially the same frequency. Moreover, at 50 Mc/sec the minimum observed range of echoes is somewhat less than at 100 Mc/sec [10,11], and at 30 Mc/sec the minimum observed range is further reduced somewhat [9]. It must be remembered, however, that

the Chapman calculations do not assume that all of the scattering by an auroral ray comes precisely from the foot of the perpendicular. A column that extended nearly down to the foot of the perpendicular could still give quite a good echo. There is some latitude available in interpreting the condition of perpendicularity, and this latitude increases with increase of wavelength. In fact, the aspect sensitivity of auroral columns, and its variation with wavelength, are surprisingly reminiscent of the corresponding observations for meteor trails [29]. A meteor shower, consisting of a large number of small meteors having the magnetic zenith as radiant, would produce radio phenomena by no means dissimilar to those observed during auroral displays.

The meteor-like behavior of auroral echoes makes the observations of Gartlein concerning the fine structure of auroral rays quite remarkable. Gartlein's observations, described in Section 4, amount to saying that an auroral ray often seems to consist of a bundle of narrow meteor-like trails or raylets, each extending for part of the length of a ray and each lasting only about a second. Gartlein's observations are tantamount to suggesting that auroral displays showing ray structure are not only meteor-like in the radio phenomena associated with them, but also in the visual phenomena. While visual observations of fine structure in the aurora are undoubtedly difficult, the photometric analysis described in Section 4 seems to establish the existence of this fine structure with some certainty.

If one accepts the reality of the raylets seen by Gartlein, and combines this information with that concerning the radio phenomena reported above, one forms the impression that auroral rays could be produced by a group of meteor-like particles entering the earth's atmosphere along the lines of the earth's magnetic field. The energy of the particles would, of course, have to be spread over a considerable range in order to explain the enormous length of rays [30]. These particles could not be individual protons, since the energy of a single proton would be ridiculously too small to produce the visual raylet and the ionized trail. A "particle" might conceivably be a group of protons having nearly the same velocity in magnitude and direction. While it is difficult to imagine how this could occur, it is also difficult to imagine how even the most obvious geometrical features of a rayed aurora could occur. These aspects of auroral displays are still wrapped in mystery. It has not even been demonstrated yet that auroras with ray structure are associated with incoming protons, since hydrogen radiation has not yet been detected in auroras of this type.

It should be said that, while we have interpreted the fact that auroral echoes are only obtained at low angles of elevation in the northern quadrant as indicating a striking aspect sensitivity for auroral scatters, this view was specifically rejected by Forsyth [10] in discussing the Saskatoon observations. There were apparently some echoes that did not fit in with the Chapman calculation, particularly at their lower operational frequency of 56 Mc/sec. A few gross discrepancies could have occurred by mistaking a long-duration meteor-echo for an auroral echo. Minor discrepancies, we feel, are due to taking the perpendicularity hypothesis of Chapman too literally.

Instead of regarding the auroral scatterers as columns or trails lying along the lines of the earth's magnetic field, Forsyth thinks of them as being roughly iso-

tropic in character, and overdense even at a frequency of 100 Mc/sec. He pictures these scatterers as existing under disturbed conditions in both the E region and in the D region (or lower part of the E region). In the E region the scatterers would reflect incident radio waves, while in the D region they would absorb them. A disturbed volume, viewed from a long distance, would be such that the E-region scatterers could reflect energy without passing through the absorbing scatters in the D region. A disturbed volume viewed at short range, or from underneath, would be such that passage through the D-region scatterers would be necessary, and this would completely absorb reflected wave. This theory does not seem tenable to us. In the first place, it would lead to a situation in which auroral echoes were equally likely on all azimuths under circumstances when auroral disturbance is equally likely to occur in all parts of the sky. This is not in accordance with our reading of the observations, even of the observations at Saskatoon. Even as an explanation of the lack of short-range echoes, the theory does not seem likely to us. It assumes that, over localized areas, complete attenuation of 100-Mc/sec waves is possible in the D region or lower E region. Observations of galactic noise [8] and discrete cosmic sources [22] have shown that some reductions do occur during auroras, but the amount is much less than would be required to support Forsyth's theory. Furthermore, if complete black-out is possible at 100 Mc/sec even locally, one would have thought that this would occasionally show up in the transmissions from Cedar Rapids to Ithaca at 49.8 Mc/sec, as described in Section 5. No occasion has even occurred when the signal was diminished below normal. On the contrary, there are more than a hundred examples of increases in signal strength in association with auroral activity. Of course, complete black-outs in association with auroral activity are common enough at HF frequencies. But this does not imply that there is any black-out phenomenon at a frequency as high as 100 Mc/sec. In the frequency-range involved, attenuation in decibels is inversely proportioned to the square of frequency. Thus, a hundred decibels of attenuation at 10 Mc/sec becomes only one decibel at 100 Mc/sec. We know of no reason for thinking that there is any important attenuation at 100 Mc/sec due to auroral disturbance.

Let us now turn our attention to the fading rates of waves reflected from the aurora. Pursuing the meteor-like concept of auroral echoes, R. K. Moore [18] suggested that the high fading-rate of aurorally reflected waves might be associated with the velocity of incoming auroral particles in the same way that the Doppler whistle of a radio echo from a meteor is associated with meteor velocity. Consider an incoming particle with velocity v whose trail is a perpendicular distance r from a radar operating on wavelength λ. The Fresnel zone along the trail, with center at the foot of the perpendicular from the radar, has length of the order of $\sqrt{r\lambda}$. The time taken by the particle to transverse this zone is $\sqrt{r\lambda}/v$, and the associated fading frequency is

$$v/\sqrt{r\lambda} \quad \ldots\ldots\ldots\ldots\ldots\ldots\ldots\ldots\ldots\ldots (1)$$

From a more elaborate formula of this type, Moore calculated that the observed fading rates of auroral reflections as seen at Ithaca could be explained with a value of v of 340 km/sec. Formula (1) would, however, imply that fading rate is proportional to the square root of frequency, whereas, in fact, it is at least pro-

portional to frequency. Moreover, 340 km/sec is a rather low velocity for incoming protons (or other ions). The incoming particles, regardless of initial speed, will produce their ionization where their speed has been reduced roughly to the orbital velocity of the outer electrons in the atmospheric gases, and this is of the order of 3,000 km/sec. According to formula (1), this would lead to fading rates of the order of 1,500 cycles/sec at a frequency of 50 Mc/sec, using typical ranges. As mentioned in Section 3, fading rates as high as this have been seen in some auroras, and in these cases Moore's explanation of fading may be appropriate. At 50 Mc/sec, however, a fading rate of 150 cycles/sec would be more usual, and some other explanation must be sought.

An alternative explanation of the fading of auroral echoes is that it is like the random fading of a meteor echo after the trail has been completely formed and the Doppler whistle associated with its creation has died away. This fading is due to drift and break-up of the trail in a wind-like motion. However, the fading of auroral echoes is about a power of ten faster than the random fading of meteor echoes. Greenhow [31] finds for meteor echoes fading rates of 10 and 20 cycles/sec at frequencies of 36 and 72 Mc/sec. Bowles [21] quotes for auroral echoes at Ithaca fading rates of 100 and 400 cycles/sec at frequencies of 50 and 145 Mc/sec. Fading rates of auroral echoes observed in Alaska by Bowles and Dyce [12] were even greater than those observed at Ithaca. Fading of auroral echoes would seem, therefore, to be due to a wind-like motion of the scattering columns of ionization, but with speeds up to a power of ten faster than the wind-speeds associated with a quiet ionosphere. Observation of the rate of movement of centers of auroral echoes in range and azimuth also give high speeds, sometimes higher than 1,000 meters/sec.

The question arises as to whether the high speeds with which auroral ionization (and luminosity [17]) seems to move are due to a genuinely high wind-speed. The answer appears to be in the negative. Bowles [12], while observing auroral echoes in Alaska at 106 Mc/sec, was frequently able to see meteor echoes at the same time. The auroral echoes were fading at a rate greater than the repetition rate (sweeps/second) of the radar. On the other hand, the meteor echoes were fading at a rate which was slower than the repetition rate of the radar and which would fit in with the meteor observations of Greenhow [31]. The implication seems to be, therefore, that auroral ionization moves at a speed much greater than simultaneously present meteoric ionization-trails. Presumably, the meteor trails are moving at the wind-speed and the auroral columns at a much higher speed, determined perhaps by motion of the source of excitation of the auroral ionization.

In common with other authors, we have interpreted all auroral echoes so far observed as coming from *E*-region levels. There does not, however, seem to be any strong reason for thinking that auroral echoes cannot come from levels above the *E* region. We have been led to the view that the echoes come from auroral columns of ionization that lie along the lines of force of the earth's magnetic field and are associated with the auroral rays observed visually. While auroral rays usually extend down to *E*-region levels, they are by no means restricted to *E*-region levels. Rays frequently extend from the *E* region up through the *F* region, sometimes to heights above 1,000 km. If this is true of the luminosity, the same might

also be true of the associated ionization. The only reason why we have interpreted the echoes as coming from the E region is that, for the comparatively northern locations of present auroral radio observing stations, the feet of perpendiculars from them onto the lines of force of the earth's magnetic field fall at roughly E-region levels, or somewhat below. To make the foot of the perpendicular (the "echo point") fall at an F-region level, it would merely be necessary to consider a location for the radar substantially nearer to the equator than has so far been used. Figure 17 (based on computations of G. C. Rumi) illustrates this for coronal

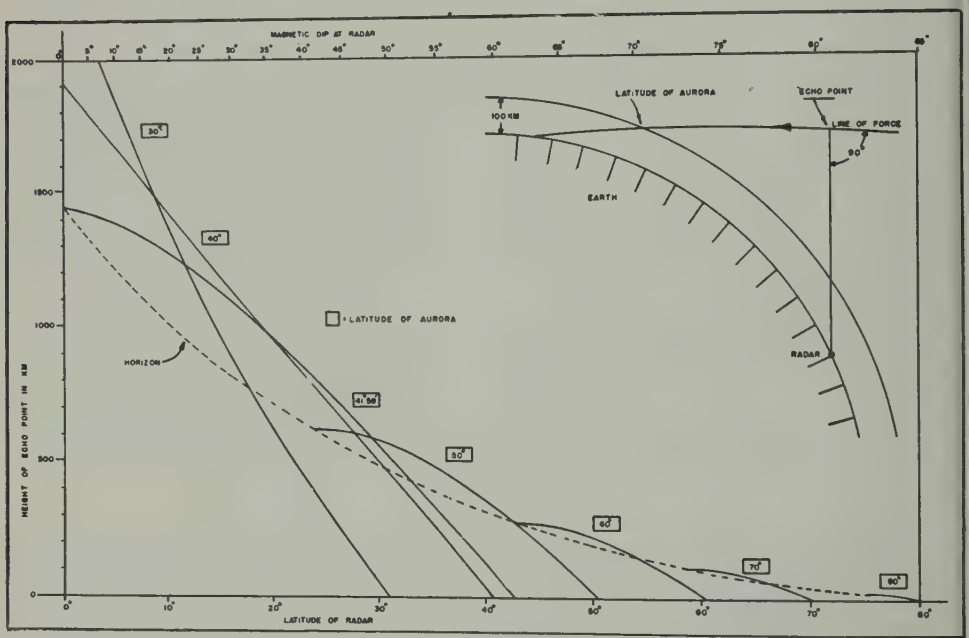

FIG. 17—Height of foot of perpendicular in meridian plane to a line of force of dipole field *vs* latitude of radar

auroras in various latitudes. It is assumed that the earth's magnetic field is the field of a dipole at the center, and magnetic latitudes are used. (Departure from this assumption can be allowed for by using an equivalent latitude designed to reproduce the proper local magnetic dip; see scale at top of diagram.) It is further assumed that the aurora is in the same magnetic meridian as the radar. An aurora is assumed to be defined by a line of force of the earth's magnetic field, and the latitude of this line at the 100-km level is defined as the "latitude of aurora." Along the horizontal axis in the Figure is plotted the latitude of the radar. Along the vertical axis is plotted the height of the echo point, that is, the foot of the perpendicular from the radar onto the line of magnetic force representing the aurora. Transequatorial echoes are disregarded; the portions of the curve not drawn correspond to situations in which the perpendicular from the radar is below the horizon of the radar and which are therefore of no practical interest. It is seen that auroras in latitudes around 50° having rays extending up through

the F region should, so far as geometry is concerned, give auroral echoes from F-region levels for radars located in latitudes around 30° to 40°. No VHF observations have ever been made, however, so far from the regular auroral zone as this.

From Figure 17 it may be seen that an aurora in latitude 40° could conceivably give auroral echoes at a radar located at the equator, provided that the auroral rays extend up to 2,000 km. The chances of this happening even at sunspot maximum are presumably negligible. It does seem likely, however, that, around sunspot maximum, auroral echoes could be obtained at locations nearer the equator than have so far been used, and that these echoes would come from F-region levels or even higher.

References

[1] E. V. Appleton, R. Naismith, and L. J. Ingram, Phil. Trans. R. Soc., A, **236**, 191-259 (1937).

[2] L. Harang, The aurorae, Chap. 8, New York, John Wiley and Sons, Inc. (1951).

[3] G. Leithäuser and B. Beckmann, Zs. Techn. Physik, **18**, 290 (1937); W. Dieminger and H. Plendl, Hochfrequenztech., **51**, 117 (1938); R. Eyfrig, G. Goubau, Th. Netzer, and J. Zenneck, Hochfrequenztech., **51**, 149 (1938); B. Beckmann, W. Menzel, and F. Vilbig, Telegraphen- Fernsprech- und Funk-Technik, **27**, 27, 245 (1938) and **28**, 130, 425 (1939).

[4] J. H. Meek, J. Geophys. Res., **54**, 330 (1949).

[5] R. K. Moore, J. Geophys. Res., **56**, 97 (1951).

[6] L. Harang and W. Stoffregen, Hochfrequenztech., **55**, 105 (1940).

[7] A. Aspinall and G. S. Hawkins, J. Brit. Astr. Assoc., **60**, 130 (1950).

[8] D. W. R. McKinley and P. M. Millman, Can. J. Phys., **31**, 171 (1953).

[9] G. Hellgren and J. Meos, Tellus, **4**, 249 (1952).

[10] B. W. Currie, P. A. Forsyth, and F. E. Vawter, J. Geophys. Res., **58**, 179 (1953); P. A. Forsyth, J. Geophys. Res., **58**, 53 (1953).

[11] L. Harang and B. Landmark, J. Atmos. Terr. Phys., **4**, 322-338 (1954).

[12] K. Bowles and R. Dyce, papers presented at Joint Meeting of URSI, IRE, and AGU, Washington, D.C., May 3-6, 1954.

[13] K. Bowles, J. Geophys. Res., **57**, 191 (1952).

[14] R. Thayer, Master's Thesis, Cornell University (1952).

[15] R. Dyce, School of Electrical Engineering, Cornell University, Res. Rep. EE 209 (1954).

[16] S. Chapman, J. Atmos. Terr. Phys., **3**, 1 (1952).

[17] A. B. Meinel, National Science Foundation Conference on "Motions in the upper atmosphere," Albuquerque, September 7-9, 1953.

[18] R. K. Moore, Trans. Inst. Radio Eng., Professional Group on Antennas and Propagation, No. 3, 217 (1952).

[19] W. A. Flood, Master's Thesis, Cornell University (1952). [School of Electrical Engineering, Cornell University, Studies on propagation in the ionosphere, Tech. Rep. No. 8.]

[20] W. Dieminger, Proc. Conference on Ionospheric Physics, Pt. A, 175 (1950).

[21] K. L. Bowles, Master's Thesis, Cornell University (1953). [School of Electrical Engineering, Cornell University, Studies on propagation in the ionosphere, Tech. Rep. No. 15.]

[22] C. A. Little and A. Maxwell, J. Atmos. Terr. Phys., **2**, 356 (1952).

[23] C. W. Gartlein, Trans. Amer. Geophys. Union, **1**, 122 (1945); paper presented at American Geophysical Union meeting, Washington, D.C., May 1-3, 1950.

[24] A. B. Meinel, Remarks at joint meeting of URSI and IRE, Ottawa, October 5-8, 1953.

[25] D. K. Bailey, R. Bateman, L. V. Berkner, H. G. Booker, G. F. Montgomery, E. M. Purcell, W. W. Salisbury, and J. B. Weisner, Phys. Rev., **86**, 141 (1952).

[26] T. L. Eckersley, J. Inst. Elec. Eng., **86**, 548 (1940).
[27] W. L. Hartsfield and R. Silberstein, Proc. Inst. Radio Eng., **40**, 1700 (1952).
[28] N. Herlofson, Nature, **60**, 867 (1947).
[29] A. C. B. Lovell, Sci. Prog., **38**, 22 (1950).
[30] D. R. Bates, J. Atmos. Terr. Phys., **3**, 212 (1953).
[31] J. S. Greenhow, Phil. Mag., **41**, 682 (1950).

THE SYSTEMATIC ELECTRIFICATION OF MIST AND LIGHT RAIN IN THE LOWER ATMOSPHERE

By Ross Gunn

Physical Research Division, U.S. Weather Bureau, Washington, D.C.

(Received July 19, 1954)

ABSTRACT

The role of ionic diffusion in placing free electrical charge on droplets falling in the atmosphere is considered. Experimentally verified expressions for the diffusion of ions onto droplets are shown to account for the sign and magnitude of the free charge observed on light rain and mist. In the lower atmosphere, such droplets are normally positive and carry a specific free charge approximating 1 esu/gm. The observed variability of the electrical conductivity of the atmosphere suggests that diffusion may occasionally transfer large negative as well as positive charges to the falling drops.

Introduction.

The free electricity carried towards the ground by falling precipitation plays an important role in determining the electrical balance of the atmosphere. The mechanisms responsible for the observed electrification are not well understood, although many possible processes have been considered in the literature.

Nearly two decades ago, R. Gunn suggested that falling cloud droplets might be likened to concentration cells charged to a potential of some 60 millivolts [see 1 of "References" at end of paper]. On this hypothesis, a quantitative description of thunderstorm electricity was developed. Although the description was not complete, it was successful in explaining many features of active thunderstorms. Two recent papers have considered new aspects of this suggestion, which attributed the electrification of precipitation to the diffusion of water molecules and ions. These new investigations by R. Gunn [2] and by B. B. Phillips and R. Gunn [3] have established a theoretical and observational understanding of the diffusion of ions onto falling droplets and have provided experimentally observed values for the magnitude of the resulting equilibrium charge. Adopting these new results, one considers here their application to the electrification of mist and light rain droplets falling in the lower atmosphere. Our conclusion may be stated in advance, namely, that the free charge observed on quietly falling mist and light rain at relatively low levels is normally a manifestation of ionic diffusion.

Systematic Equilibrium Charge on Drops Falling Through on Ionized Environment.

The rate of transfer of positive and negative charge by diffusion of ions to a conducting sphere moving with respect to its environment has been worked out in detail and compared with controlled laboratory measurement [2, 3]. These

measurements show that the average equilibrium charge, Q, transferred to conducting spherical droplets is given by

$$Q = a\left(1 + F\sqrt{\frac{aV}{2\pi D}}\right)\left[\frac{kT}{e}\, ln\, \frac{\lambda_+}{\lambda_-}\right] \quad \text{.....(Eq. 1)}$$

where the effective diffusion coefficient, D, is

$$D = \frac{n_+D_+ + n_-D_-}{n_+ + n_-} \quad \text{.....(Eq. 2)}$$

In these relations, a is the radius of the sphere, V is its velocity relative to the ionized environment, n_+ and n_- are the ionic densities of the positive and negative ions respectively, D_+ and D_- are the diffusion coefficients for the positive and negative ions, k is the Boltzmann constant, T is the absolute temperature, e is the electronic charge, F is a dimensionless constant approximating unity, determined by the character of the air flow around the drop, while λ_+ and λ_- are the positive and negative ion conductivities of the environment respectively.

It is important to notice in Eq. 1 that the ratio of the positive and negative ionic conductivities determines the sign of the charge acquired by the droplet. When the positive conductivity is in excess, the droplet will acquire a positive charge; and when the negative conductivity is greater, the negative charge predominates. It is clear, therefore, that free space charge due to light ions will normally modify the equilibrium charge acquired by a drop. For example, the normal space charge in the lower atmosphere is positive, and this has a marked tendency to skew the charge on atmospheric droplets towards positive values. This asymmetry is observed [5]. It may be noted, however, that a large random electrification persists even when the conductivities are equal. The electromechanics of this random electrification will be considered elsewhere.

It may be noted that the term in square brackets in Eq. 1 is the potential of a concentration cell [1] whose value depends only on atomic constants and the relative conductivities due to the positive and negative ions. This fundamental cell potential is increased by a factor depending on the relative velocity of the droplet and its environment. The augmentation of the free charge by this relative

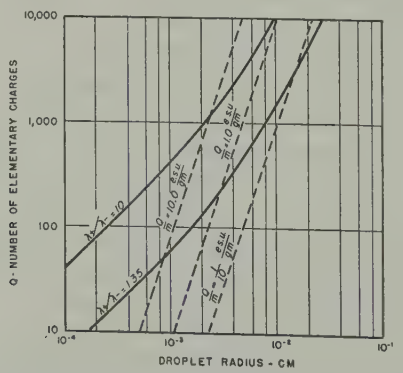

FIG. 1—The equilibrium charge on falling droplets expressed as a function of the droplet radius and the relative conductivities due to the positive and negative ions; the dashed lines define values of constant charge per unit mass of the falling precipitation

motion is given by the terms in round brackets in Eq. 1 and may amount to a factor of 35 for the largest raindrops. The increase is important even for mist and light rain.

By the use of Eq. 1, the magnitude of the equilibrium charge carried by droplets of various sizes is plotted in Figure 1, assuming that the relative positive and negative ion conductivities are those indicated on each curve. Since the velocity of free fall in Eq. 1 is known as a function of the droplet radius [4], it is clear that the magnitude of the charge is determined when the conductivity ratio has been assigned. Also shown on the same Figure are dotted lines of equal specific charge corresponding to 10, 1, and 0.1 esu/gm of precipitation. Referring to Figure 1, it may be seen that for droplets of the size of mist or light rain (*circa* 0.01 cm), the charge per unit mass of precipitation approximates 1.0 esu/gm. Attention is drawn to the fact that falling droplets normally associate by collision to form larger droplets. Since the mass and charge are both conserved in such associations, the charge per unit mass of the fully grown drop may under favorable conditions be as great as 5 esu/gm, the exact value depending on the size of the fundamental droplet.

The Observed Systematic Electrification of Mist and Light Rain.

A large number of experimenters have collected data on the free charge carried by falling rain and have subdivided the measurements according to the droplet size and precipitation rate [5, 6]. Although the measured free charges brought down by moderate and heavy precipitation scatter badly, nearly all observers agree that the free charge on quietly falling light rain and mist is positive. For example, F. J. Scrase [6] made continuous determinations of the charge on rain over a two-year period. For precipitation rates less than 0.01 mm/min, he found that 93 per cent of the rain carried positive charges. As the precipitation rates increased, the relative amounts of positive charge steadily decreased until rain of cloudburst proportions was observed. The average of Scrase's measurements shows that the charge transferred per unit mass of falling rain approximated 0.46 esu/cm^3. This value is consistent with the specific free charge density inferred from Eq. 1 and plotted in Figure 1.

In addition to the systematic charge of a single sign carried by many raindrops, charges of both signs in equal amounts are normally distributed at random among the other drops. Under certain conditions, these charges also contribute to the over-all electrification.

Relative Conductivities Due to the Positive and Negative Ions.

The sign of the free charge carried by droplets falling in the atmosphere according to Eq. 1 depends upon the logarithm of the ratio of the positive and negative conductivities in the environment. It is important, therefore, to examine the observational data on the relative conductivities for an indication of the sign of the charge to be expected under various conditions.

Measurements of the relative conductivities of positive and negative ions have been made by a large number of observers. All measurements clearly show that the positive conductivity is about 30 per cent greater than the negative in

regions near the earth. For example, K. L. Sherman [7] measured the relative conductivities in Alaska for nearly a year and concluded that the average value of $\lambda_+/\lambda_- = 1.36$. He also found that the ratio of the ionic density of the positive ions to that of the negative ions averaged 1.32. In the reduction of his data, he estimated the mobilities for the positive and negative ions and found that the typical negative ionic mobility exceeded that of the positive by about 25 per cent. These coherent ground measurements in relatively pure polar air establish beyond reasonable doubt that the positive ion conductivity is in marked excess. Recently, G. R. Wait [8] summarized conductivity measurements made at the Tucson, Arizona, Observatory over a period of 17 years. His summarized values are not unlike those of Sherman and show that the positive ion conductivity exceeds that of the negative ions.

Measurements of the relative conductivities make in aircraft are sometimes inconsistent. O. H. Gish and G. R. Wait [9] give curves showing both the positive and negative conductivities as a function of the altitude. Their measurements show that the ratio of the positive and negative conductivities approximates 3.75 near the earth, but decreases slowly with increasing altitude to about 0.94 at 35,000 feet. The conductivities are essentially equal at 25,000 feet. More recently, R. C. Callahan, S. C. Coroniti, A. J. Parziale, and R. Patten [10] report later measurements and conclude that the relative conductivities are essentially the same for all altitudes, although their presented curves of average values do not well support their conclusions. Further measurements are required before the matter can be entirely settled, but it is fair to observe that the measurement of atmospheric conductivity from moving high-speed aircraft is beset with many pitfalls. In attempting to circumvent some of the difficulties, Fritz Rossmann [11] has made extensive measurements using motorless gliders. His conductivity values scatter badly and serve principally to emphasize the large variability normally encountered in the free atmosphere.

In the lower levels of the atmosphere, where mist and very light rain usually originate, the available data indicate clearly that the positive ion conductivity notably exceeds the negative. In this region, therefore, droplets charged by diffusion would be positively charged. On the other hand, according to Gish and Wait's measurements, droplets above 25,000 feet might be expected to carry negative charges. Moreover, it is apparent from measurements like those reported by J. J. Nolan and P. J. Nolan [12] and by Rossmann [11] that rather large excursions of positive and negative ion abundance occur whenever precipitation is present For example, the Nolan measurements at the surface show that n_+/n_- varied from 1.01 to 0.16, according to the character of the precipitation. It is fair to infer that gross fluctuations of ionic abundance induce reflected changes in the conductivity ratio and thus diffusion modifies the free charge carried by the falling droplets. In typical regions of the lower atmosphere, it seems proper to assume that λ_+/λ_- will approximate 1.35 throughout. This value has been adopted in preparing the lower curve in Figure 1.

Since large fluctuations in the ionic conductivity ratio are sometimes observed, the upper curve of Figure 1 is plotted showing the free charge carried by droplets when the relative conductivity for the positive and negative ions is 10. Such charges

probably approach the maximum that would be transferred to droplets by ionic diffusion in the free atmosphere. These values closely approximate those adopted in the theory of thunderstorm electricity worked out in reference [1].

The excess positive conductivity measured in the lower atmosphere implies that droplets there would be positively charged. Neutralizing mechanisms are at work, however. Since large numbers of droplets will selectively absorb positive ions, the positive conductivity will thereby be reduced. If new air and new ions were not constantly brought into the precipitating regions, the positive and negative conductivities would finally approach equality. Selective charging would then vanish. However, it is well known that all precipitation processes involve the mixing of large volumes of air. Therefore, ionic charges transported out of the region by precipitation will be replaced by new ions swept in with the air from adjacent areas and by new ion pairs formed by cosmic rays or radioactivity.

Conclusion.

The diffusion of ions onto atmospheric particles is a universal process, taking place wherever appreciable ionic conductivity is present. The occurrence of large numbers of droplets in the free atmosphere provides an extensive "wall" surface upon which the ions may selectively diffuse. It is not surprising, therefore, that important electrical effects are frequently observed to accompany various types of precipitation. The magnitude of such ionic charging is great enough to describe the electrification of quietly falling rain droplets and may be of marginal significance in thunderstorm electricity. However, other electrifying influences, such as the C. T. R. Wilson effect, probably are present in active thunderstorms and these must be quantitatively evaluated before final decisions may be reached as to their relative importance.

References

[1] R. Gunn, The electricity of rain and thunderstorms, Terr. Mag., **40**, 79-106 (1935).
[2] R. Gunn, Diffusion charging of atmospheric droplets by ions and the resulting combination coefficients, J. Met., **11**, 339-347 (1954).
[3] B. B. Phillips and R. Gunn, Measurements of the electrification of spheres by moving ionized air, J. Met., **11**, 348-351 (1954).
[4] R. Gunn and G. D. Kinzer, The terminal velocity of fall for water droplets in stagnant air, J. Met., **6**, 243-248 (1949).
[5] J. A. Chalmers and F. Pasquill, The electric charges on single raindrops and snowflakes, Proc. Phys. Soc., **50**, 1-15 (1938).
[6] F. J. Scrase, Electricity of rain, London, Met. Office, Geophys. Mem., **9**, No. 75 (1938).
[7] K. L. Sherman, Atmospheric electricity at the College-Fairbanks Polar Year Station, Terr. Mag., **42**, 371-390 (1937).
[8] G. R. Wait, Investigation of electrical properties of atmosphere, Air Force Contract No. AF19-(604)-251, p. 7 (1953).
[9] O. H. Gish and G. R. Wait, Thunderstorms and the earth's general electrification, J. Geophys. Res., **55**, 473-484 (1950).
[10] R. C. Callahan, S. C. Coroniti, A. J. Parziale, and R. Patten, Electrical conductivity of the air in the troposphere, J. Geophys. Res., **56**, 545-551 (1951).
[11] F. Rossmann, Luftelektrische messungen mittels segelflügzeugen, Ber. D. Wetterdienst US-Zone, No. 15 (1950).
[12] J. J. Nolan and P. J. Nolan, Observations on atmospheric ionization at Glencree Co., Wicklow, Proc. R. Irish Acad., A, **40**, 11-59 (1931).

NOTE ON THE OCCURRENCE OF WORLD-WIDE S.S.C.'S DURING THE ONSET OF NEGATIVE BAYS AT COLLEGE, ALASKA*

BY JAMES P. HEPPNER†

California Institute of Technology, Pasadena, California

(Received June 14, 1954)

ABSTRACT

World-wide sudden commencements which appear during the night hours at College, Alaska, are found to occur most frequently during the onset, or decreasing H stage, of negative bays. As this stage of magnetic disturbance accompanies a distinct change from homogeneous to rayed aurora, it is suggested that s.s.c.'s have an atmospheric source which is related to sudden changes in auroral activity.

In the course of studying the relationships between nightly geomagnetic variations and aurora, the writer encountered some striking cases in which s.s.c.'s (sudden commencements followed by a period of storminess) occurred when homogeneous arcs broke into brilliant rayed forms at College, Alaska. The number of s.s.c.'s which occurred when very detailed aurora observations were being taken at College during 1950-1952 was too small to test this coincidence statistically. However, an indirect test is possible. As previously demonstrated [see 1 of "References" at end of paper], the change from homogeneous arcs to rayed aurora at College is accompanied by the onset of a negative bay. Thus, if there is a statistical coincidence between s.s.c.'s and the onset or first stage of negative bays, one may infer that there is also a statistical coincidence between s.s.c.'s and the change from homogeneous arcs to rayed aurora.

For this purpose, disturbance of the horizontal component at College was divided into eight stages, as illustrated in Figure 1. College magnetograms were obtained from the United States Coast and Geodetic Survey for all days on which an s.s.c. was reported in the *Journal of Geophysical Research* by two or more stations for the period January 1951 through June 1953. The local times of the s.s.c.'s were marked on the magnetograms and classified as occurring in the eight stages as follows:

(1) A period when H was comparatively quiet
(2) The onset or increasing H stage of a positive bay
(3) A period of significant $+ \Delta H$ disturbance
(4) The decay or decreasing H stage of a positive bay
(5) A period separating a positive and negative bay
(6) The onset or decreasing H stage of a negative bay

*Contribution No. 701, Division of Geological Sciences.
†Now at the Naval Research Laboratory, Washington 25, D.C.

(7) A period of large $-\Delta H$ for the particular night
(8) The decay or increasing H stage of a negative bay and the interval of $+\Delta H$ which usually follows a negative bay [for more information on this interval of $+\Delta H$, see reference 1]

S.s.c.'s which did not fit this classification were designated Group (9). In some cases, the s.s.c. was located where it was equally well classified in two groups. For example, the H component may decrease directly from large $+\Delta H$ to large $-\Delta H$, thus eliminating Group (5); an s.s.c. occurring at this time is equally well classified in Groups (4) and (6). Many other situations are obvious. To distinguish between the clearly-defined cases and those where two classifications were possible, the classifications were designated "definite" and "indefinite." For the "indefinite" cases, the alternative groups were each given the value one-half. A distinction between s.s.c.'s reported by five or more stations and those reported by two, three, or four stations was also made, as indicated in Figure 1. To distinguish between the often disturbed "night" hours and the often quiet "day" hours, the corre-

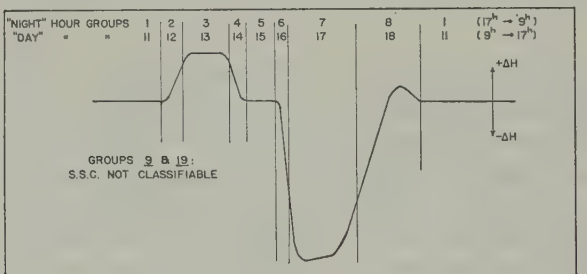

GROUPS (NUMBER OF OCCURRENCES IN 1)

S.S.C.

"NIGHT" HOURS (17h → 9h)	GROUPS	1	2	3	4	5	6	7	8	9
S.S.C. REPORTED BY	DEFINITE	3	6	0	0	0	7	0	0	1
5 OR MORE STATIONS	INDEFINITE	3	1½	½	1	0	1½	0	½	3
S.S.C. REPORTED BY	DEFINITE	2	2	1	1	0	7	0	1	3
2, 3, OR 4 STATIONS	INDEFINITE	0	1	1½	0	2½	3	1½	1	½
	TOTAL	8	10½	3	2	2½	18½	1½	2½	7½

S.S.C.

"DAY" HOURS (9h → 17h)	GROUPS	11	12	13	14	15	16	17	18	19
S.S.C. REPORTED BY	DEFINITE	13	3	0	0	0	0	0	0	1
5 OR MORE STATIONS	INDEFINITE	½	½	0	0	0	½	0	0	½
S.S.C. REPORTED BY	DEFINITE	2	1	0	0	0	0	0	0	0
2, 3, OR 4 STATIONS	INDEFINITE	1	0	0	0	0	½	0	0	½
	TOTAL	16½	4½	0	0	0	1	0	0	2

S.I.

"NIGHT" HOURS (17h → 9h)	GROUPS	1	2	3	4	5	6	7	8	9
S.I. REPORTED BY	DEFINITE	1	3	2	1	0	4	1	2	0
5 OR MORE STATIONS	INDEFINITE	½	0	0	0	0	2	1	0	1½

S.I.

"DAY" HOURS (9h → 17h)	GROUPS	11	12	13	14	15	16	17	18	19
S.I. REPORTED BY	DEFINITE	4	1	0	0	0	1	1	2	1
5 OR MORE STATIONS	INDEFINITE	0	0	0	0	0	½	0	0	½

FIGURE 1

sponding groups, (11) through (19), were used for s.s.c.'s occurring between 09h and 17h. Sudden impulses not followed by a period of storminess, s.i.'s, were

classified in the same manner for cases where they were reported by five or more stations.

From the results tabulated in Figure 1, it is obvious that the number of occurrences of s.s.c.'s during the onset or decreasing H stage of negative bays is large compared to the other stages of a typical disturbance. As this stage (Group 6) is consistently associated with the change from homogeneous arcs to rayed aurora, a relationship between this change and sudden commencements is clearly indicated. The s.s.c.'s of Group (6) are found either at the origin of a negative bay or during a rapid decrease in H; hence the time relationships do not suggest that the s.s.c. precedes the change in aurora. In specific cases where detailed aurora observations are available, the s.s.c. appears during the change. A concentration of occurrences in Groups (2) and (12) would be expected from the usual description of the initial phase of a magnetic storm [see reference 2]. The writer has not found a remarkable coincidence between changes in auroral activity and the s.s.c.'s of Group (2); in most cases, an arc or glow is already present above the north horizon at the time of a Group (2) s.s.c., and the auroral activity after this s.s.c. follows the same general pattern as on other nights. The concentration of occurrences in Groups (1) and (11) illustrates that many s.s.c.'s are not followed by an initial phase of $+\ \Delta H$ disturbance. The number of occurrences in Groups 3-13, 4-14, 5-15, 16, 7-17, and 8-18 is relatively insignificant. The distribution of occurrences of s.i.'s appears quite similar to that of s.s.c.'s.

Previous studies of the diurnal variation of s.s.c.'s have led to the conclusion that any local time dependence is very slight, if present at all [see reference 3]. As the onset of a negative bay may occur any time between roughly 22^h and 07^h, it is apparent that a coincidence between the onset and s.s.c.'s would not appear as a diurnal variation of the type previously sought. The possibility that the coincidence is a consequence of the number of hours per night of Group (6) may be readily dismissed by merely inspecting the magnetograms. The number of hours per night which could conceivably be designated Group (6) rarely exceeds three; in the majority of cases, this group occupies less than two hours and in many cases less than 30 minutes. An attempt has been made to see if there is any particular geographical distribution of stations reporting the s.s.c.'s of Group (6). A tendency for the stations to be concentrated in Europe is present, but is of doubtful significance considering the over-all concentration of stations in that region.

From the coincidence indicated here, it seems reasonable to speculate that a high percentage of the s.s.c.'s occurring during the "day" hours, 09^h to 17^h, at College may coincide with Group (6) at a station located roughly 12 hours from College at the same geomagnetic latitude. If this proves true, an extension of the study to other stations offers the possibility of establishing the indicated relationship between sudden commencements and aurora. A relationship in which s.s.c.'s and s.i.'s depend on the previous existence of homogeneous arcs suggests that sudden commencements have an atmospheric origin in the auroral zones. The world-wide, but variable, character of sudden commencements might then be attributed to a transient current traveling in the most conducting regions of the ionosphere. This transient could be expected from a sudden reversal or increase of potential in the auroral zones.

References

[1] J. P. Heppner, J. Geophys. Res., **59**, 329-338 (1954); for a complete presentation, see, Ph.D. thesis, California Institute of Technology (1954).
[2] S. Chapman and J. Bartels, Geomagnetism, Oxford, Clarendon Press (1940).
[3] V. C. A. Ferraro, W. C. Parkinson, and H. W. Unthank, J. Geophys. Res., **56**, 177-195 (1951).

SOLAR CORPUSCLES RESPONSIBLE FOR GEOMAGNETIC DISTURBANCES*

BY JEAN-CLAUDE PECKER AND WALTER ORR ROBERTS

High Altitude Observatory, Boulder, Colorado

(Received June 21, 1954)

ABSTRACT

A qualitative hypothesis is given that attributes recurrent "*M*-region" geomagnetic disturbances to the arrival at the earth of solar corpuscles that have been gathered into beams by the deflecting action of coronal-region fields, presumably magnetic, associated with centers of heightened solar activity. The hypothesis identifies the source of solar corpuscles that produces *M*-region magnetic disturbances with "quiet areas" of the solar surface. A related hypothesis associates non-recurrent magnetic storms, the greatest ones, with a different solar corpuscular source, found in the active region itself.

I. INTRODUCTION

Numerous investigators have given evidence for the solar origin of geomagnetic urbances. About ten years ago, C. W. Allen [see 1 of "References" at end of per] published an important paper that discussed the solar origin of geomagnetic urbances. His paper contained the principal ideas that we have developed e; we regret only that we have pursued these ideas, most of them reached ependently, so many years later, instead of doing so at once following Allen's portant analysis, as it should have been possible to do.

Most authors have suggested corpuscular emission from the sun as the cause geomagnetic disturbances, though some, notably Wulf and Nicholson [2], have ght to explain the effects by radiation alone. Many important facts have erged from past work. Among the most interesting is the marked difference ween the time of magnetic disturbance near central meridian passage (CMP) active solar regions for great magnetic storms in years near sunspot-activity ximum as compared with the lesser but still substantial magnetic storms that pen near sunspot minimum. This material is well discussed by Allen. Par-ularly baffling has been the origin of the latter magnetic disturbances, which erally fall into 27-day recurrent series, but their formation seems nonetheless pear no simple relationship to the formation or decline of centers of visible solar ivity.

Allen clearly shows, for the 27-day recurrent disturbances, that approximately

*This research was sponsored in part by the Geophysics Research Directorate of the Air ce Cambridge Research Center, Air Research and Development Command, under Contract 19(604)-969.

three days after CMP of active centers characterized by sunspots, bright calciun and hydrogen plages, strong coronal-line emission, and related phenomena, ther is generally a definite diminution of geomagnetic disturbance ratings, presumably signifying a decrease in the intensity of the solar corpuscular stream at the earth

Our work reports the results of a detailed study of the period July 1952-July 1953, a time near minimum solar activity when 27-day recurrent M-region dis turbances dominated the geomagnetic disturbance ratings. The work has led u to formulate a qualitative hypothesis for the origin of solar M-regions, and complementary hypothesis for the formation of other geomagnetic disturbances We relate both of these, moreover, to the electron corona (the K-component) o the sun in a fashion concordant with an earlier explanation we have given for th changes of shape of the principal features of the electron corona with changes o solar activity [3]. Both of these hypotheses were implicit in the conclusions of Allen We hope soon to extend our analysis to other periods, and to make other tests o our hypotheses.

We stress, at the outset, that it appears to us very likely that the phenomen of the aurora, sporadic magnetic storms, and the M-regions, as well as certain aspects of cosmic-ray and ionospheric changes, can all be ascribed to solar cor puscular emission. However, it seems to us that the following properties of th solar sources of corpuscular emission must be considered: (1) The velocity of th ejected particles; (2) their stream density or total energy; (3) the location of th sources, of which there may be many at one time; (4) the geometry of the deflectin magnetic fields; and (5) the state of ionization of the stream particles. The difficult of explaining all of these terrestrial phenomena in a single homogeneous pictur results in part from the diversity of these variable factors, and from the imper fectness of our knowledge of them. In the following work, we have endeavored t deal with a simple solar situation, in order to confront at one time as few as possibl of the variable factors.

II. MAGNETIC DISTURBANCES IN 1952-53

The sun's activity during this period was moderate, confined to well-define regions, and well observed. Moreover, there were excellent cases of well-isolate and pronounced recurrent magnetic disturbances within the period.

We first attacked the question of the distribution of dates of geomagneti disturbance with respect to the CMP dates of centers of heightened solar activity To fix the presence and position of a solar active region, we used the High Altitud Observatory maps of solar activity [4]. These give much weight to the location an intensity of the emission corona, which generally maximizes over active region marked by bright plages, flares, active sunspots, and other disturbed-sun characte istics.

Our first result is given in Figure 1*A*. There we present the frequency of occur rence of "internationally quiet" (Q days) or "internationally disturbed" (D days days in geomagnetism occurring N days of solar rotation away from (either befor or after) CMP of the nearest active center. The pronounced maximum of Q day about three days after CMP of active centers suggests that the corpuscles re

onsible for geomagnetic disturbances were less numerous then, or that there s a "cone of avoidance" above the active center that reached the earth at two d one-half to three days after CMP. The *D*-curve minimum similarly expresses e lesser frequency with which disturbances occurred within this cone of avoidance. ie *D* curve involves 58 days and the *Q* curve 56, and both include 46 active regions.

The frequencies given in Figure 1*A* were not the actually observed frequencies occurrence of *Q* and *D* days, but were values which, for the following reason, had corrected. If we had plotted observed frequencies as a function of the mber of days *N* from an active region, these frequencies would have gradually clined with *N* because of the distribution of active regions on the sun; there re in 1952-53 very few cases of any region of the sun being so isolated that there s no other region within, for example, eight or ten days of solar rotation. Thus,

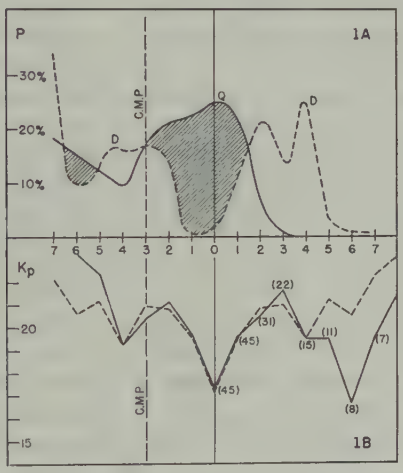

g. 1—(*A*) Distribution of magnetically quiet, *Q*, days and magnetically disturbed, *D*, days with pect to the central meridian passage of active solar regions. *N* is given in days of solar rotation m the assumed center of the nearest cone of avoidance, which is considered to reach the earth proximately three days after CMP of the active region. Frequencies of occurrence *P* are given percentages of all days, so that the mean values for *Q* and *D* are about 15 per cent.

) Average planetary geomagnetic disturbance index K_p corresponding to different angular tances from active solar regions. The angular distances from solar regions are given in terms of e number of days of solar rotation *N* before or after the assumed center of the nearest cone of oidance sweeps the earth, which is considered to be approximately three days after CMP of the active region.

corrected frequencies would drop to 0 at some value of *N*, but this drop would t signify an active-center-induced variation of corpuscular streams, which is iat our analysis was designed to discover. Thus, we corrected the observed day and *D*-day frequencies by dividing them by the observed frequencies with iich any solar longitude occurs *N* days of solar rotation away from an active nter.

Figure 1*B* represents the same facts shown by the above figures, but in different d perhaps more useful fashion. There we have given the average planetary omagnetic *K*-index, K_p, for *N* days before and after the assumed center of the

nearest cone of avoidance was at the earth. The assumed centers of the cones of avoidance we took to sweep the earth three days after CMP of the active centers.

This method of analysis has the advantage of safely separating out the effects of overlapping periods of activity. It is an improvement over the Chree-type superposed-epoch analysis used earlier by Shapley and Roberts [5] and by Barbara Bell (unpublished). Both of these earlier applications, as well as recent unpublished superposed-epoch analyses of Trotter and Roberts, agree in showing a definite minimum in geomagnetic disturbance ratings three days after CMP of the active regions. In fact, this minimum was the only common feature of all of these superposed-epoch analyses, in spite of the fact that Shapley and Roberts paid little attention to the minimum and much to the maximum of geomagnetic disturbance four or five days before CMP, a feature that does not show up consistently in M-region data for all periods now analyzed.

Figure 1B clearly shows the minimum in K_p , corresponding to the center of the cone of avoidance, and also the rather definite maxima symmetrically located at about ± 2.5 days from the minimum. Farther away from the minimum, beyond five days, the statistics become unreliable because of the small numbers of values involved in the means, as shown in parentheses beside each point. This result suggests that either side of the cone of avoidance is a region where the corpuscular stream density rises above the values it would have had in the absence of the cone of avoidance. This tempts one to conjecture that the deficiency of particles over the active center has been compensated at the fringes of the cone of avoidance.

We next attempted to find out the effect of two moderately-spaced active centers, on the expectation that the interaction of two cones of avoidance would result in the formation of a stronger corpuscular beam half-way between the two active centers. Figure 2 exhibits the results of this analysis for the year period. Here we have again plotted mean K_p as ordinates. The abscissae, however, represent

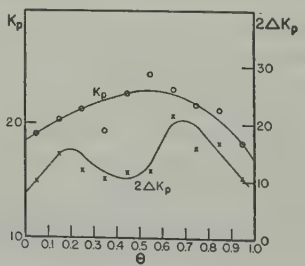

FIG. 2—Average planetary geomagnetic disturbance index K_p plotted as a function of the fractional separation between pairs of active centers. The fractional separations, θ, range between $\theta = 0$ and $\theta = 1$, corresponding to the times when the assumed centers of the cones of avoidance associated with the active centers sweep the earth, three days after CMP's of the centers. The lower curve gives the dispersion of the K_p values from the mean K_p corresponding to each value of θ.

tenths of the angular distance in longitude between active centers on the sun. For the abscissae, we have, in all cases, assumed the relevant dates to be the active-center CMP dates plus three days. Thus, the abscissae range from $\theta = 0$ to $\theta = 1$ where $\theta = t - t_1/t_2 - t_1$, t being the date studied, and t_2 and t_1 are the

lates of CMP plus three days of the active regions making up the pairs. Thus, t s always taken between t_2 and t_1 . The active-center pairs were always taken in pposite hemispheres of the sun to assure that on the average they were of opposite let magnetic polarity. We feel some doubt that this assumption of opposed olarities is entirely safe. Thirty-six pairs of regions entered the analysis, with pacings ranging from two to 25 days.

Obviously, we expected to find, as we did find, minima in K_p corresponding o each of the active centers and thus to $\theta = 0$ and $\theta = 1$, and the maximum at $= 0.5$ was also expected, even if no actual physical interaction of active-center airs were involved. But we also found another result that may be of significance, hough it is weakly established. The dispersion of K_p values entering the means or $\theta = 0$, 1, and 0.5 was small, while for values of θ near 0.25 and 0.75 the dis- ersion of values was larger. The curve marked ΔK_p expresses the dispersion alues quantitatively, a point the significance of which we discuss below.

III. MAGNETIC AND SOLAR DATA, 6 AUGUST–3 SEPTEMBER 1953

We recently made a careful examination of solar and geomagnetic phenomena or the month period from 6 August through 3 September 1953, in connection vith an intensive group-study project sponsored by the Air Force Cambridge

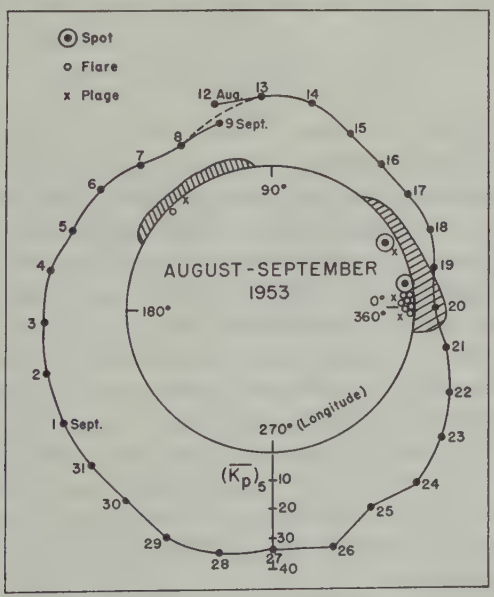

IG. 3—Solar and geomagnetic disturbance data for August-September 1953. The circle represents chematically the different solar longitudes presented to the earth on successive dates for this eriod. The longitudes of occurrence of the principal phenomena of solar activity for the period re shown. The shaded zones represent schematically the relative intensities of the green coronal mission regions occurring during the period. The line surmounting the circle gives in polar repre- entation the mean K_p values for the dates shown. The scale of dates is displaced three days with espect to the solar longitudes shown, in order to place the centers of the assumed cones of avoid- ance at the earth above their corresponding active solar centers.

Research Center. The period had been chosen for special solar-terrestrial analysis because we felt that it exhibited clear-cut confinement of substantial solar activity to a limited region of the sun's disk. It offered several days when the solar disk was almost perfectly free of signs of activity. Moreover, detailed auroral, cosmic-ray, geomagnetic, ionospheric, weather, and solar observations were available for study—a study, by the way, that suggests the kind of analysis that will be possible with data from the forthcoming International Geophysical Year.

This particular period provides a confirmation of the above statistical studies. Figure 3 represents relevant solar and geomagnetic data for the period. Two pronounced centers of solar activity were in evidence, at the heliographic longitudes shown. The corresponding CMP dates appear in the inner portion of the diagram. Mean coronal intensities in λ 5303 are shown, as indices of the active-center location, together with symbols to represent sunspots, solar flares, and bright plages. The polar graph above the solar disk represents the five-day mean K_p, suggested by Pecker and Roberts [6], on the basis of recent study, as the optimum for such analyses. The K_p graph was displaced three days with respect to the CMP dates shown. Clear minima correspond to the active regions, suggesting cones of avoidance above them, with maxima between. The large magnetic disturbance that began on August 23 had a sudden commencement and reached a rather disturbed level, even though the solar disk was quiet, and it is highly unlikely that the sudden commencement was associated with a solar flare.

IV. OTHER OBSERVATIONAL DATA

C. W. Allen's analysis [1] revealed clearly the same cone-of-avoidance effect when magnetic disturbances within the sequence of 27-day recurrences were considered. It also revealed that for non-recurrent magnetic disturbances there was, instead of a minimum, a maximum a few days after CMP of the associated active center, which he attributed to solar corpuscles from the active center.

To explain the origin of the magnetic disturbances, both recurrent and non-recurrent, Allen appealed to the observable features of the white-light coronal streamers that are visible as a result of the scattering of photospheric light by free electrons in the streamers. Eclipse observations have failed to reveal conclusively, however, the directions of the coronal streamers in space, but have indicated their orientation only in the plane of the sky. Thus, no general agreement has been reached as to the locations of sources of these streamers on the surface of the sun. The details of their geometry have remained a mystery, in spite of the important clues in Allen's work, and the explicit suggestion of Allen that they are deflected away from sunspot regions.

K. O. Kiepenheuer suggested [7] in 1947 that solar filaments, far removed from active centers, were the source of the corpuscular radiation responsible for the 27-day recurrent disturbances. Active regions, he postulated, could deflect these particles and interfere with the correlation. He developed a hypothesis consistent, in the main, with Allen's results and with additional observations of his own. We feel that a simpler explanation along the lines suggested by Allen and further development below is possible. We shall, nevertheless, later evaluate the results

of comparison of geomagnetic activity with filaments, and with active regions alone, for the same observing periods.

Another group of observations, collected by Wulf and Nicholson [2] and discussed by them and by Waldmeier [8], fits coherently into this picture, in spite of the rather different interpretations given it by these other authors. Figure 4 is reproduced from the paper of Waldmeier, who in turn reproduced part of it from

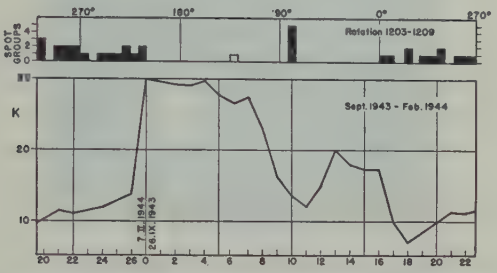

FIG. 4—Mean sunspot activity at different solar longitudes for five rotations, above; corresponding mean geomagnetic disturbance ratings, below. In this Figure, taken without change from Waldmeier [reference 8], the geomagnetic disturbance data have been displaced in time by two days, instead of the three days used elsewhere in this paper.

Wulf and Nicholson. However, he displaced the geomagnetic character curve by two days, instead of three, as suggested by our work above. The correspondence of minima with active regions measured by sunspots is evident. The maxima, on the other hand, appear over quiet regions, as expected from Allen's and our own work.

A still further group of highly interesting observations is available. Becker and Denisse [9] found that the CMP of a solar radio-noise-producing sunspot is followed a day or two later by a substantial rise of mean geomagnetic disturbance ratings. This suggests that the radio-noisy sunspots produce large numbers of active-center corpuscles. On the other hand, these authors show that radio-quiet sunspots are followed by a pronounced minimum in geomagnetic disturbance, corresponding to the cone-of-avoidance effect for weak corpuscle-producing sunspots. Other authors have, of course, shown that active centers, particularly those with large and frequent solar flares, are likely to produce radio noise and to have particle streams associated with them (Payne-Scott and Little [10]; Dodson, Hedeman, and Owren [11]; Wild, Murray, and Rowe [12]).

Recently, we developed some new notions about the relationship of the shape of the corona to the extensive space-streamers assumed responsible for geomagnetic disturbance [3]. We postulated the existence of deflecting fields diverging from active centers, of the general type suggested by the above cone-of-avoidance concept. From this, we concluded that one could easily account for the apparent changes of coronal shape with phase of the sunspot cycle. Figure 5 is a schematic drawing of coronal forms found in the presence of active centers, on the left, and in their absence, on the right. The Figure is a somewhat idealized composite from many eclipse observations. It was to explain these forms that we developed our concept of the formation of the electron-scatter component (K-component) of the

white-light corona. In our view, the electron corona during low solar activity is formed by the deflection of ions fed into the corona from small spicules distributed over the whole surface of the sun. During high activity, the active centers deflect these ions in the different directions shown, to produce the observed forms. The

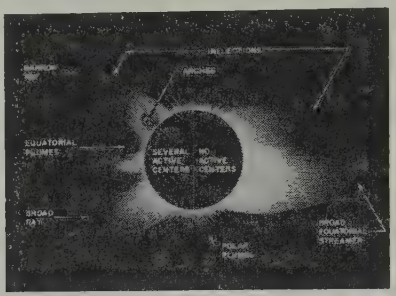

Fig. 5—Schematic drawing of the electron corona as seen at eclipse, for a period with no active regions near the solar limb, and for a period with several active centers at the limb. The white-light streamers shown are assumed responsible, when they sweep the earth, for geomagnetic disturbances. No dense streams of active-region corpuscles are shown; streamers shown are principally of the type that originate all over the solar surface.

concentration of all-surface corpuscles to the solar equatorial plane, and thus to the general direction of earth, at times of low solar activity is also illustrated by the Figure.

V. THE ORIGIN OF GEOMAGNETIC DISTURBANCES

The above considerations led us to develop a qualitative hypothesis regarding the origin of the solar corpuscular streams responsible for geomagnetic disturbances. We stress that the ideas implicit in this hypothesis have, for the most part, been stated at one time or another by previous authors. We assumed, first, that geomagnetic disturbance is produced by the arrival at earth of solar corpuscles. We then concluded that there are two different kinds of solar sources of corpuscles, as follows:

(a) *Small jets of corpuscles, distributed in a fine network all over the entire solar surface, and presumably associated with chromospheric spicules or photospheric granules*—These jets, in the absence of deflecting fields, would send radial streams of corpuscles in all directions, and, of course, the streams would always be present, regardless of the level of sunspot activity. The corpuscles are undoubtedly principally protons and electrons, making up ion streams that are electrically neutral as a whole.

(b) *Larger irregular streams of ions associated with active regions, and probably most intense at the time of solar flares*—Such streams are probably always associated with active centers, but it is likely that not all centers have strong streams of this type present at all times. There is probably a high dispersion of particle velocities and stream energies for this type of corpuscular stream.

In the absence of any active centers on the sun, the corpuscular emission would be confined to the first type, and would result in a steady stream of particles into the solar atmosphere. In accord with our earlier hypothesis [3], the general magnetic field of the sun would deflect large numbers of these particles, however, as shown on the right of Figure 5, into directions near the equatorial plane of the sun. The resulting distribution would not produce day-to-day changes at the earth, as the sun rotates with its roughly 27-day period, because of the uniformity of the distribution of ions in the solar equatorial plane.

If, however, an active center does exist, it will be quite near the equator. If we postulate that it possesses an ion-deflecting field, presumably magnetic, extending well above the active region, it is possible to predict space distributions of corpuscles that suggest the main features observed for *M*-regions. Such fields would destroy the uniformity of distribution in the equatorial plane, and, in particular, would reorganize the ion flow so as to produce regions of deficiency at solar longitudes above the active center.

Figure 6 illustrates the type of ion deflection we suggest above centers of activity. The arrows represent the trajectories of the ion jets that leave the solar surface near the center of activity, and are deflected by the active-center field. If the active center has a field with approximately the geometry shown, there will be a

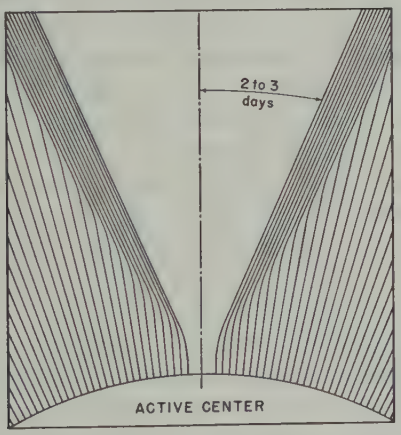

FIG. 6—A highly schematic representation of the suggested trajectories of spicule-type particles emitted from the solar surface in the vicinity of an active center, and assumed responsible for geomagnetic disturbance of *M*-region character. Note the cone of avoidance above the active region, and the compensation in particle density at the edges of the cone.

cone of avoidance of four to six days in angular width. If the fields above the active centers are magnetic, and if it can be assumed that the ion flow is parallel to the field, then the field shape near the active region must diverge as from one pole of a long bar-magnet. This is the shape we assumed earlier [3]. It is also that suggested by the mean trajectories of sunspot prominences, which usually are found converging towards a center of activity. And it is the shape found by Allen for the "equatorial plumes" in the white-light corona.

The jets, which we shall assume are identical with spicules, thus produce, as

shown, a concentration of ion density in directions corresponding approximately to the edges of the cone of avoidance. Thus, a single center of activity in an otherwise quiet sun should produce a cone of avoidance, the terrestrial consequence of which is several days of lowered geomagnetic disturbance, flanked by two periods of geomagnetic activity greater than the mean for the whole solar rotation, and a longer period with a more or less uniform level of disturbance. That such a situation actually exists is strongly suggested by Figures 1*A* and 1*B*, as well as by the work of others described above.

We consider it likely that at some distance above the center of activity, as proposed earlier [3], the kinetic energy of the ion jets is sufficient to overcome the magnetic field, so that the guiding effect of the active-center field controls the ion flow only near the center. After the ions have reached distances of the order of a solar radius or so, they are probably governed otherwise—perhaps held in self-focused beams, as suggested by Bennett and Hulburt [13], or otherwise [14]. It seems likely that the three-day lag between the CMP of the active center and the receipt of the center of the cone of avoidance at the earth represents a three-day transit time for the solar corpuscles.

A further result of Allen may be understood from this picture. If the angle of aperture of the cone of avoidance is assumed to vary with the history of the active center, being small at the start and the finish, and large in the middle of the lifetime of the *M*-regions, then the strong tendency of Allen's mid-sequence geomagnetic storms to show a minimum, and the lesser tendency of the earliest and latest ones of the series to do so, are explained. This is quite reasonable, since the angular width of the cone probably corresponds to the strength of the field, and this probably is weakest at the start and end of a series.

Moreover, the dispersion curve of Figure 2 is explained. If the angle of the cone of avoidance is sometimes large and sometimes small, then at the mean width of the cone one will find, statistically, a large dispersion of K_p corresponding to the fact that at such angles there is the change either to the reduced ion density just inside the cone, or the increased ion density just outside the cone. Over the center, on the other hand, the values will be consistently low (providing the center is not a strong corpuscle producer, and this was the case in 1952-53); at the mid-point between the two centers, similarly, the ion density will be consistently high.

Photographs taken of the white-light corona at eclipse reveal electron corona distributions that in the main are entirely consistent with this picture. However, over active centers there are generally found to be, in the first few tenths of a solar radius, well-marked maxima of ion density, corresponding in position also to the emission corona maxima found in the regions. At first, this seems discordant. If, however, the deflecting fields of the active center are not at large angles to the radius just at the solar surface, as seems likely, the cone of avoidance will not be very marked until heights of the order of a radius of the sun are reached. Moreover, if the center itself is *also* a producer of ions, as seems most likely, then the near-to-the-sun maxima in active centers are rather to be expected. It is the divergence of the deflecting fields, above the active centers, that causes a steeper height gradient of ion density over the center than elsewhere. The effect of an active center is thus very like that of the general deflecting fields found over the poles of the sun, save

that at the poles the only producers of ions are the surface-distributed spicule jets.

The concentrated jets from active centers, diverse evidences suggest, are often very intense, and they are highly variable with time. Their particles fill in the cone of avoidance. Presumably they are of higher velocity than the spicule ions, and their disruptive effect on the field is also probably far greater, and less predictable. Ions from this source are considered, in our hypothesis, to be responsible for the greatest magnetic storms, and for most of the non-recurrent storms so frequent during periods of great solar activity. It seems attractive to consider, as well, that the same ions are responsible for the radio noise of noise-producing sunspots [9], perhaps by producing plasma oscillations. At times of solar flares, the ion production is probably most intense, and it may even be that appreciable numbers of active-center ions are ejected with cosmic-ray velocities.

The active-center ions thus should have just the CMP relationships found by Allen, and known for some time for the great sunspot regions. The great auroral displays, ionospheric upsets, and magnetic storms, like that of Easter 1940, fall into this category, with the maximum effects usually about one day after CMP of the responsible regions.

VI. RECOMMENDATIONS FOR FUTURE WORK

The work we have done was confined to a small period of time chosen for extreme simplicity of phenomena. However, the working hypotheses are capable of numerous further tests. Simplest, of course, is the extension of the analysis of Figures 1 and 2 to other periods, and to extend this type of analysis to the data used by Allen. A great deal of benefit can probably also be derived from study of individual case histories now that detailed solar observations are available, and we plan to undertake studies of this nature. The work should now be pursued with vigor, because separation of the effects of the two types of solar corpuscles, if these suggestions stand the test of time, will be most important to the work of the International Geophysical Year.

Most important, however, is for further work to be done to explain when *M*-region geomagnetic storms will occur. We have suggested that when they do occur there will be a rather quiet sun, and also active centers with deflecting fields, but without strong ion production. However, such conditions occasionally occur without strong *M*-region storms. Probably many suitable ion streams never strike the earth. However, further work must be done before we are able to predict with any accuracy the rise and decline of individual *M*-region disturbances from the location and now-known properties of the associated active regions.

Extension of the type of analysis suggested by Becker and Denisse is most important. It seems likely that additional test and development of the hypothesis can be made with the aid of these powerful radio-astronomy techniques. Knowledge of the magnetic fields of the various active centers is also of great importance, so that routine observations of the sort recently published by Babcock [15] are of highest interest. Radio-astronomical efforts to study coronal-region magnetic fields, as suggested by Payne-Scott and Little [10], also deserve attention.

Direct observations of the electron corona outside of eclipse by means of the polarization of scattered white light are also of high importance. From such

measures, three-dimensional models of electron corona streamers should be possible, as they are not possible from eclipse observations. They should be a powerful test of the hypothesis that M-region streamers are deflected away from the axes of active regions, in contrast to the suggestions made by some authors that M-region corpuscular streams originate over the locations of active centers of the emission corona or of sunspots. To be useful, such measures of the electron corona must be carried to heights of at least one solar radius. Present coronagraphic and electronic techniques suggest that such measurements are feasible, and we have proposed that they be undertaken for the International Geophysical Year.

The importance of solar corpuscles in terrestrial phenomena is rapidly becoming evident. The effects are of great significance in auroral, ionospheric, and geomagnetic phenomena, as well as in newer fields. Even in meteorology, as shown by Shapiro [16], there is now evidence for effects of practical importance. It seems reasonable, therefore, to concentrate great effort on understanding the origin and behavior of this form of solar emission.

VII. ACKNOWLEDGMENTS

We acknowledge with appreciation the many discussions we have had with our colleagues, Drs. Joseph H. Rush, R. Grant Athay, and Donald E. Billings.

References

[1] C. W. Allen, Mon. Not. R. Astr. Soc., **104**, 13 (1944).
[2] O. R. Wulf and S. B. Nicholson, Pub. Astr. Soc. Pacific, **60**, 37 (1948).
[3] W. O. Roberts, R. Grenchik, and D. E. Billings, Astr. J., **58**, 225 (1953).
[4] D. E. Trotter and W. O. Roberts, Quarterly summaries of solar activity, Nos. HAO-NBS 10, 13, 14, 16, 17, 19, 21, and 22 (1952-1953). [Available from High Altitude Observatory, Boulder, Colorado.]
[5] A. H. Shapley and W. O. Roberts, Astropy. J., **103**, 257 (1946).
[6] J.-C. Pecker and W. O. Roberts, Science, **120**, 721 (1954).
[7] K. O. Kiepenheuer, Astrophy. J., **105**, 408 (1947).
[8] M. Waldmeier, Zs. Astrophy., **27**, 42 (1950).
[9] U. Becker and J. F. Denisse, J. Atmos. Terr. Phys., **5**, 70 (1954).
[10] R. Payne-Scott and A. C. Little, Aust. J. Sci. Res., A, **4**, 508 (1951); **5**, 32 (1952).
[11] H. W. Dodson, E. R. Hedeman, and L. Owren, Astrophy. J., **118**, 169 (1953).
[12] J. P. Wild, J. D. Murray, and W. C. Rowe, Nature, **172**, 533 (1953).
[13] W. H. Bennett and E. O. Hulburt, Phys. Rev., **91**, 1562 (1953).
[14] H. Alfvén, Phys. Rev., **75**, 1732 (1949); On the origin of cosmic radiation, Tellus, **6**, 232 (1954).
[15] H. W. Babcock, Astrophy. J., **118**, 387 (1953).
[16] R. Shapiro, J. Met., **11**, 424 (1954).

FFECTS OF RADIOACTIVE DEBRIS FROM NUCLEAR EXPLOSIONS ON THE ELECTRICAL CONDUCTIVITY OF THE LOWER ATMOSPHERE

By D. Lee Harris

Scientific Services Division, U.S. Weather Bureau, Washington, D.C.

(Received October 15, 1954)

ABSTRACT

An increase in the ionization near the ground due to the fall-out from a radioactive cloud formed by a nuclear explosion will increase the conductivity and lower the potential gradient in the lower atmosphere. Records of atmospheric conductivity and potential gradient from the Tucson Magnetic Observatory are compared with records of the deposition of atomic debris on the ground following the Nevada tests. The observed changes are not inconsistent with values computed from theoretical considerations. Most of the effects are confined to a very shallow layer, within a few meters of the ground.

It has been suggested on several occasions that the ionization produced by the lebris from the atomic-bomb tests in Nevada might produce significant changes n the normal electrical parameters of the lower atmosphere on either a local or vorld-wide scale [Herzog (1946), Hess and Luger (1946), Weekes and Weekes 1946)]. Recently, the Scientific Services Division of the United States Weather Bureau decided to investigate the magnitude of these changes.

The Weather Bureau, in cooperation with the Atomic Energy Commission, has maintained a network of observation stations to measure the spread of radio-ictive debris across the country after each of the last several atomic-test series. An estimate of the debris deposited on the ground is obtained by exposing one-foot square sheets of gummed paper on a horizontal stand about 30 inches above the ground at a large number of stations scattered throughout the country. These papers are exposed for a 24-hour period, and are sent to the New York Operations Office of the Atomic Energy Commission for a count of the radioactivity. In most cases, two or three papers were exposed simultaneously. In general, the simul-taneously exposed papers at any one station showed good agreement, but differences of an order of magnitude were observed in a few cases. A description of these observations has been given by Atomic Energy Commission (1953), Eisenbud and Harley (1953), and List (1954).

The Tucson Magnetic Observatory, at Tucson, Arizona, makes continuous measurements of the positive and negative conductivity, as well as of the potential gradient. These instruments have been described in detail by Torreson (1939) and by Wait and Parkinson (1953). The following brief description will be sufficient

for the present purposes. A schematic diagram of the observatory, a flat-roofed structure three meters high, is given in Figure 1. The potential gradient is measured by a radioactive probe, extending outward from one wall at a height of 2.45 meters above the ground. Both positive and negative conductivities are measured by

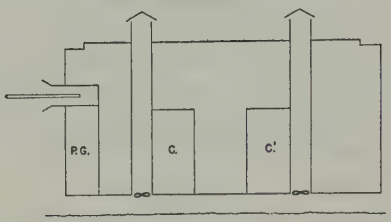

FIG. 1—Schematic diagram of the atmospheric electricity observatory, Tucson, Arizona; P.G. is the potential gradient meter and C. and C'. the conductivity meters

means of modified Gerdien apparatus. The air is drawn into the instrument through vent-pipes on the roof and is exhausted under the floor of the building by means of a fan at floor level. According to Torreson, the air is drawn through the system at a velocity of not less than 2 meters per second.

Fortunately, Tucson is in the network of stations which record the fall-out of atomic debris, and so it is possible to make a reasonably direct comparison of these two sets of records. Although Tucson is near the Nevada test-site, the winds

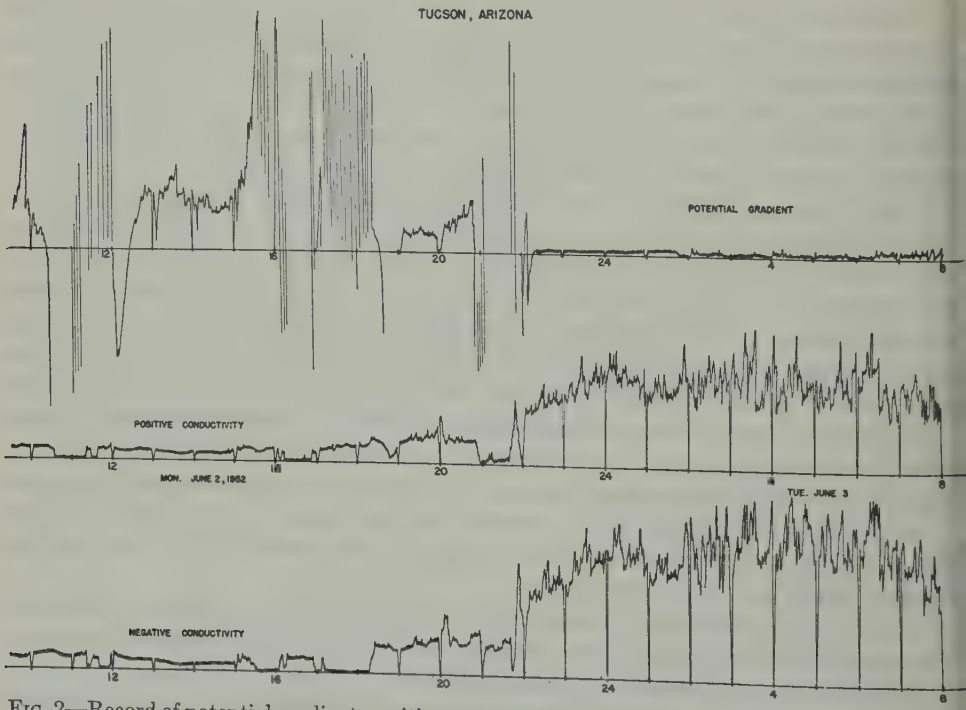

FIG. 2—Record of potential gradient, positive and negative conductivity, June 2-3, 1952, at Tucson

om the proving grounds generally pass north of Tucson, and only a few cases of gnificant fall-out have occurred. The greatest fall-out recorded at this station as measured from the gummed paper exposed between $11^h\ 30^m$ MST, June 2, nd $11^h\ 30^m$ MST, June 3, 1952. In this case, three papers were exposed, and they nowed good agreement, indicating a fairly homogeneous fall-out. A tracing of the ecords of atomospheric conductivity and potential gradient corresponding to this eriod is given in Figure 2. The record prior to $21^h\ 00^m$ is typical of that recorded or several days prior to that time. The record after $24^h\ 00^m$ is typical of that ecorded for the next four or five days.

The hourly mean values of the potential gradient and conductivity for the eriod $08^h\ 00^m$, June 1, to $08^h\ 00^m$, June 5, are shown in Figure 3. Since the cali-

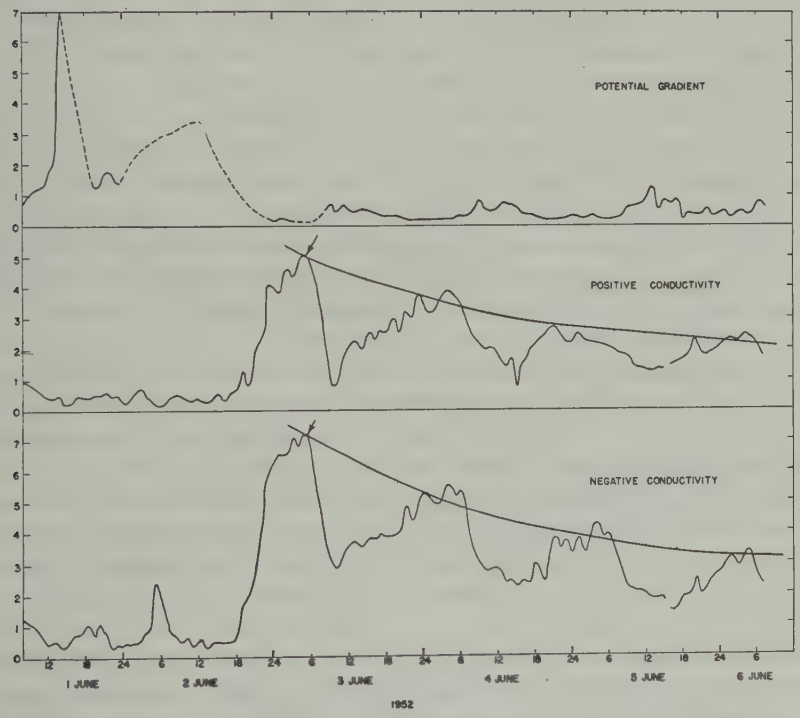

IG. 3—Record of potential gradient, positive and negative conductivity, June 1-6, 1952, at Tucson

ration factors necessary to reduce these observations to absolute units over the ange of values observed are not available, the deflections of the instrumental ecords from the zero values are shown in arbitrary units. The smooth lines drawn n the right-hand portion of the conductivity records represent the theoretical onductivity due to both natural causes and fission products, based on certain ssumptions to be discussed below.

There were several thundershowers at Tucson on June 2, and the abrupt change n the character of the record occurred at the end of the last shower. A study of he upper winds indicates that only a thin portion of the radioactive cloud passed

over Tucson at an altitude of about 16,000 feet. The available data indicate that this debris must have been carried downward by the last shower of the day.

The conductivity appears to have been increased about tenfold, and the potential gradient when not affected by the showers appears to have been decreased by a factor of about six following this fall-out. The observer's log indicates that he investigated every likely source of instrumental failure without learning the cause of the unusual disturbance in the record. The records of both conductivity and potential gradient were clearly abnormal for four or five days following this fall-out. The conductivity record appears to have been somewhat abnormal for a longer period, but the values observed were within the range of natural variability.

It is interesting to compare the recorded change in conductivity and potential gradient with theoretical calculations. According to the Atomic Energy Commission (1950), the fission products are primarily beta and gamma emitters. The average maximum energy of the beta particles is 1.3 Mev, but most of the particles have smaller energies, so that the over-all mean is about 0.4 Mev. The range of a beta particle in air is a little less than 5 meters for a particle of 1.3 Mev energy and less than 0.75 meter for 0.4 Mev particles. Since the beta particles are being continuously deflected by electrons and nuclei of the atoms in the air, they follow a very tortuous path, and the effective range in a straight line is very much less than that indicated above. The average energy of the gamma radiation from fission products is about 0.7 Mev. The gamma rays do not have a definite range, but their intensity decreases about an order of magnitude by passing through 240 meters (788 ft) of air. It is assumed that the source is an infinite plane.

On the average, 33.2 electron-volts will be consumed in the production of each ion pair. Thus, the average beta particle will produce 1.2×10^4 ion pairs, and most of these will be produced within 50 cm of the source. The Atomic Energy Commission (1950) gives graphs relating the contamination at the ground in terms of megacuries per square mile to roentgens of gamma radiation per hour as a function of height above the ground and the initial energy. By making the proper conversions, it can be shown that one disintegration per square foot per minute will produce about 2.9×10^{-5} ion pair per second, at an elevation of one meter above the ground.

The fall-out observed at Tucson in this case was about 4×10^5 disintegrations per square foot per minute on the day of fall-out. Thus, the gamma rays would have produced about 11.5 ion pairs per cc per second in the lowest few meters, or just a few more than are normally produced by natural processes. The total ion production due to gamma rays from fission products and the average natural production does not exceed the largest values of the natural production which are commonly observed near the surface over land. However, the beta particles would have produced approximately 4.8×10^9 ion pairs per minute per square foot. If these were all produced in the lowest 50 cm above the ground, this would amount to an average production of 1.7×10^3 ion pairs per cc per second.

The true relation between ion production and conductivity for these conditions is not known. However, we can make an estimate of the relation by consideration of the simple expression for equilibrium conditions:

$$q = \alpha n^2 + \beta n \quad \ldots\ldots\ldots\ldots\ldots\ldots\ldots\ldots\ldots\ldots (1)$$

where q is the number of ion pairs produced per cc per second, α is the recombination coefficient for small ions, n is the number of small ions per cc, and β is a complex factor which is a function of the number of large ions and natural condensation nuclei present. It is assumed that conductivity is proportional to n.

The value of beta pertaining to this problem is not known with sufficient accuracy to permit an exact evaluation of the effect of the above ionization on the conductivity. However, it may be safely assumed that conduction will not increase faster than the ionization. For very large values of q, such as may prevail in the region in which beta particles are most effective, we may expect conductivity to approach $(q/\alpha)^{\frac{1}{2}}$, and may be even less than this value because of the ions lost by vertical diffusion. The ions produced by beta particles cannot affect a very deep layer of the atmosphere, for their source region is the lowest few centimeters of the atmosphere and as they diffuse upward there will be an excess above the equilibrium ion density and recombination will be very rapid. Stergis (1954) has shown that under such conditions the ion density in the non-equilibrium system may decrease by an order of magnitude within the first minute away from the source region and equilibrium conditions will normally be reached within 5 to 15 minutes.

The increase in conductivity at Tucson, which cannot be explained by the ions produced by gamma rays, is probably due to the diffusion of the ions produced by the beta particles. Since the ion concentration decreases rapidly in any particle of air which leaves the source region, it is believed that any increase in conductivity due to ions produced by beta particles from atomic debris on the ground would be greatest during the day when vertical mixing is greatest. However, the highest values of conductivity are found in the early morning hours, when it is unlikely that the vertical mixing could lift the ions produced near the ground rapidly enough to account for the increased conductivity.

Since the observatory has a flat roof, it is likely that much of the original radioactive material which fell on the roof remained there. If we assume that the increase in conductivity is due mainly to the beta particles from radioactive material on the roof, it becomes easy to account for the recorded changes in conductivity, and for the fact that the change in the potential gradient, which depends largely on the conductivity through a layer of 2.5 meters, is less than that which would be expected from the recorded change in conductivity.

If the above interpretation is correct, the conductivity will be sharply stratified in the lowest few meters. At night, when the local turbulence is at a minimum, the air sampled by the Gerdien apparatus will consist largely of air which has been ionized by the beta particles from the debris on the roof of the observatory. During the day, there will be more mixing with air which has been over the roof a shorter period of time, and the conductivity would be expected to drop. The addition of more condensation nuclei from the ground would also lead to a decrease in conductivity during the daytime. It appears that the actual conductivity should be expected to conform to the theoretical value more closely during the night than during the day. The theoretical curve shown in Figure 3, was fitted at the time of the first maximum of conductivity. This computation is based on the assumptions that the response of the conductivity recording instrument is linear; the total conductivity may be expressed as the sum of an average value due to natural causes

and an additive term due to ionization by fission products; and conductivity is proportional to ionization. That is to say, it is assumed that

$$\lambda = \bar{\lambda} + \lambda_B t^{-1.2} \quad \ldots\ldots\ldots\ldots\ldots\ldots\ldots\ldots\ldots\ldots (2)$$

where $\bar{\lambda}$ is the average conductivity for each 24-hour period just preceding the fall-out, λ_B is a constant determined by the data, and t is measured in hours after the explosion.

In this case, it appears that most of the change in conductivity is due to the beta particles which originate within a meter or so of the measuring instrument. It is doubtful if the conductivity or the electric field would be significantly modified at any great distance from the ground. Some confirmation for this point of view is provided by Figure 4, which was furnished by Dr. Parkinson of Fordham University. The continuous line represents the ion production at 12 cm above an iron plate exposed above a flat roof at Fordham University. The circled dots and crosses indicate the conductivity measured by a Gerdien apparatus about four feet above the roof of a six-story building at Mt. St. Vincent College in New York City. Each point represents the average conductivity for a 12-hour period. It is noted that the ion production at 12 cm above the plate on March 19 is about ten times the natural ion production, yet the average conductivity is increased by a factor of less than two. The increased ion production and conductivity on March 19 is due to a radioactive fall-out from the atomic bomb detonated on March 17.

The next highest fall-out at Tucson was about an order of magnitude less than

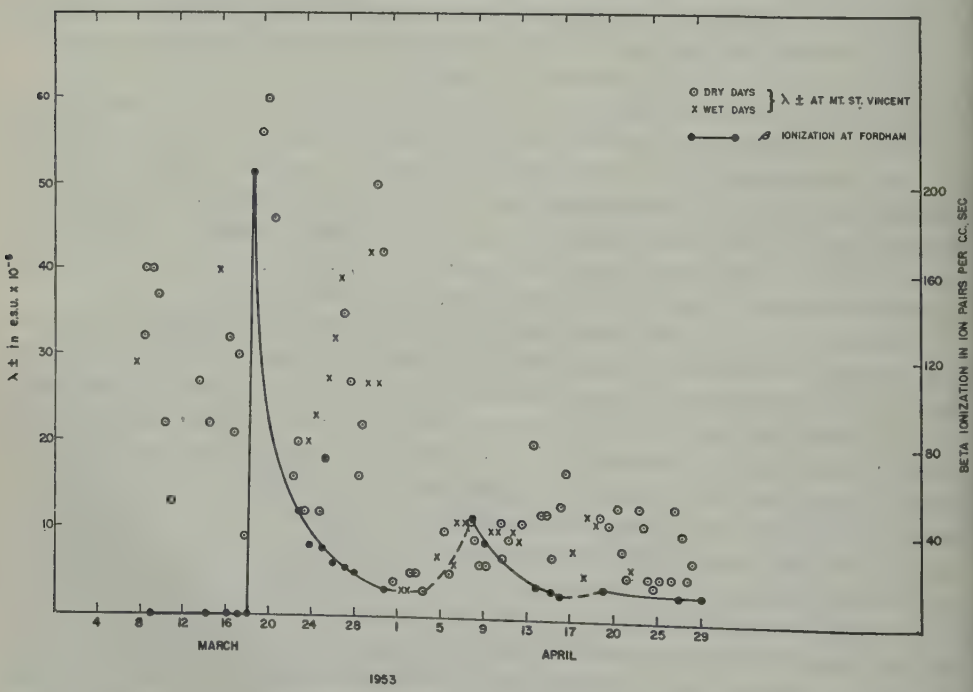

FIG. 4—Record of conductivity and beta-ray ionization at New York City, March and April, 1953

the one discussed here, and occurred on April 19, 1952. There is no clear-cut evidence that the artificial radioactivity due to atomic bombs affected the electrical records at Tucson on this date or at any other time, aside from the above-mentioned case.

The General Electric Research Laboratory maintains a corona-discharge current meter at Schenectady, New York. This instrument has been described by Falconer (1949, 1953). The records from this instrument have been compared with the fall-out values observed at the Albany airport, a few miles from Schenectady.

The Albany records show only one fall-out of the magnitude of that discussed above. This occurred between 07^h 30^m EST, April 26, and 07^h 30^m EST, April 27, 1953, and was about 40 times greater than that at Tucson. The discharge current dropped sharply during this period and the fair-weather field remained about an order of magnitude below normal for several days. However, this instrument is not a satisfactory device for detecting the presence of radioactive debris. The records for all periods during which atomic weapons were being tested were examined by Mr. Falconer to determine if there were other periods in which the records of discharge current were similar to those observed following April 26. Other periods with similar records were found in which there was little likelihood that bomb debris might be involved. In one case, April 1-10, 1952, the period of low discharge current began a few hours before the bomb was detonated and several days before any artificial radioactivity was observed at Albany.

Radioactive fall-outs of the magnitude of that discussed for Tucson have occurred in some part of the United States during each of the last three test-series at the Nevada Proving Grounds, but not following each individual test. Fall-out of ten times this value has occurred over some part of the United States on several occasions. The largest single measurement of fall-out, more than 300 miles from the test site, was 40 times as great as that discussed above. It is to be expected that surface measurements of the atmospheric electrical parameters made within a few days following a fall-out of this magnitude will be significantly altered by this artificial radioactivity. However, large changes in conductivity and potential gradient are not sufficient evidence to indicate the presence of radioactive debris from atomic bombs. No evidence has been found which would indicate that changes in the electrical parameters of the magnitude discussed above will have a measurable effect on the weather.

Acknowledgments—I wish to express my appreciation to the Carnegie Institution of Washington for lending the records of the Tucson Observatory, to Mr. Raymond Falconer and the General Electric Company for the use of the Schenectady records, and to Dr. Parkinson for providing me with the data shown in Figure 4 and for several helpful comments during the preparation of the final manuscript.

References

Herzog, G. (1946); Gamma-ray anomaly following the atomic bomb test of July 1, 1946, Phys. Rev., **70**, 227-228.

Hess, V. F., and P. Luger, Jr. (1946); The ionization of the atmosphere in the New York area before and after the Bikini atom bomb test, Phys. Rev., **70**, 564-565 (1946).

Weekes, E. D., and D. F. Weekes (1946); Effort to observe anomalous gamma-rays connected with atomic bomb test of July 1, 1946, Phys. Rev., **70**, 565.

Atomic Energy Commission (1950); The effects of atomic weapons, Washington, D.C., U.S. Government Printing Office.

Atomic Energy Commission (1953); Assuring public safety in continental weapons tests, Washington, D.C., U.S. Government Printing Office.

Eisenbud, M., and J. H. Harley (1953); Radioactive dust from nuclear detonations, Science, **117**, 141-147.

Falconer, R. E. (1949); Some correlations between variations in the atmospheric potential gradient at Schenectady and certain meteorological phenomena, Project Cirrus Occ. Rep. No. 18, G.E. Research Lab., Rep. No. RL-287.

Falconer, R. E. (1953); A correlation between atmospheric electrical activity and the jet stream, Final report ONR Project, G.E. Lab., Rep. No. RL-1007.

List, R. J. (1954); Transport of atomic debris, Bull. Amer. Met. Soc, **35**, 315-325.

Stergis, C. G. (1954); Study of atmospheric ions in a non-equilibrium system, J. Geophys. Res., **59**, 63-66.

Torreson, O. W. (1939); Instruments used in observations of atmospheric electricity, Physics of the Earth Series, Vol. VIII, Terrestrial magnetism and electricity, edited by J. A. Fleming, New York, McGraw-Hill Book Co., Inc., pp. 231-269.

Wait, G. R., and W. D. Parkinson (1953); Appendix to final report on investigation of electrical properties of the atmosphere, Contract No. AF 19 (604)-251, May 12, 1953.

OBSERVATIONS OF DISTANT METEOR-TRAIL ECHOES FOLLOWED BY GROUND SCATTER

BY W. L. HARTSFIELD

*Central Radio Propagation Laboratory, National Bureau of Standards, Washington 25, D.C.**

(Received October 20, 1954)

ABSTRACT

Observations of backscatter on 13.7 Mc over a southeasterly path from Sterling, Virginia, revealed the existence of meteor-trail reflections just ahead of the main body of the backscatter, demonstrating that the latter was from the ground in these instances. The existence of apparent two-hop backscatter without the appearance of one-hop was noted in a number of cases. Possible reasons for this behavior are discussed.

Reflections from meteor trails in the E region have been recognized on recordings of high-frequency backscatter echoes since the early experiments by T. L. Eckersley [see 1 of "References" at end of paper]. Whereas it was relatively easy to guess that the large numbers of short-duration echoes within one or two milliseconds after the transmitter pulse were caused by meteor trails, distant echoes were more of a problem, partly because of the lack of resolution of the early equipment and partly because distant echoes propagated by the $F2$ layer could conceivably originate either from the ground at the skip distance or from the distant E region along the ray path to the ground at that distance.

Eckersley concluded that the observed distant echoes were always from the distant E region. Observations by many later workers led to the conclusion that most of the distant echoes were from the ground. One group of experiments on about 13.7 Mc conducted at Sterling, Virginia, by the National Bureau of Standards in 1947-48 are noteworthy, in that over the westerly path along which transmissions were beamed it was possible, at this time of a sunspot maximum, to obtain echoes at recordable skip distances all night [2]. Thus, very strong signals could be obtained at hours of minimum interference and great meteor activity. Using photographs and visual observations of an A-plan oscilloscope presentation, it was possible to observe strong, discrete echoes of short duration just ahead of a steadier echo group. The separations observed were approximately correct for the brief echoes to be from meteor trails and the steadier echoes to be distant ground scatter along the same ray. Figure 1 is a reproduction of Figure 5 of the reference, showing this effect on October 2, 1947, between $09^h\ 00^m$ and $10^h\ 15^m$ GCT.

During a sunspot-minimum period, the ionosphere will not support 13.7-Mc $F2$-layer propagation at night over a path to the west of Sterling at any time of year. However, over paths to the southeast on winter nights after the first early-evening ionization drop, when the skip distance may go to infinity, the ionization recovers sufficiently for night backscatter observations, offering the same advantages noted in the previous case.

*Now an Audio Consultant, Washington, D.C.

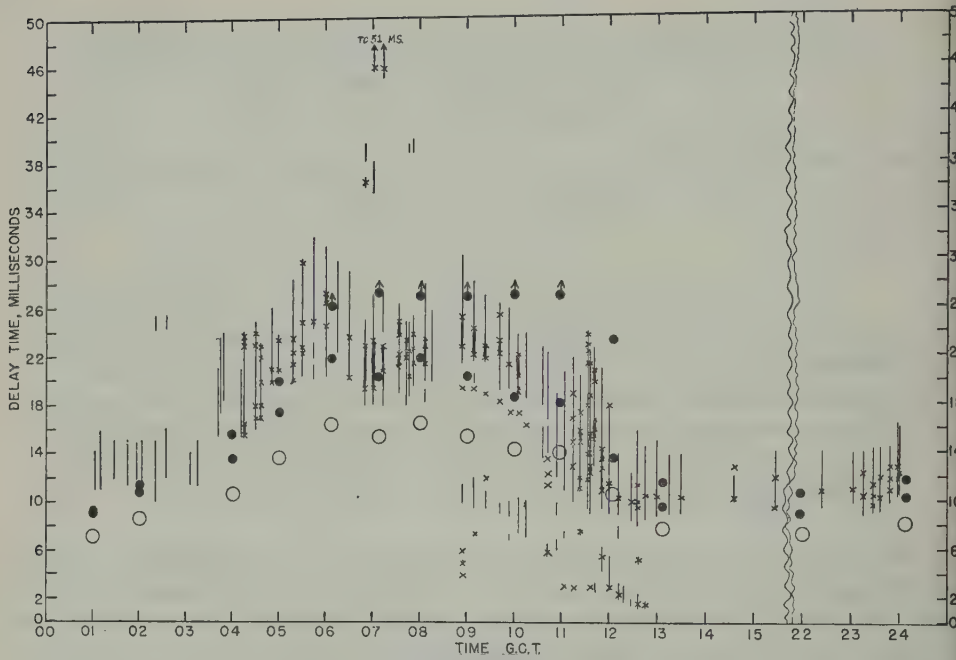

FIG. 1—Backscatter observations on 13,660 kc at Sterling, Virginia, 01h 00m–24h 00m GCT, Oct. 2, 1947

Crosses indicate amplitude peaks.
Heavy line between crosses indicates high amplitude between peaks.
Solid circles indicate shortest and longest of ground scatter delay times derived at any time from *F*2 skip-distance maps.
Arrows pointed vertically upward indicate skip greater than 4,000 km.
Open circles indicate *E*-layer long scatter corresponding to shortest derived ground-scatter delay time.

Such night echoes were photographed on a high-resolution range-time recorder constructed since the earlier tests. Figure 2 is a sample record taken on the night of December 3-4, 1953. In this Figure, the regularly-spaced vertical lines are hour markers, time shown being EST, and the horizontal lines represent delays in milliseconds. At the 25-per-second repetition rate used, the total time between pulses is 40 milliseconds. The 39th millisecond marker is at the bottom of the Figure, and is followed by a dark trace representing the transmitter pulse and the recovery period of the receiver. This trace, in turn, is followed by a field of dots extending in cases out to as much as 6 milliseconds. These dots, sparsely distributed during the sunset period and increasing in rate of occurrence towards sunrise, are the well-known meteor-trail echoes returning directly from the *E*-region level.

There is a broad dense line starting at approximately 19h 00m EST at about 21 milliseconds delay which extends across the record in an irregular manner and terminates at 05h 00m EST and at the same delay. Ahead of this line is a band of dots of a similar contour and with a density distribution similar to that of the known meteor-trail echo distribution noted above. If it is assumed that the broad dense line represents ground scatter propagated via the *F*2 layer, calculations indicate that the dots represent echoes from the meteor trails as the beam of the transmitter passes through the *E* region ahead of the distant ground.

TABLE 1—*Maximum heights of meteor trails above distant ground region as deduced from Fig. 2*

EST	Surface distance to ground scatter	Height
h m	*km*	*km*
19 55	2742	80
20 10	2425	65
21 20	2025	85
21 55	2345	75
22 30	2150	75
01 10	1950	75
02 45	1643	90
03 38	1860	85
04 28	2515	105
04 38	2550	125
04 55	2700	60

In Table 1 are noted some computed maximum heights above ground of the distant meteor trails of Figure 2, assuming that the solid distant trace represents ground scatter propagated via the *F*2 layer, and that the virtual height of the layer is 300 km.

There is considerable variability in the computed maximum heights of the observed meteor trails. Some of the variability may be due to a lack of knowledge of the virtual heights of the *F*2-layer reflection points existing at the time. Thus, if 90 km is assumed as the real maximum virtual height at which distant meteor

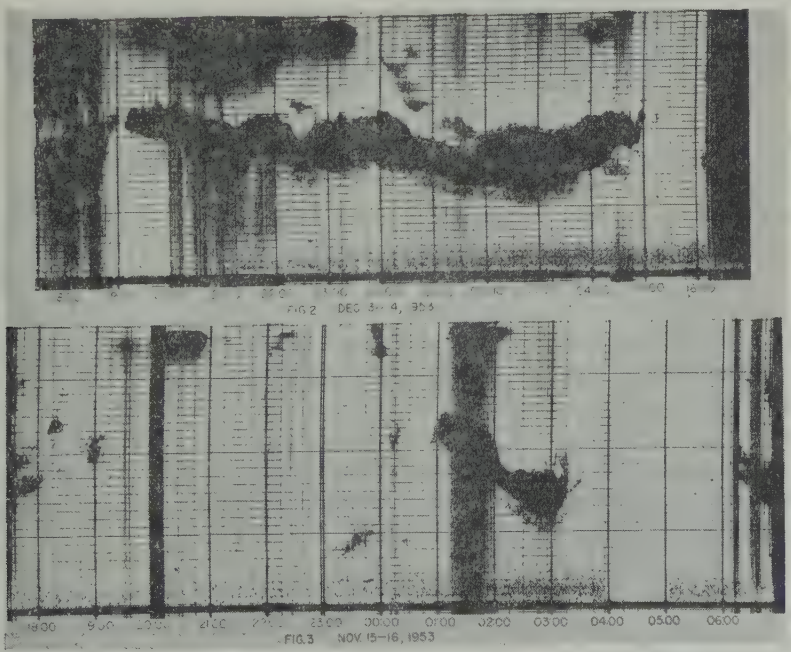

FIG. 2—Backscatter echoes from southeast of Sterling, Virginia, 13.7 Mc, Dec. 3-4, 1953
FIG. 3—Backscatter echoes from southeast of Sterling, Virginia, 13.7 Mc, Nov. 15-16, 1953
(Times in Figs. 2 and 3 are EST)

trails at $21^h\ 55^m$, $22^h\ 30^m$, and $01^h\ 10^m$ EST could have existed and been observed at Sterling, instead of 75 km as computed, the $F2$-layer virtual height would have had to be more nearly 400 km than 300 km, which is a reasonable possibility.

On some records, when the source of the ground scatter moves in after sunrise to a distance corresponding to a delay of the order of 7 milliseconds, the band of meteor echoes ahead of it moves in to merge with the nearby meteor echoes following the transmitter pulse. This leaves the possibility that a single meteor trail could yield as many as three echoes, corresponding to Eckersley's three characteristic modes [1].

The maximum delay ordinarily expected for 1-hop echoes with a high main lobe, such as possessed by the antenna array at Sterling, is something considerably less than 27 milliseconds. In Figure 3 are several instances of apparent 2-hop ground-scatter echoes, some with one-hop ground scatter showing and some without. The cases without appear, however, to exhibit the meteor region just ahead of where one-hop ground scatter would be expected. There are also some cases of just the distant meteor trails being noticeable.

At ranges centering roughly around 20 milliseconds, echoes of the meteor-trail type are found from $19^h\ 00^m$ to $20^h\ 00^m$, from $22^h\ 00^m$ to $22^h\ 30^m$, and from $23^h\ 45^m$ to $00^h\ 20^m$. The group appearing from $22^h\ 00^m$ to $22^h\ 30^m$ is followed at a delay time of 34 milliseconds by what appears to be two-hop ground scatter. At about $00^h\ 00^m$, a similar two-hop echo, beginning at 33 milliseconds, follows the meteor-type dots at around 20 milliseconds. From $01^h\ 00^m$ to $03^h\ 15^m$, the usual ground scatter preceded by meteor trails appears. Some two-hop echoes are seen to follow but are almost obliterated by interference.

Two explanations may be offered as to why two-hop ground scatter could be seen without one-hop ground scatter but with meteor trails apparently in the region ahead of one-hop ground skip range being visible. One explanation is the presence of dense homogeneous E-layer "clouds." Two-hop propagation would take place by means of two $F2$-layer reflections and an oblique M reflection from the top of the E layer. With large smooth dense areas, this could take place without noticeable one-hop scattering from the E layer or the ground (or ocean) below. In this type of reflection, the wave coming down after the first $F2$ reflection would be bent around in the upper region without penetration. However, meteor trails would be encountered as the chief discontinuities and these would be observable at the transmitting site as scattering sources. Another possible explanation is a one-hop ground return point on the ocean during a very calm period.

Thus, observation of meteor reflections on backscatter records affords additional evidence in support of the now widely accepted view that the ground is the principal source of backscatter. The meteor echoes, when present, could be used to discriminate between ground scatter and E-layer scatter in interpreting backscatter records for communication problems.

References

[1] T. L. Eckersley, Analysis of the effect of scattering in radio transmission, J. Inst. Elec. Eng., 86, 548 (1940).

[2] W. L. Hartsfield, S. M. Ostrow, and R. Silberstein, Back-scatter observations by the Central Radio Propagation Laboratory—August 1947 to March 1948, J. Res. Bur. Stan., 44, 199 (1950).

MOVEMENT OF THE *F*-REGION

By Kurt Toman

Cruft Laboratory, Harvard University,
Cambridge 38, Massachusetts

(Received October 30, 1954)

ABSTRACT

In the course of a fixed-frequency ionospheric study, employing a pulse-triggered transmitter operating on 3.5 Mc/s and three spaced-receivers, the transmission delay was continuously recorded. Aside from a vertical-incidence transmission, two oblique transmissions were thus available with 62 and 109 km as base lines, the latter being correspondingly oriented in an approximate west-east and northwest-southeast direction.

An analysis of the echoes from the *F*-region was made for the period between August 1952 and December 1953. Successive irregularities observed simultaneously on three records displayed frequently consistent time-displacements. Assuming the midpoints of the transmissions to be characteristic and preferred areas for the reflection of the h.f.-pulses, the time-displacements were interpreted as being due to a mechanical motion of the *F*-region. Direction and speed of this movement were thus obtained, and semiannual and annual periods of these components became apparent.

Introduction

Several methods have been used to pursue the study of winds in the upper atmosphere: Optical observations of noctilucent clouds and meteor trails, the radio method, the meter-wavelength emission of radio stars, observations of the night air-glow, and the measurement with rockets.

Using the radio method, which is also of primary interest in this investigation, Mitra [see 1 of "References" at end of paper] employed a 4-Mc/s transmitter, together with a receiver triangulation system of about 100-meter base lines, and recorded simultaneously time-displaced fading-curves of the amplitude of the sky wave. He considered the time-displacements to be produced by a movement of the reflecting portion of the ionosphere. However, the atmospheric level of the wind could not be specified. Munro [2] recorded simultaneous transmission-delays by using three triangularly-sited 5.8 Mc/s transmitters and three receivers with base lines of the order of 20 km. Time-displaced occurrences of large-scale irregularities, observable as a marked change in the group delay, were interpreted as a translational progression of a disturbance in the *F*-region due to a horizontal drift or a pressure wave.

In this analysis, the continuously recorded *F*-region transmission-delay was used to investigate the movement of the *F*-region, during the period between

August 1952 and December 1953, utilizing also the presence of large-scale irregularities. The apparatus employed in this experiment comprised a pulse-triggered transmitter, operating on 3.5 Mc/s, with a trigger rate of 10 cps and three spaced-receivers. The transmitter and one receiver were located in Concord, Massachusetts, with the latitude of 42°.4 north and the longitude of 71°.2 west. Additional receivers were installed in Gloucester, Massachusetts, with a base line of 61.2 km, and in Sandwich, Massachusetts, with a base line of 108.8 km, as shown in Figure 1. A 43.5 Mc/s transmitter at Great Blue Hill, Massachusetts, maintained synchronization between the transmitter and the receivers.

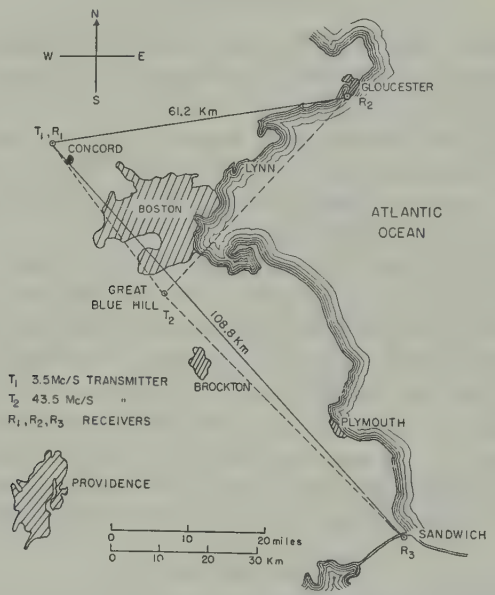

FIG. 1—Geographical arrangement of the triangulation system

Transmission-Delay Recording

During intervals which range from one-half hour to sometimes five and six hours, the variations of the *F*-region group-retardation were similar for all transmissions, except for a consistent time-displacement between them. Assuming the midpoints of the transmissions to represent characteristic and preferred areas for a specular reflection, these time-lags were interpreted as being due to a mechanical horizontal motion of the observed region. They were determined either by direct inspection or by sampling the records and cross-correlating the time-series thus obtained. The sampling was made in reference to the time of arrival of the leading edge of the pulse without correcting for varying amplitudes, neglecting the apparent and small variations of the transmission delay produced by intensity variations of a nonrectangular pulse.

Some examples of simultaneous transmission-delay records for Concord, Gloucester, and Sandwich are shown in Figure 2 for September 18, 1952. The abscissa carries the hour of the day, EST, and the ordinate the transmission delay. The upper trace represents the *F*-region echo of the ordinary ray, and the

nore regular trace at the bottom is the ground wave. This type of record is obtained rom an intensity-modulated beam of a cathode-ray tube whose horizontal sweep s a measure of the transmission time and is calibrated in 133 μsec intervals by neans of appropriate time-markers. The 133 μsec delay units were converted into ilometers of virtual path-length as it is indicated along the ordinates of Figure 2.

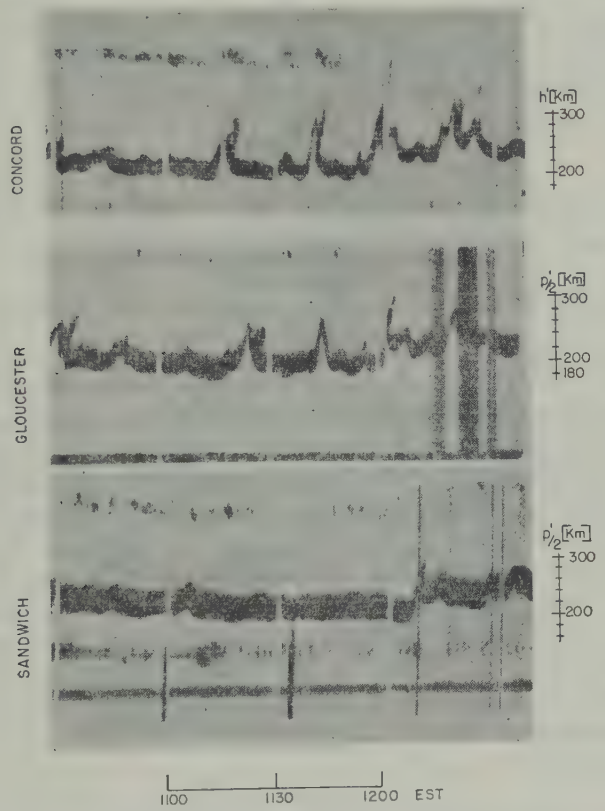

FIG. 2—Samples of simultaneous transmission-delay records for 3.5 Mc/s of September 18, 1952, midday

The photographic paper was advanced perpendicularly to the sweep with a speed of 6 cm/hr.

The Cross-Correlation Method

Of the records seen in Figure 2, the lower edge of the sky-wave trace was redrawn in Figure 3. The abscissa represents the time of day (EST) and the ordinate the virtual path-length. The three traces correspond to Concord, Gloucester, and Sandwich records. It is possible to note the variations on one record being repeated on the other records after several minutes have elapsed. In this example for September 18, 1952, the displacements obtained by direct inspection were found to be 4.7 minutes between Concord and Gloucester and 10 minutes between Concord and Sandwich.

Other examples of transmission-delay records obtained at the three receiving-

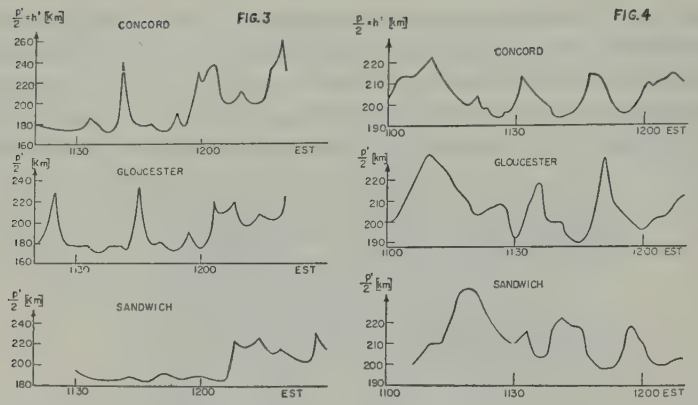

FIG. 3—Redrawn samples of simultaneous 3.5 Mc/s transmission-delay records of September 18, 1952, midday

FIG. 4—Redrawn samples of simultaneous 3.5 Mc/s transmission-delay records of October 8, 1952, midday

sites for October 8, 1952, midday, were redrawn as shown in Figure 4. The virtual path-length is indicated along the ordinate and the time of day along the abscissa. As observable in this illustration, the general pattern of the F-traces revealed time-displacements, although a point-to-point comparison of the displaced transmission-delay records yielded some differences. On those days the records had to be sampled and cross-correlated. The sampling was performed from minute to minute and one-tenth of a delay unit could be estimated with reasonable accuracy. In view of the following cross-correlation, primary interest was directed towards obtaining distinct maxima of the cross-correlation curve. This determined the choice of reference line with respect to which the sampling was performed. For each record it was chosen to lie one-tenth of a unit below the minimum delay observed during a selected period.

Using the formula

$$r(\tau) = \frac{\sum [x(t) \cdot y(t-\tau)]}{\{\sum [x(t)]^2 \cdot \sum [y(t-\tau)]^2\}^{1/2}} \quad \ldots\ldots\ldots\ldots\ldots\ldots (1)$$

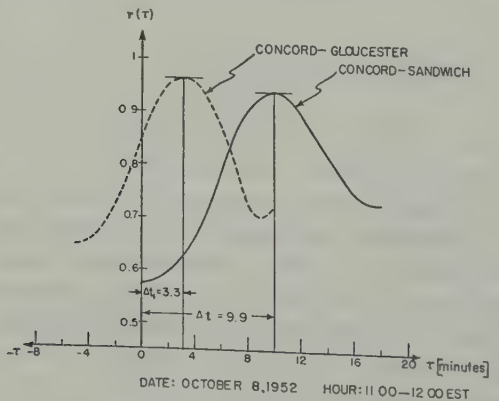

FIG. 5—Cross-correlation of Concord-Gloucester and Concord-Sandwich F-transmission-delay records for 3.5 Mc/s

where $x(t)$ is the departure from reference line for one record and $y(t)$ is the departure from reference line of the other record, cross-correlograms were obtained, as shown in Figure 5 for October 8, 1952, midday, indicating $r(\tau)$ as a function of the time-displacement τ in minutes for the Concord-Gloucester and Concord-Sandwich analyses. Correspondingly, the maxima were found at 3.3 and 9.9 minutes.

In order to be assured of a consistent time-displacement between records, it was also desirable to cross-correlate after sampling from a reference line lying above the lower edge of the trace. Figure 6 illustrates both methods. The sampling

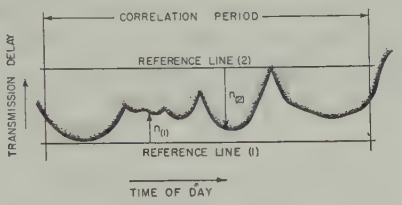

FIG. 6—Normal (1) and reversed (2) method of sampling of a transmission-delay record

from reference line 1 was denoted normal and from reference line 2, reversed. Figure 7 displays such normal and reversed cross-correlograms for January 21, 1953, midday, which yielded a displacement of 4.6 minutes for C-G and of 8 minutes for C-S. The fact that both sampling methods rendered identical time-

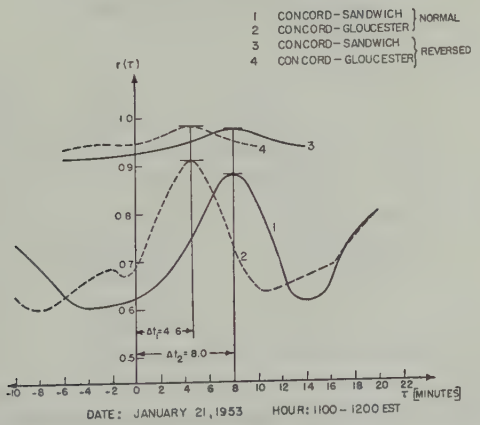

FIG. 7—Cross-correlation of Concord-Gloucester and Concord-Sandwich F-transmission-delay records for 3.5 Mc/s

lags confirmed the relative shift between entire echo structures, including the small as well as the large values of the transmission delay during the particular period. This eliminated the possibility of the time-displacements to be produced by electrical effects due to the unlike effective frequencies of the three transmissions.

The obtained time-lags were utilized in order to obtain the speed and direction of motion of the F-region. For this purpose, two geometries were taken into consideration.

The Straight-Front Geometry

It was simple to assume the presence of straight frontal irregularities within the *F*-region which pass over the receiving sites in a direction perpendicular to their orientation. Figure 8 illustrates the geometry of the stations, including the angles between the base lines and their orientation with respect to the geographic north-south. The three midpoints of the transmissions, which were assumed to be preferred areas for optical reflection, are reached by a progressing front at certain instances of time. Under the condition of horizontal uniform motion during a given period, time was linearly related with distance. Since the reference point was the zenith at Concord, with respect to which the time-lags were desired, the distances between Concord and the midpoints of the oblique trajectories were calculated and their ratio was related to the ratio of the time-displacements. For

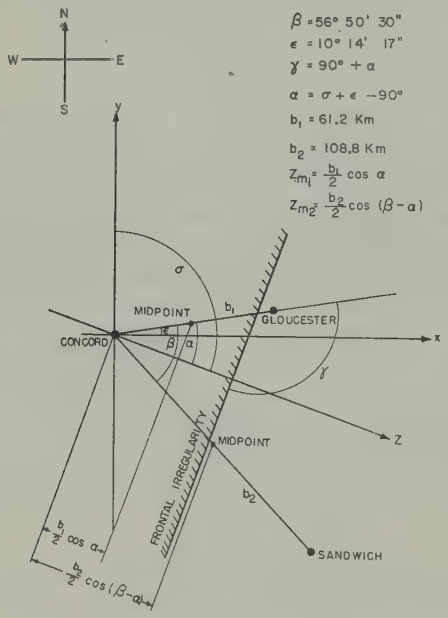

Fig. 8—Straight-front geometry

the particular geometry of the triangulation system, the following formula was derived, relating the ratio of the time-lags with the orientation of the progressing front,

$$\Delta t_2/\Delta t_1 = 0.972 - 1.488/tg\gamma \quad \ldots\ldots\ldots\ldots\ldots\ldots (2)$$

where γ is the angle between the front and the Concord-Gloucester base line, and Δt_1 , Δt_2 are the time-displacements in minutes. Since

$$\gamma = \sigma + 10°14'$$

a relation was obtained between the ratio $\Delta t_2/\Delta t_1$ and the direction of movement of the region σ in degrees east of north, which was plotted in Figure 9. Since the time-displacements can assume positive and negative values, the lower portion

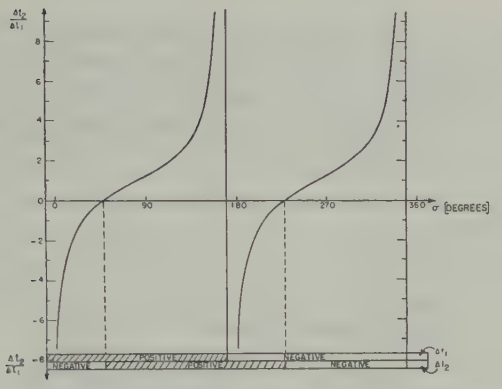

FIG. 9—Ratio of cross-correlation time-displacements $\Delta t_2/\Delta t_1$ as a function of the direction of movement σ

of Figure 9 includes specifications regarding the sign of each time-lag relative to Concord. It was considered positive if like irregularities occurred first on the Concord record and subsequently on the other record. It was negative if the opposite was true.

Knowing now the time-displacements Δt_1 and Δt_2 from the cross-correlation analyses, it was possible to obtain the horizontal direction of movement by the use of Figure 9. From the resulting value σ or γ, the speed of movement was calculated, using the formula

$$v = \frac{30 b_1 \sin \gamma}{\Delta t_1} = \frac{30 b_2 \sin (\gamma - \beta)}{\Delta t_2} \quad \ldots\ldots\ldots\ldots\ldots\ldots (3)$$

where

v is the speed of movement in kilometers/hour
Δt_1 is the Concord-Gloucester time-lag in minutes
Δt_2 is the Concord-Sandwich time-lag in minutes
γ is the angle between the front and the Concord-Gloucester base line
b_1 = 61.2 km, the Concord-Gloucester base line
b_2 = 108.8 km, the Concord-Sandwich base line
β = 56° 50′ 30″

Here it may be anticipated that the straight-front method was used in this analysis. However, the physical concept of frontal irregularities may not seem very appealing to the mind. Hence for comparison, and also to be accessible to analytic evaluation, the *F*-region was considered to be composed of individual clouds (electron or ion concentrations) which act like point reflectors. During the period of a consistent time-lag between two records, clouds had to be assumed to move with equal speed in the same direction (laminar flow). It was of interest to study the geometry of moving clouds so as to know what time-displacements to expect between transmission-delay records.

The Point-Reflector Geometry

The choice of point reflectors eliminated the consideration of retardation effects. Accordingly, only geometrical path-lengths were the subject of investiga-

tion. Figure 10 displays the three-dimensional geometry of the triangulation system. The path of a moving point-reflector is indicated by z. This path is specified by the angle σ of its deviation from the north, the height above ground h, and the shortest distance s between the projection of z on the ground plane and the location

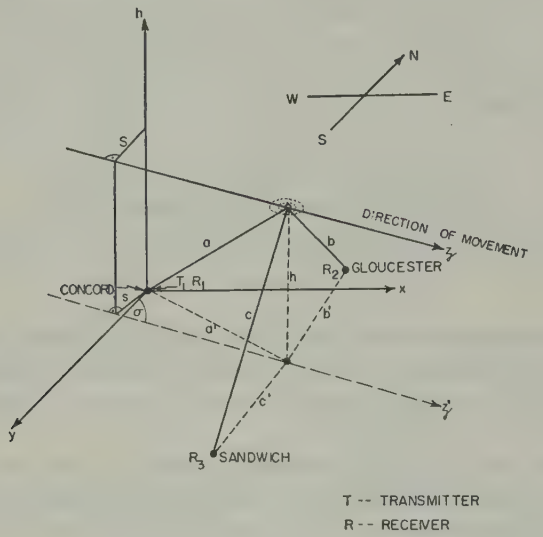

FIG. 10—Point-reflector geometry

of Concord. Neglecting the curvature of the earth and its surrounding atmosphere, the various path-lengths were evaluated during the course of travel of a patch. An example is shown in Figure 11 for $\sigma = 120°$ east of north, an altitude of 200

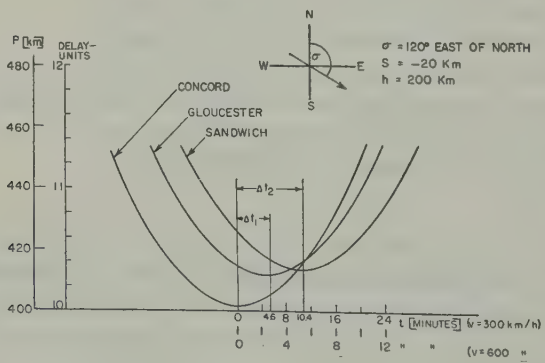

FIG. 11—Ideal point-reflector passing over receiving sites

km, and $s = -20$ km. Along the abscissa, two time-scales were included in correspondence with two speeds of 300 km/hr (83 m/s) and 600 km/hr (166 m/s). Time was chosen to begin at zero, when the point reflector is closest to Concord. The time-displaced curves correspond to the three transmissions between the transmitter, the point reflector, and each receiver. The indicated scales on the ordinate describe the path-length in kilometers as well as its equivalent 133-μs delay units. For a speed of 300 km/hr, the time-displacements of the minima

ere calculated with $\Delta t_1 = 4.6$ minutes between Concord and Gloucester and $_2 = 10.4$ minutes between Concord and Sandwich. Comparing these values with e time-lags of $\Delta t_1 = 4.7$ and $\Delta t_2 = 10.4$ minutes, obtained by the straight-front alysis for the same specifications, the error was found to be very small.

Assuming several patches to move in succession along the path z, one obtains, ring a desirable period, a series of such traces which could synthesize trans-ission-delay records similar to those observed experimentally. There will be a nsistently uniform displacement if the speed of such successive patches is the me and remains unchanged during the appearance of its echoes on the record.

An analysis of the expected error between the straight-front method and the int-reflector method for all directions of movement yielded values of less than .4, 2°.4, and 1°.4 for 100, 150, and 200 km altitude, respectively. Consequently, the actual height of the 3.5 Mc/s contour of the F-region was above 150 km, e error remained below 2°.4. This result was obtained with respect to a series of tches moving in succession along the path z. In practice, there are patches which ve to be assumed randomly distributed and, if long correlation-intervals relative the fading period of the transmission delay are chosen, the above-mentioned rors were compensated in time.

It was also of interest to know what kind of physical conditions, more feasible an point reflectors, can exist in the F-region without invalidating the interpre-tion of the time-displacements which were attributed to its horizontal movement. or the purpose of this study, it was found that the patches can have finite dimen-ons if either the areas of constant ionization-density are concentric spheres, or the cloud is at least symmetrical with respect to the plane normal to the direction movement. In the former, the amount of retardation remains essentially constant ring the appearance of an echo on the record, and for the latter, although rying, the magnitude of retardation will also not affect the time-displacements.

From the preceding discussion, it was believed that the use of the straight-ont concept is justifiable.

Horizontal Direction of Movement

From the time-displacements obtained by cross-correlation, or direct inspection d employing the straight-front method (formula 2), it was possible to calculate e directions of movement of the F-region during the period between August 52 and December 1953. This period included 510 days. Useful data were available · 177 days. Because of equipment failure, 130 days did not provide three simul-neous records. On the remaining unusable daily records, no reliable time-dis-acements could be obtained, either because of the absence of F-region irregu-ities (smooth record), or because simultaneous records were not alike. In addition, ta had to be eliminated if blanketing effects of underlying regions obscured the transmission delay-echoes. The analysis was restricted to intervals around noon, ce the rate of change of ionization-density for this time of day was zero or very all.

Figure 12 displays a polar histogram of the directions of movement. The dius indicates the number of observations of $\bar{\sigma}$, as well as the percentage of read-gs lying within 10° intervals. More than 90° deviation of $\bar{\sigma}$ was comprised by e F-region, which moved predominantly towards the southeast. The angular

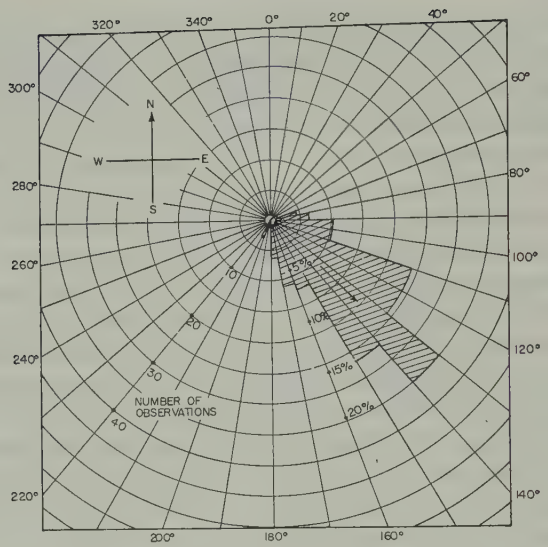

FIG. 12—Distribution of the direction of movement of the F-region during the period of August 1952 to December 1953 midday

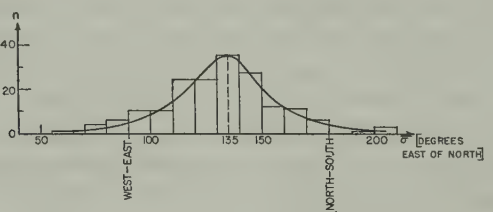

FIG. 13—Number of measured mean directions of motion of the F-region as a function of the angle $\bar{\sigma}$ for the period from August 1952 to December 1953 midday

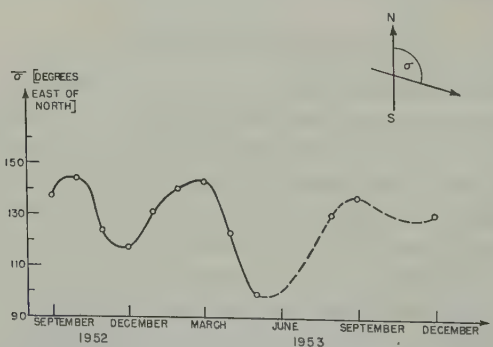

FIG. 14—Mean direction of motion of the F-region at midday

distribution was better illustrated in Figure 13, where the number of observation was plotted as a function of $\bar{\sigma}$. The obtained curve showed a maximum at 135 east of north. For the investigated period, the monthly averages of the resultin directions were plotted in Figure 14. A semiannual period was observed wit maximum deviation east of north close to the equinoxes.

Munro [2] reported for Sydney, Australia, a direction of movement of the egion between 30° and 60° towards east of north. In later experiments, Munro found an annual period of the direction of movement with a predominant t-to-east component. Many other results were summarized by Deb [4] and xwell [5]. From these sources, it appeared that the prevailing direction of move- nt of the *F*-region had a west-to-east component during the day, which compares ntially with the results presented here. Some discrepancies, however, are ex- ted, since observations were made on different continents and at various tudes. A world-wide wind-circulation system in the upper atmosphere is therefore gested. The conception of such a system relies on data to which it is hoped t the results obtained here are contributing.

The horizontal speed of movement was derived from the same source as the ction of movement of the *F*-region. As reported in the following paragraph, it found to be in good agreement with values obtained by other workers.

Horizontal Speed of Movement

By averaging monthly observations, the seasonal variation of the horizontal ed of the *F*-region was obtained, as shown in Figure 15. In contrast to the

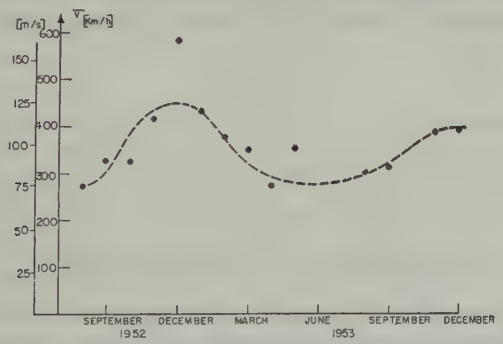

15—Average speed of the *F*-region at noon deduced from 3.5 Mc/s transmission-delay records

iannual period of $\bar{\sigma}$, the speed $\bar{v}$ was found to have an annual period and its nthly averages varied between 250 and 600 km/hr, with higher values in winter n in summer. A histogram of $\bar{v}$ is displayed in Figure 16. The most frequently urring speed was about 350 km/hr. The average speed of the *F*-region for the

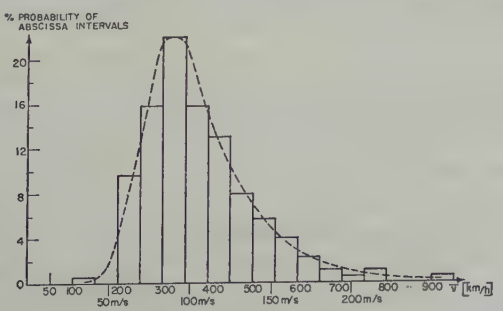

16—Per cent probability of average speed of the *F*-region deduced from 3.5 Mc/s transmission-delay records

period between August 1952 and December 1953 was found to be 362 km/hr, or about 100 m/s. The median values of $\bar{v}$ were plotted in Figure 17, of which the ordinate reads the percentage exceeding the value of the abscissa. From this diagram, a 50 per cent median speed of 392 km/hr, or 110 m/s, was obtained.

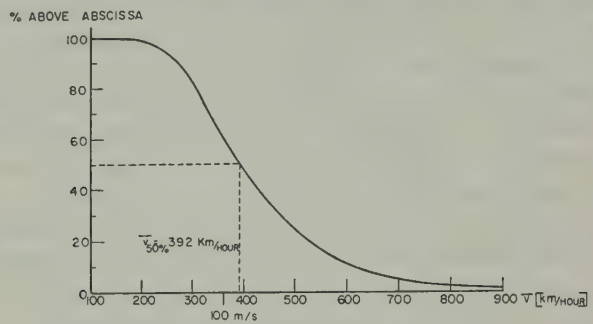

FIG. 17—Mean speed distribution of the F-region for the period from August 1952 to December 1953 midday

For midday, the virtual-height median-values were derived from the Concord record and their monthly averages are shown in Figure 18, indicating greater

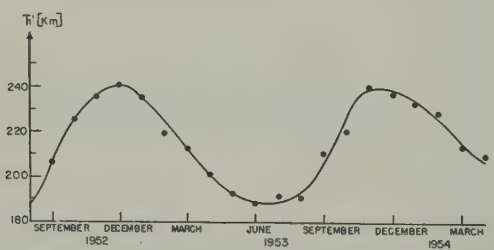

FIG. 18—Mean virtual-height $\bar{h}'$ of the F-region at midday derived from 3.5 Mc/s transmission-delay records (Concord, Massachusetts; latitude: 42°.4 north, longitude: 71°.2 west)

delays in winter than in summer of the 3.5 Mc/s signal. Similar to the behavior of the monthly averages of the speed, the mean virtual-height also revealed an annual period. The relation between both was indicated in Figure 19. The monthly averages of the virtual height plotted as the ordinate were related to the monthly averages of the speed read along the abscissa. Although the data used in this diagram were collected during a long period, increase of speed with increasing height seems consistently indicated.

Operating with a frequency close to the penetration frequency of the region, Munro [2] in Australia reported speeds for the F-region between 288 and 480 km/hr. Beynon [6] in England referred to a speed of 430 km/hr for the $F2$-region around sunrise. From later experiments, Munro [3] obtained horizontal speeds of the F-region between 300 and 600 km/hr. Maxwell and Dagg [5] in England observed a most-frequently-occurring drift-speed of 360 km/hr for the upper F-region. In America, Salzberg and Greenstone [7], and in Canada, Chapman [8], obtained an average speed of 360 km/hr. From these references, it may be concluded that the average horizontal speed of the F-region reported in this study is in good agreement with the results of other investigations.

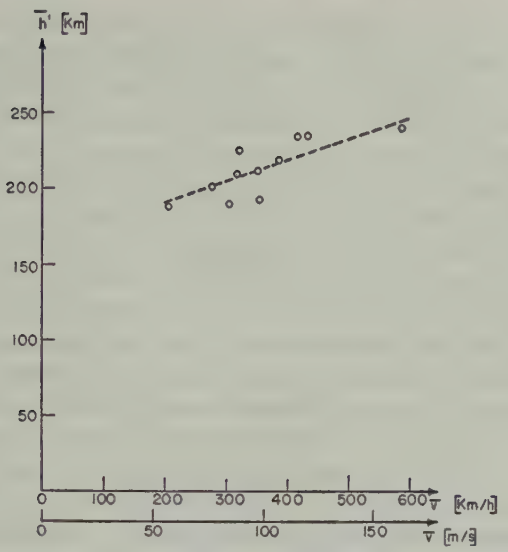

G. 19—Relation between mean virtual-height and mean speed of the *F*-region for the period of ugust 1952 to December 1953 midday deduced from 3.5 Mc/s transmission-delay records

Discussion

The irregularities of the *F*-transmission-delay records were assumed to be oduced by physical irregularities within the *F*-region. If these variations were used by irregularities of the *E*-region, for example, the direction of movement otained here would have to be attributed to the latter. If it were possible to oss-correlate simultaneous *E*-region records, similar to the *F*-region analysis, a mparison of the time-displacements would resolve the ambiguity. Unfortunately, henever the *E*-region was present, its virtual height was too regular in time to ovide appropriate conditions. Daytime data of sporadic *E*'s suitable for move-ent studies were meager. During the night, sporadic-ionization clouds seem to ove predominantly towards south-southwest. However, during this time, no eful 3.5 Mc/s *F*-echoes were available for comparison. It was therefore necessary look for qualitative indications capable of resolving the *E-F* calamity. These dications were available by inspecting the *E*-region activities throughout the ar. During the winter months, while extensive correlation data were obtained, e midday monthly averages of the *E*-region critical-frequency for 1952 were und to lie below 3.0 Mc/s, and for 1953 even below 2.6 Mc/s, as reported for ashington, D.C., by the National Bureau of Standards [9]. The monthly rate of currence of sporadic *E*'s also displayed a minimum during the winter months. oreover, the inspection of the records gave only a few indications of strong *E*2 ivity during the winters of 1952 and 1953.

For the 510-day period, the *F*1-region showed substratifications on 261 days ound noon, as observed in Washington, D.C. Consequently, critical frequencies re observed within the *F*1-region, which were distributed below the normally-erred-to critical-frequency of *F*1, and the 3.5 Mc/s signal was exposed to egularities which were duly attributed to this region. The number of days per nth for which stratification was observed reached a maximum around the

equinoxes, similar to the geomagnetic activity. However, the F-region echoes were unusable for cross-correlation studies when the K-index exceeded perhaps 3 or 4. Days of strong geomagnetic activity were therefore by themselves excluded from the monthly averages of the directions and speed of movement. Although a notable but small effect of the K-index upon the speed of the F-region has been pointed out by Chapman [8], its seasonal variation seems predominantly influenced by the variations of the virtual height, as shown in Figure 19. On the other hand, the seasonal variation of the direction of movement which displayed a semiannual period as depicted in Figure 14, may be related to the behavior of the geomagnetic activity.

In winter, the $F2$-region merges with $F1$, the combined region being referred to as the F-region. It may be pointed out that, for the relationship between the monthly mean values of virtual height and speed of movement, a separation of the F-region into $F1$ and $F2$ becomes irrelevant for this discussion [10].

It is concluded that the transmission-delay variations are mainly produced by physical irregularities within the F-region and that the results of this analysis describe its actual movement. This is also supported by the good agreement with the results obtained by other workers who employed different methods.

Summary

Using the time-displacements between 3.5 Mc/s F-transmission-delay records obtained from three triangularly-sited receivers, during the period between August 1952 and December 1953, the horizontal speed and direction of movement of the F-region were obtained. At an average virtual-height of 215 km during this period, the average speed was found to be 362 km/hr, with a mean direction of movement of 135° east of north, not quite parallel to the earth magnetic field [8]. The monthly averages of the mean direction revealed a semiannual period, with maximum deviation east-of-north around the equinoxes. The monthly averages of the speed, varying between 250 and 600 km/hr, indicated an annual period with higher values in winter than in summer. It was also found that the speed increased with height.

Acknowledgment

Gratitude is due to Prof. Harry R. Mimno for his support and encouragement, and to Mr. David Davidson with whom equipment maintenance was shared. The help of various members of Cruft Laboratory is also gratefully acknowledged.

References

[1] S, N, Mitra, Proc. Inst. Elec. Eng., **96**, 441 (1949).
[2] G. H. Munro, Nature, **162**, 886 (1948).
[3] G. H. Munro, Proc. R. Soc., A, **202**, 208 (1950).
[4] S. Deb, J. Atmos. Terr. Phys., **4**, 28 (1953).
[5] A. Maxwell and M. Dagg, Phil. Mag., **45**, 551 (1954).
[6] W. J. G. Beynon, Nature, **162**, 887 (1948).
[7] C. D. Salzberg and R. Greenstone, J. Geophys. Res., **56**, 521 (1951).
[8] J. H. Chapman, Can. J. Phys., **31**, 120 (1953).
[9] National Bureau of Standards, Ionospheric data, September 1952 to January 1954, Nation. Bur. Stand., Washington, D.C., CRPL Series F.
[10] K. Rawer, Die Ionosphäre, Groningen, P. Noordhoff, Ltd., p. 117 (1953).

JOURNAL OF GEOPHYSICAL RESEARCH VOLUME 60, No. 1 MARCH, 1955

ANNUAL VARIATION OF THE MAGNETIC ELEMENTS

BY R. P. W. LEWIS, D. H. McINTOSH, AND R. A. WATSON

Meteorological Office, Edinburgh, Scotland

(Received October 1, 1954)

ABSTRACT

Annual variations of the horizontal intensity (H force) were computed for a number of stations, using values for magnetically quiet days where available. These are expressed in terms of Fourier components. Differences found between one pair of stations suggest that the annual variation arises from local as well as world-wide influences.

A. M. van Wijk has in a recent note [see 1 of "References" at end of paper] called attention to the annual variation of the magnetic elements, using as illustration 19 years of results from the magnetic observatory at Hermanus. Part of this variation is apparently due to the known six-monthly variation of magnetic disturbance (itself unexplained, as he points out), but there is also a 12-monthly wave with maximum in the early local summer.

The Department of Terrestrial Magnetism, of the Carnegie Institution, has published curves [2] showing mean annual variations for a large number of stations, including variations appropriate to Q days only, D days only, and years of maximum and minimum solar activity. These curves show that a real variation in the vertical component is, if present, too small to be satisfactorily disentangled from errors of measurement; that variations in the E-W component are probably systematic but very small (much less than the effect due to secular change); and that a real annual variation of H or X exists with two significant harmonic components: a second harmonic dependent on magnetic disturbance and sunspot cycle, and a first harmonic independent of these factors and antisymmetrical with respect to the equator, its maximum falling in the early local summer.

Some of these results were based on only a few years of data, and as errors in measurement (chiefly due to uncertainties in the base-line) tend to be rather large, annual variations of H force were computed anew for a number of stations, including some not dealt with in the publication mentioned above. Where available, values for Q days were used as being more likely to give a true representation of the real annual variation. For some stations (for example, Batavia), accidental errors are still well marked even after averaging over 36 years of data, pronounced features of the mean curve being manifestly due to the data for one or two years only. The conclusions reached about the 12- and six-monthly components of the annual H variation are still however unaltered.

The scatter of the phase angles deduced for the 12-monthly component is considerably greater than the scatter of the phase angles for the six-monthly component, the variation of date of maximum of the former being roughly four

TABLE 1—*Amplitudes and phases for annual variation of H force, assumed given by* $[C_1 \sin (t + \phi_1) + C_2 \sin (2t + \phi_2)]$, *where t is measured in degrees from January 1 (unless stated otherwise, values refer to Q days)*

Station	C_1	ϕ_1	C_2	ϕ_2
	γ	°	γ	°
Tromsö	6.4	− 97	8.7	−256
Lerwick	1.7	− 59	4.0	−252
Sitka	3.8	− 61	5.0	−261 (all days)
Eskdalemuir	2.9	− 65	3.7	−249
Abinger	2.6	− 46	2.4	−259
De Bilt	3.3	− 2	1.8	−263
Cheltenham	4.5	− 56	3.3	−271
Tucson	4.3	− 60	4.5	−262 (all days)
Zikawei	6.5	− 19	1.4	−279 (all days)
Honolulu	2.3	− 38	1.9	−262
Porto Rico	4.6	− 70	3.7	−277 (all days)
Huancayo	1.1	−271	2.6	− 33
Apia	5.6	−232	1.9	−285
Mauritius	4.2	−234	3.2	−288 (all days)
Watheroo	6.3	−272	3.4	−255
Hermanus*	4	−225	7	−270
Amberley	4.7	−240	5.2	−271 (all days)

*Values for Hermanus were estimated from reference [1].

times that of the latter. This result probably corresponds to a really greater variability of phase of the 12-monthly component, for the amplitudes of the two components are (for Q days or all days) about the same size. For example, the mean annual variation at De Bilt has a phase differing by 44° (that is, about six weeks) from the corresponding phase for Abinger. The De Bilt figures are based on an average for the years 1911-35, and the Abinger figures on an average for 1926-40. The variations for individual years were also analysed and the results plotted on a harmonic dial (Fig. 1). This showed that the mean phase difference was probably, but not quite certainly, real. The distance between the stations is only 250 miles (approximately), so it seems that local factors may influence the 12-monthly component considerably; an explanation of the annual variation solely in terms of such world-wide events as seasonal changes in the high atmosphere (winds and/or temperatures; see Vestine [3]), could hardly account for such rapid changes in a small distance. (No systematic year-to-year change is apparent on the harmonic dial.)

We have spoken above of annual variations of H force, meaning annual variations of the daily mean of H, usually on Q days only. The significance of such a variation is obscured by the fact that the amplitude of the hour-to-hour diurnal variation of H is considerably greater than the amplitude of the annual variation of the daily mean (see Fig. 2). Since the diurnal variation on Q days (S_q) itself has a marked annual variation, it is possible that the annual variation of the

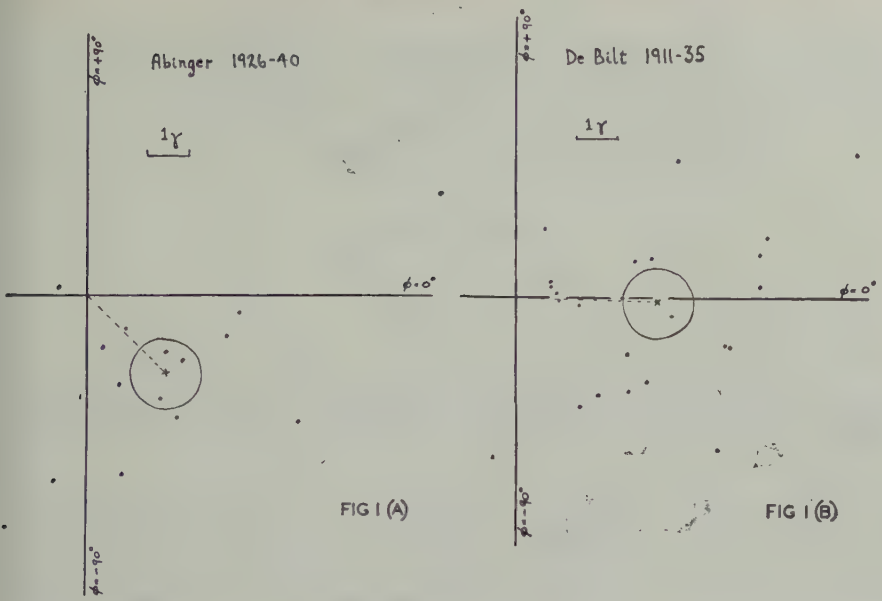

FIG. 1—Harmonic dials for 12-monthly component $C_1 \sin(t + \phi_1)$ of annual H variation for individual years at Abinger and De Bilt, t being measured in degrees from January 1 (mean amplitude vectors indicated by pecked lines, and their standard errors by circles)

daily means is merely a by-product of the annual variation of S_Q . Annual variations of H measured over one particular hour of the day show considerable differences from one another (Fig. 3). It is thus difficult to say what is the "true annual variation of the general level of H."

There is some reason for thinking [4] that the datum line for S_Q is the midnight value; if so, Figure 3*a* gives the best idea of the annual variation at Abinger, which

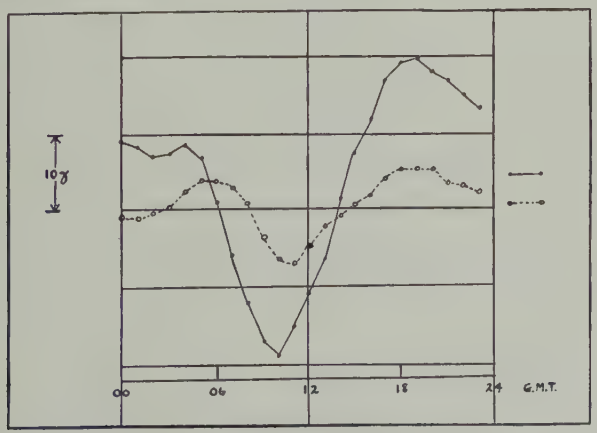

FIG. 2—Quiet-day variations at Abinger referred to the same absolute level after allowing for six months of secular change, ·——· June, o——o December, 1926-40 (daily means indicated at right-hand side of Fig.)

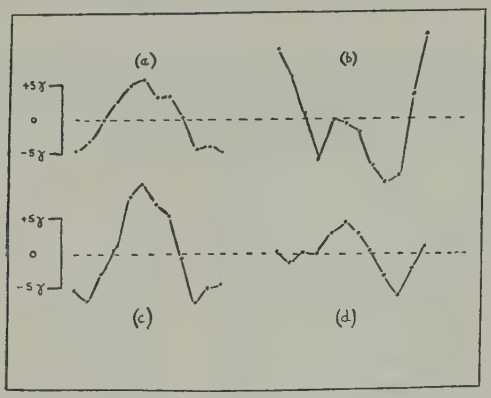

Fig. 3—Annual variation, January to December, of H at Abinger, 1926-40: (*a*) at 00^h GMT, (*b*) at 10^h GMT—time of minimum, (*c*) at 19^h GMT—time of maximum, and (*d*) for daily mean

is even larger than that obtained by considering the daily means, although the six-monthly component is considerably reduced. The amplitudes of the first and second harmonics are, in fact, 5.3γ and 0.3γ, respectively, compared with 2.6γ and 2.4γ. (The phases are $-76°$ and $-238°$, compared with $-46°$ and $-259°$.) These considerations do not affect the statistical validity of the results in Table 1 but render their meaning very obscure.

References

[1] A. M. van Wijk, J. Geophys. Res., **58**, 418 (1953).
[2] E. H. Vestine, L. Laporte, I. Lange, and W. E. Scott, The geomagnetic field, its description and analysis, Washington, D.C., Carnegie Inst. Pub. 580 (1947).
[3] E. H. Vestine, J. Geophys. Res., **59**, 93 (1954).
[4] S. Chapman and J. Bartels, Geomagnetism, Vol. I, p. 242, Oxford, Clarendon Press (1940).

THE EFFECT OF RESONANCE ABSORPTION ON THE DETERMINATION OF THE HEIGHT OF AIRGLOW LAYERS

BY T. M. DONAHUE AND A. FODERARO*

University of Pittsburgh, Pittsburgh, Pennsylvania

(Received September 30, 1954)

ABSTRACT

The theory of the self-absorption of resonance photons within a luminescent airglow layer is developed and expressions obtained analogous to the Van Rhijn equation for the variation of intensity as a function of zenith angle. The measured flux is shown to be a function of $L_0/\sqrt{T}$, where L_0 is the vertical thickness in atoms/cm^2 and T the absolute temperature of the layer. The attenuation at large zenith angles in the case of the sodium D lines is shown to be large enough when L_0 is between 1 and 2 $\times$ 10^{10} cm^{-2} and T between 160° and 220° to cause a layer at 70 km to simulate a non-absorbing (Van Rhijn) layer between 200 and 300 km. If self-absorption is important, it is shown that the ratio of D_1 to D_2 intensity should vary with zenith angle and different apparent heights found for the two components. Accurate measurements of L_0 and T are shown to be necessary for even good approximate height deductions where resonance radiation (for example, Na and OI) is concerned.

1—INTRODUCTION

Most of the difficulties encountered in understanding the emission of the sodium resonance doublet in the night sky are related to the great height at which the excited atoms apparently exist during the night. The most reliable measurements made in recent years seem to place them at nearly 300 km above the surface of the earth [see 1, 2, 3, 4, and 5 of "References" at end of paper]. This conflicts with twilight observations which show about 10^{10} sodium atoms per square centimeter distributed in equilibrium with the rest of the atmosphere somewhere between 70 and, say, 115 km [6, 7, 8, 9, 10, and 11], and introduces serious trouble for any photochemical explanation of the excitation [12].

It is the purpose of this paper to show that absorption of resonance photons within the emitting layer itself may alter significantly the flux of radiation below the layer when the layer thickness is as large as 10^{10} atoms/cm^2 and give an intensity variation with zenith angle very similar to the Van Rhijn variation for a much higher layer.

2—IMPRISONMENT OF RESONANCE RADIATION

Although the considerations here will hold no matter what is the excitation mechanism, they arose from a study of the effect of imprisonment of resonance

*Now at Westinghouse Electric Corporation, Atomic Power Division, Pittsburgh, Pa.

radiation in causing the nocturnal excitation of such lines as the sodium D lines and the red forbidden line of OI [13]. The fundamental quantity which controls this as well as all imprisonment phenomena has been shown by Holstein [14] to be the probability that a resonance photon emitted by an atom somewhere in a region containing similar atoms will travel a distance r through them without being absorbed. If $P(\nu)\ d\nu$ is the probability that an atom will emit a photon having a frequency in the range ν to $\nu + d\nu$, then

$$T(r, \nu) = P(\nu)e^{-k(\nu)r}\ d\nu \quad \ldots\ldots(1)$$

is the probability that this photon will be emitted and travel a distance r without being absorbed, where $k(\nu)$ is the absorption coefficient at frequency ν. (We assume for the present that $k(\nu)$ is not a function of r.)

$$T(r) = \int P(\nu)e^{-k(\nu)r}\ d\nu \quad \ldots\ldots(2)$$

is the probability that an excited atom will emit a resonance photon which will travel at least a distance r without being absorbed. Holstein [14] has given arguments to show that under a wide variety of conditions the absorption and emission probabilities have the same shape, that is,

$$P(\nu) = \alpha k(\nu) \quad \ldots\ldots(3)$$

Under such conditions and for a specified line shape, the calculation of $T(r)$ is possible.

Consider, for example, the pure Doppler shape which almost certainly obtains in the case of the airglow D lines [15],

$$k(\nu) = k_0 \exp\left[-\frac{c^2}{v_0^2}\left(\frac{\nu - \nu_0}{\nu_0}\right)^2\right] \quad \ldots\ldots(4)$$

or

$$k(x) = k_0 e^{-x^2} \quad \ldots\ldots(5)$$

where

$$x = \frac{\nu - \nu_0}{\nu_0}\frac{c}{v_0} \quad \ldots\ldots(6)$$

The relationship between emission and absorption probability follows from the fact that

$$\int P(\nu)\ d\nu = \alpha \int k(\nu)\ d\nu = 1 \quad \ldots\ldots(7)$$

Thus, since

$$\int k(\nu)\ d\nu = k_0 \int_{-\infty}^{+\infty} e^{-x^2}\ dx = k_0\sqrt{\pi} \quad \ldots\ldots(8)$$

it follows that

$$\alpha = 1/k_0\sqrt{\pi} \quad \ldots\ldots(9)$$

and

$$P(x) = \frac{1}{\sqrt{\pi}} e^{-x^2} \quad \ldots\ldots(10)$$

Hence

$$T(r) = \frac{1}{\sqrt{\pi}} \int_{-\infty}^{+\infty} e^{-x^2} \exp\left(-k_0 r e^{-x^2}\right) dx \quad \ldots\ldots\ldots\ldots\ldots (11)$$

Holstein [14] calculates as asymptotic expression for large $k_0 r$

$$T(r) \approx (k_0 r \sqrt{\pi \ln k_0 r})^{-1} \quad \ldots\ldots\ldots\ldots\ldots\ldots\ldots (12)$$

On the other hand, for purposes of calculation at small $k_0 r$, it is possible to develop a rapidly convergent series for $T(r)$. Since

$$\exp\left(-k_0 r e^{-x^2}\right) = 1 - k_0 r e^{-x^2} + \frac{(k_0 r)^2 e^{-2x^2}}{2} - \cdots \quad \ldots\ldots\ldots (13)$$

the integrand in (11) may be written as an absolutely convergent series and integrated term by term:

$$T(r) = 1 - \frac{k_0 r}{\sqrt{2}} + \frac{(k_0 r)^2}{2\sqrt{3}} - \frac{(k_0 r)^3}{6\sqrt{4}} + \cdots \quad \ldots\ldots\ldots\ldots (14)$$

By making use of the small and large $k_0 r$ expressions, (14) and (12), it is possible to plot a smooth function $T(k_0 r)$ for all $k_0 r$. It is obvious that $T(k_0 r)$ is a universal function of $k_0 r$. Since

$$k_0 = \frac{\lambda_0^3}{8\pi} \frac{1}{\sqrt{\pi}\, v_0 \tau} \frac{g_2}{g_1} N \quad \ldots\ldots\ldots\ldots\ldots\ldots\ldots (15)$$

where λ_0 is the wavelength at the center of the line, τ the lifetime of the excited state, g_2 and g_1 the statistical weights of the upper and ground states, N the density of atoms, and

$$v_0 = \sqrt{2RT/M}$$

it follows that $T(k_0 r)$ is a function of $N(r)$, or, more generally, of L, the thickness of absorbing matter traversed, where

$$L = \int N(r')\, dr' \quad \ldots\ldots\ldots\ldots\ldots\ldots\ldots\ldots (16)$$

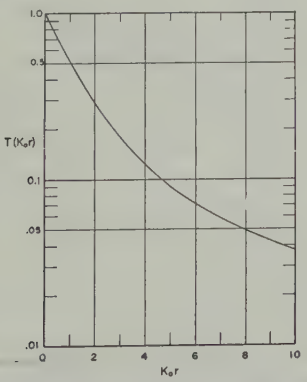

FIG. 1—Probability that a resonance photon will travel a distance r without being reabsorbed as a function of $k_0 r$, where k_0 is the absorption coefficient at the center of the line

$T(k_0 r)$ is plotted in Figure 1. It will be noticed that when $k_0 r = \sigma_0 L = 1$, where σ_0 is the cross-section for absorption at the center of the line, there is appreciable chance of absorption. Since σ_0 is of the order of 10^{-11} cm^2 for the sodium D_2 line at normal temperature, this means that a resonance photon has roughly only a 0.5 chance of traversing 10^{11} atoms/cm^2 in one flight. The cross-section at the center of the Doppler line is given through (15) by

$$\sigma_0 = \frac{\lambda_0^3}{8\pi} \sqrt{\frac{M}{2\pi RT}} \frac{1}{\tau} \frac{g_2}{g_1} \quad \ldots\ldots\ldots\ldots\ldots\ldots\ldots\ldots (17)$$

At the center of the D lines ($^2S_{1/2}$-$^2P_{3/2}$) and ($^2S_{1/2}$-$^2P_{1/2}$),

$$\sigma_0 = \frac{21.3 \times 10^{-11}}{\sqrt{T}} \text{ cm}^2 \qquad \text{for } D_2 \ldots\ldots\ldots\ldots\ldots\ldots (18)$$

and

$$\sigma_0 = \frac{10.7 \times 10^{-11}}{\sqrt{T}} \text{ cm}^2 \qquad \text{for } D_1 \ldots\ldots\ldots\ldots\ldots\ldots (19)$$

Now, it is clear that if the thickness of the emitting sodium layer in the atmosphere is greater than 10^{10} atoms/cm^2 and, if the emitting atoms have a velocity distribution which is the same as the unexcited sodium atoms surrounding them, the large thicknesses of sodium which must be traversed by photons traveling slantwise through the layer will considerably reduce the intensity of light observed on the ground at large zenith angles. If this absorption is not taken into account, the effect would clearly be to simulate a layer of greater than the true height.

3—THEORY OF SELF-ABSORPTION IN AIRGLOW LAYERS

Consider, in Figure 2, atoms distributed in a layer between h_0 and h_1 above the earth's surface. We calculate first the probability that a resonance photon originating somewhere in this layer at a distance between r and $r + dr$ from a telescope at O will emerge through the bottom of the layer in such a direction that

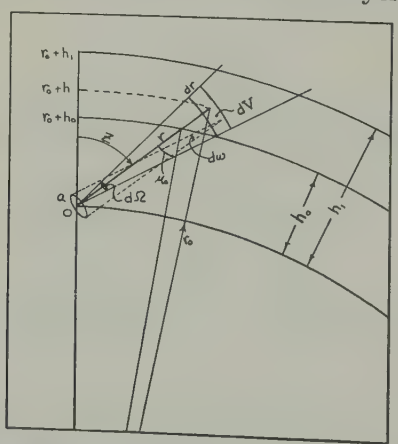

FIG. 2—Geometry of the absorbing layer problem; dΩ is the solid angle seen by the photometer telescope at O, dω is the angle subtended by the telescope objective of area a at the site of an atom which can send a photon into the telescope when it is oriented at zenith distance z

it could pass through the optical train of the telescope. Let the axis of the telescope be fixed at zenith distance z and $d\Omega$ be the solid angle seen by the telescope.

Of all the excited atoms which lie in a shell between r and $r + dr$ from the telescope, only those contained within a volume element $dV = r^2\, d\Omega\, dr$ can emit photons which would be traveling in the proper direction to pass through the telescope if they should strike it. And of these only the ones emitted into the solid angle $d\omega = a/r^2$ can strike the telescope objective if the telescope is well enough collimated that the projected area of the objective may be approximated by its total area a. Some of these selected photons will be lost on their way to the bottom of the layer, absorbed by atoms in their ground states. The probability of escape depends on the slant thickness to the bottom of the layer and is given by Holstein's function T for an argument which measures the thickness of absorbers along the telescope axis between the volume element dV and the bottom of the layer. If $n(h)$ is the density of excited atoms, the number of photons which originate in dV at r and leave the layer in such a way that they can pass through the telescope if they reach it is

$$T(h, z)(d\omega/4\pi)n(h)\, dV = T(h, z)(a\, d\Omega/4\pi)n(h)\, dr \quad \ldots\ldots\ldots\ldots (20)$$

Here dr is given by

$$dr = \frac{\partial r}{\partial h}\, dh \quad \ldots\ldots\ldots\ldots\ldots\ldots\ldots\ldots\ldots\ldots (21)$$

z being held fixed, where

$$(r_0 + h)^2 = r^2 + r_0^2 + 2rr_0 \cos z \quad \ldots\ldots\ldots\ldots\ldots\ldots (22)$$

defines the functional relationship between r, h, and z.

The total number of photons passing out toward the telescope at zenith distance z is then

$$B^0(z) = \frac{a\, d\Omega}{4\pi} \int_{r(h_0, z)}^{r(h_1, z)} T(h, z)n(h)\, dr \quad \ldots\ldots\ldots\ldots\ldots\ldots (23)$$

The superscript on B^0 emphasizes that these are the photons at the base of the layer, with the lower atmosphere yet to be traversed.

The calculation from this point on is considerably simplified by the fact that the function $T(\sigma_0 L)$ may be approximated closely by the sum of two exponential functions in the range of $\sigma_0 L$ of interest for this problem:

$$T(\sigma_0 L) \cong 0.9 \exp(-0.716\sigma_0 L) + 0.1 \exp(-0.101\sigma_0 L) \quad \ldots\ldots\ldots (24)$$

If it is now assumed that the absorbing atoms are distributed in the layer according to

$$N(h) = N_0 e^{-h/H} \quad \ldots\ldots\ldots\ldots\ldots\ldots\ldots\ldots\ldots\ldots (25)$$

then

$$\sigma_0 L = \sigma_0 N_0 \int_{r(h_0, z)}^{r(h, z)} e^{-h'/H}\, dr' \quad \ldots\ldots\ldots\ldots\ldots\ldots\ldots (26)$$

and we may write

$$T(\sigma_0 L) = \sum_{i=1}^{2} A_i \exp\left[-\alpha_i \sigma_0 N_0 \int_{r_0}^{r} e^{-h'/H}\, dr'\right] \quad \ldots\ldots\ldots\ldots (27)$$

where $r_0 = r(h_0, z)$ and $r = r(h, z)$, as given by (22). Then

$$B^0(z) = \frac{ad\Omega}{4\pi} \int_{r_0}^{r_1} \sum_{i=1}^{2} A_i \exp\left[-\alpha_i \sigma_0 N_0 \int_{r_0}^{r} e^{-h'/H}\, dr'\right] n(h)\, dr \quad \ldots\ldots(28)$$

It is necessary at this point to make some assumption about the density of excited atoms as a function of altitude. Because it is simple, more or less natural, and no information whatever is available on the subject, the assumption made here will be that the density of excited atoms is everywhere proportional to the total density of the atoms involved,

$$n(h) = \beta N_0 e^{-h/H} \quad \ldots\ldots(29)$$

However, it should be pointed out that the method of calculation used here assumes that $n(h)$ is a "final" distribution of excited atoms, including those excited by the primary mechanism, if there is any, and also by absorption of resonance quanta. A purely photochemical distribution, for example, would have to be corrected for a contribution to excited atoms because of imprisonment. On the other hand, the density yielded by a calculation based exclusively on an imprisonment mechanism will be precisely the distribution to be used in the present calculation.

Under assumption (29),

$$B^0(z) = \frac{ad\Omega}{4\pi} \beta \int_{r_0}^{r_1} \sum_{i=1}^{2} A_i \exp\left[-\alpha_i \sigma_0 N_0 \int_{r_0}^{r} e^{-h'/H}\, dr'\right] N_0 e^{-h/H}\, dr \quad \ldots\ldots(30)$$

Since

$$L(r) = N_0 \int_{r_0}^{r} e^{-h'/H}\, dr' \quad \ldots\ldots(31)$$

and

$$dL = N_0 e^{-h/H}\, dr \quad \ldots\ldots(32)$$

it is possible to write

$$B^0(z) = \frac{ad\Omega}{4\pi} \beta \int_0^{L(h_1, z)} \sum_{i=1}^{2} A_i e^{-\alpha_i \sigma_0 L}\, dL \quad \ldots\ldots(33)$$

Then

$$B^0(z) = \frac{ad\Omega}{4\pi} \beta \frac{1}{\sigma_0} \sum_{i=1}^{2} \frac{A_i}{\alpha_i} (1 - e^{-\alpha_i \sigma_0 L}) \quad \ldots\ldots(34)$$

In general, L the thickness is a function of the density distribution and the height and extent of the layer. For the cases discussed in the present paper, it is a sufficiently good approximation, because of the rapid decrease of the integrand in (31) with altitude, to take

$$L = L_0 \sec \mu_0 \quad \ldots\ldots(35)$$

where L_0 is the vertical thickness, and the angle μ_0 is measured at the *base* of the layer, so that

$$\sin \mu_0 = \frac{r_0}{r_0 + h_0} \sin z$$

L thus depends, for a given zenith angle, on L_0 and the height h_0 of the base of the layer, in strict correspondence with the assumptions in the Van Rhijn analysis. We have then

$$B^0(z) = \frac{a d\Omega}{4\pi} \beta \frac{1}{\sigma_0} \left\{ \frac{A_1}{\alpha_1} [1 - \exp(-\alpha_1 \sigma_0 L_0 \sec \mu_0)] + \frac{A_2}{\alpha_2} [1 - \exp(-\alpha_2 \sigma_0 L_0 \sec \mu_0)] \right\} \quad \ldots (37)$$

Instrumental factors drop out of the ratio $B^0(z)/B^0(0)$ and

$$\frac{B^0(z)}{B^0(0)} = \frac{\frac{A_1}{\alpha_1} [1 - \exp(-\alpha_1 \sigma_0 L_0 \sec \mu_0)] + \frac{A_2}{\alpha_2} [1 - \exp(-\alpha_2 \sigma_0 L_0 \sec \mu_0)]}{\frac{A_1}{\alpha_1} [1 - \exp(-\alpha_1 \sigma_0 L_0)] + \frac{A_2}{\alpha_2} [1 - \exp(-\alpha_2 \sigma_0 L_0)]} \quad \ldots (38)$$

For $L_0\sigma_0$ sufficiently small that absorption is negligible, it is evident that this expression reduces, as a first approximation, to the Van Rhijn expression,

$$B^0(z)/B^0(0) = \sec \mu_0 \quad \ldots (39)$$

4—THE SODIUM LAYER

In the particular case of the sodium resonance doublet, the variation with z is

$$B_2^0(z) = \frac{a\beta_2 d\Omega}{4\pi} \frac{1}{\sigma_0} \left\{ 1.26 \left[1 - \exp\left(-15.2 \times 10^{-11} \frac{L_0}{\sqrt{T}} \sec \mu_0 \right) \right] + 0.99 \left[1 - \exp\left(-2.15 \times 10^{-11} \frac{L_0}{\sqrt{T}} \sec \mu_0 \right) \right] \right\} \quad \ldots (40)$$

for $(^2S_{1/2}\text{-}^2P_{3/2})$, and

$$B_1^0(z) = \frac{a\beta_1 d\Omega}{4\pi} \frac{2}{\sigma_0} \left\{ 1.26 \left[1 - \exp\left(-7.60 \times 10^{-11} \frac{L_0}{\sqrt{T}} \sec \mu_0 \right) \right] + 0.99 \left[1 - \exp\left(-1.07 \times 10^{-11} \frac{L_0}{\sqrt{T}} \sec \mu_0 \right) \right] \right\} \quad \ldots (41)$$

for $(^2S_{1/2}\text{-}^2P_{1/2})$.

If β_1 is taken to be half β_2, that is, the $^2P_{1/2}$ state assumed to be everywhere half as fully populated as the $^2P_{3/2}$, the factor to the left of the brackets is the same in both cases. However, this ratio need not necessarily obtain. Even if it does, it is obvious that the observed ratio of intensities will not be exactly 2/1 and will surely be a function of the zenith angle. In other words, the apparent height of the D_1 and D_2 layers, if deduced under the assumption that the layers are of Van Rhijn type, would be different.

Actually, the measurements which give the anomalously high layers in sodium are made for the unresolved doublet. The ratio of the brightness at the bottom

of the layer at angle z to that at the zenith, uncorrected for scattering and absorption in the lower atmosphere, and with $\beta_1 = \beta_2/2$, is then

$$\frac{B^0(z)}{B^0(0)} = \frac{F_2(z, L_0/\sqrt{T}) + F_1(z, L_0/\sqrt{T})}{F_2(0, L_0/\sqrt{T}) + F_1(0, L_0/\sqrt{T})} \quad \ldots\ldots\ldots\ldots (42)$$

where F_2 is the part of (40) in curly brackets and F_1 the corresponding expression from (41). The ratio of D_2 to D_1 intensity at any angle is the ratio of F_2 to F_1 .

For comparison with observed intensity ratios, this expression needs to be corrected for scattering and extinction in the lower atmosphere, just as do the ratios derived for a thin clear layer. It is perhaps easier to see the effect of absorption, however, if curves plotted from (42) for absorbing layers at various heights are compared with Van Rhijn curves before corrections are made in either case. In Figure 3, Van Rhijn curves for 325, 225, and 70 km layers are compared with

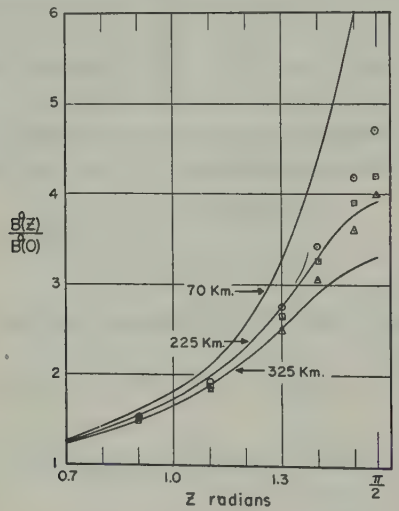

FIG. 3—Van Rhijn curves for surface brightness ratios at base of glowing layers of 70, 225, and 325 km altitude compared to the predicted ratios for layers at 70 km when absorption of sodium resonance photons is accounted for. Points for three different values of the parameter $L_0/\sqrt{T}$ are shown: ⊙ for $L_0/\sqrt{T} = 1.4 \times 10^9$, ⊡ $L_0/\sqrt{T} = 1.8 \times 10^9$, and △ $L_0/\sqrt{T} = 2.12 \times 10^9$ atoms/cm²/deg$^{1/2}$

the results predicted from (42) for a layer whose base is at 70 km and for various values of the parameter $L_0/\sqrt{T}$. Where formerly only h_0 was a parameter, now of course there are three, h_0 , L_0 , and T. $L_0/\sqrt{T}$ is now the natural parameter to use for each fixed height h_0 . It appears that a layer whose base is at 70 km would, for values of $L_0/\sqrt{T}$ between about 1.4 and 2.12×10^9 cm^{-2} degrees$^{-1/2}$, agree at least as well with observation (after correction for lower atmospheric scattering) as any Van Rhijn curve between 225 and 325 km, the limits given by Roach and Pettit [1]. This range of $L_0/\sqrt{T}$ corresponds to sodium thicknesses between 1.8×10^{10} cm^{-2} and 3.12×10^{10} cm^{-2}, for temperatures between 160° and 218°.

The effect of lower atmosphere extinction on the curves of Figure 3 is illustrated in Figure 4, where the Barbier corrections [16] are applied to the Van Rhijn curves

at 325 and 225 km and to our curves at 70 km. An extinction coefficient of 0.09/atmosphere [12] is used. The effect of increasing the extinction coefficient is great enough to warrant a careful appraisal of the proper value of this parameter. Effectively, of course, an increase in extinction relaxes the requirement on the

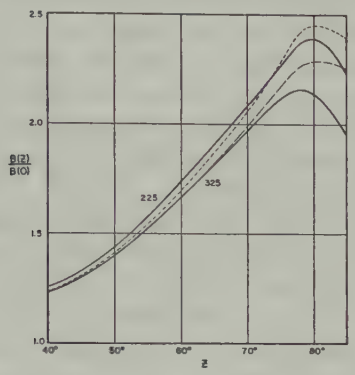

FIG. 4—Predicted variation of intensity with zenith angle for an atmospheric extinction coefficient of 0.09/atmosphere; the solid curves are for Van Rhijn layers at 225 and 325 km, the upper broken line —— is for an absorbing Na layer at 70 km with $L_0/\sqrt{T} = 1.8 \times 10^9$, and the lower dashed curve — — — for an Na layer at 70 km with $L_0/\sqrt{T} = 2.12 \times 10^9$

sodium thickness. An extinction coefficient of 0.10 would reduce $B(80°)/B(0)$ to 2.27 and 2.39 from the values 2.30 and 2.45 shown in Figure 4 for the two values of $L_0/\sqrt{T}$ plotted.

For somewhat higher altitudes, even lower $L_0/\sqrt{T}$ can be tolerated. However, in the region between 70 and 100 km, the reduction in $L_0/\sqrt{T}$ needed to give a certain ratio $B(z)/B(0)$ as the altitude increases results in little change in the thickness L_0 required, such is the temperature variation. Thus, a ratio of 2.27 for $B(80°)/B(0)$ could be achieved for $L_0/\sqrt{T} = 1.9 \times 10^9$ at 100 km, 2.01×10^9 at 85 km, and 2.12×10^9 at 70 km. Because of the change in $\sqrt{T}$ with h_0, however, these translate to requirements that L_0 be 2.79×10^{10}, 2.82×10^{10}, and 3.12×10^{10} cm^{-2}. An extinction coefficient of 0.1/atmosphere was used to correct for the effect of the atmosphere in these cases, and the temperatures are taken from data given by the Rocket Panel [17].

If the layer were truly based at 85 km and contained only 10^{10} atoms/cm^2, distributed as we have assumed, it would give rise to an uncorrected $B^{0'}(z)/B^0(0)$ close to that for a Van Rhijn value curve for 160 km. To bring the ratio at 80° down to the mean value of 2.21 given by Roach and Barbier [2] would require an extinction coefficient of 0.15/atmosphere rather than the 0.09/atmosphere usually assumed for 5893Å. A coefficient of 0.12/atmosphere would reduce the observed ratio in this case to 2.39, which scarcely seems an impossibility for $B(80°)/B(0)$, but at the moment seems very large for the extinction coefficient. On the other hand, if there is a considerable background of starlight in this spectral region as Chamberlain and Oliver have suggested [18], while the entire problem becomes somewhat more complex, the effect would still be to produce the measured ratio with the aid of less scattering. It does not seem to us at this time that a

layer located in the 70 to 100 km region is to be excluded, even if it contains as few as these 10^{10} atoms/cm^2.

The thick layer curves tend to rise somewhat above the corresponding high altitude thin layer curves at large angles and to fall a little below at lower angles. Around 90°, where the difference would be most noticeable, observation is of course virtually impossible, and there are no data available which would distinguish between the two types of zenith angle variation on this basis. The fact that published experimental curves generally appear to indicate less light than the Van Rhijn curves allow at small angles and more at large angles (giving lower altitudes at large angles) agrees—possibly fortuitously—with the thick layer predictions. Detailed comparison would be needed on this point.

The prediction of this theory most directly accessible to verification, if the sodium is indeed optically thick, is that the intensity ratio of the D lines should vary with zenith angle. Unless the excitation of the $^2P_{1/2}$ state varies with position in the night atmosphere in a way remarkably different from that of the $^2P_{3/2}$ state, different variation with zenith angle should be found for the two lines. The D_2/D_1 ratio for three layers of different $L_0/\sqrt{T}$ and assumed to be based at 70 km is plotted in Figure 5 as a function of zenith distance. For this range of optical thicknesses, the ratio varies from about 1.9 at the zenith to about 1.5 at 90°.

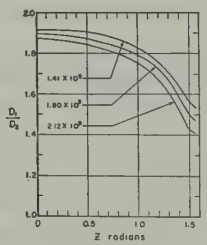

FIG. 5—Predicted variation of D_2 to D_1 intensity with zenith angle at the base of the luminous layer

5—MAXIMUM TOLERABLE THICKNESSES

An estimate of the maximum optical thickness which may be tolerated for the actual brightness ratios at a given zenith angle to differ by less than ten per cent from the simple secant law is readily obtained from an expansion of the expression for $B^0(z)/B^0(0)$. In the case of the unresolved sodium doublet, for example, it follows from (42) that to second order

$$\frac{B^0(z)}{B^0(0)} \cong \sec \mu_0 \frac{1 - 5.8 \times 10^{-11}(L_0/\sqrt{T}) \sec \mu_0}{1 - 5.8 \times 10^{-11}(L_0/\sqrt{T})}$$

$$\cong \sec \mu_0[1 - 5.8 \times 10^{-11}(L_0/\sqrt{T})(1 + \sec \mu_0)] \quad \ldots\ldots (43)$$

Therefore, $B^0(z)/B^0(0)$ will differ from sec μ_0 by no more than ten per cent if

$$L_0/\sqrt{T} \lesssim 1.72 \times 10^9/(1 + \sec \mu_0) \quad \ldots\ldots (44)$$

For a layer actually at 70 km, this means that at a zenith angle about 80° ($z = 1.4$ radians) the condition becomes

$$L_0/\sqrt{T} \lesssim 3.15 \times 10^8 \text{ cm}^2 \text{ deg}^{-1/2} \quad \ldots\ldots (45)$$

that is, $L_0 \lesssim 4.4 \times 10^9$ cm^{-2} at $T = 200°$, $L_0 \lesssim 4 \times 10^9$ cm^{-2} at 160°. A ten per cent error in sec μ_0 amounts to about 50 per cent error in estimating h_0 when the Van Rhijn technique is applied. The criterion (44) leads to somewhat relaxed conditions on $L_0/\sqrt{T}$ for higher layers observed at the same zenith angle because of the decrease in sec μ_0—the geometrical thickness. Thus, for a layer actually at 200 km,

$$L_0/\sqrt{T} \lesssim 3.9 \times 10^8 \quad \text{.....(46)}$$

will hold the error in using $B^0(z)/B^0(0)$ for sec μ_0 to less than ten per cent. Because of the rising temperature (and decreasing cross-section) at high altitudes, there is a considerable relaxation in the condition on L_0 . Thus, if the sodium layer at 200 km is at 625°, it is only necessary that L_0 be less than about 10^{10} atoms/cm^2 for the Van Rhijn method to give the altitude as about 300 kn. Similarly, for a layer at 250 km ($T \cong 900°$), the Van Rhijn measurement would scarcely give higher than 325 km as long as there were less than 1.33×10^{10} atoms/cm^2.

6—CONCLUSIONS AND REMARKS

At this time, therefore, the observed intensities do not seem to be inconsistent with a layer located below 100 km unless the thickness is less than about 1.5×10^{10} atoms/cm^2, nor between 200 and 300 km unless the thickness is greater than about 1.5×10^{10}/cm^2. Even a layer only 10^{10} atoms/cm^2 thick near 85 km cannot be excluded if extraterrestrial light and lower atmosphere extinction are larger effects than has been supposed in the past. More precise measurement of the thickness of the sodium atmosphere, as well as a knowledge of its temperature, are necessary to a good determination of the layer height. Present methods for the deduction of the thickness from twilight observations are open to objection when the degree of attenuation possible during the passage of sunlight through sodium layers containing 10^{10} atoms/cm^2 is taken into account. A detailed discussion of the twilight problem will be published separately.

Broadly speaking, these considerations might well apply also to the oxygen red line. Although the lifetime τ of the ^{1}D state of O is about 10^{10} times as long as the ^{2}P state of sodium and σ_0 more like 10^{-21} cm^2 than 10^{-11} cm^2, a 6300Å photon originating fairly low in the atmosphere might readily traverse 10^{21} atoms/cm^2. In the case of oxygen, however, some further consideration of the effect of temperature variation on imprisonment, of the fact that the ground state is a triplet, and the possibly large geometrical height of the layer which would make dubious the validity of the secant law approximation (35) is needed.

References

[1] F. E. Roach and H. Pettit, Mém. Soc. roy. sci. Liége, **12**, 13 (1952).
[2] F. E. Roach and D. Barbier, Trans. Amer. Geophys. Union, **31**, 7 (1950); Astr. J., **54**, 193 (1949); Pub. Astr. Soc. Pacific, **61**, 88, 184 (1949).
[3] D. Barbier and H. Pettit, Ann. Géophys., **8**, 232 (1952).
[4] C. T. Elvey, Amer. J. Phys., **18**, 431 (1950).
[5] J. Dufay and Tcheng Mao-Lin, Ann. Géophys., **2**, 189 (1946) and **3**, 158, 282 (1947).
[6] D. M. Hunten and G. G. Shepherd, J. Atmos. Terr. Phys., **5**, 44, 57 (1954).
[7] D. Barbier, Ann. Géophys., **4**, 193 (1948).

[8] R. Penndorf, Zs. Meteorol., **1**, 345 (1947) and **5**, 152 (1948); Phys. Rev., **78**, 66 (1950).
[9] L. Vegard, E. Tönsberg, and G. Kvifte, Geofys. Pub. 18, No. 4 (1951).
[10] J. Bricard and A. Kastler, Ann. Géophys., **1**, 53 (1944) and **6**, 286 (1950); Mém. Soc. roy. sci. Liége, **12**, 87 (1952).
[11] C. T. Elvey and A. Farnsworth, Astrophy. J., **96**, 451 (1942).
[12] D. R. Bates and M. Nicolet, J. Geophys. Res., **55**, 235 (1950); D. R. Bates and A. Dalgarno, J. Atmos. Terr. Phys., **4**, 112 (1953).
[13] A. Foderaro and T. M. Donahue, Phys. Rev., **91**, 1561 (1953).
[14] T. Holstein, Phys. Rev., **72**, 1212 (1947) and **83**, 1159 (1951).
[15] J. Bricard and A. Kastler, Paris, C.-R. Acad. sci., **216**, 878 (1940); Ann. Géophys., **1**, 53 (1944); International Council of Scientific Unions, 6th Rep., 159-165 (1948).
[16] D. Barbier, Ann. Géophys., **1**, 144 (1944).
[17] The Rocket Panel, Phys. Rev., **88**, 1027 (1952).
[18] J. W. Chamberlain and N. J. Oliver, Astrophy. J., **118**, 197 (1953).

VISCOSITY IN THE HIGH ATMOSPHERE*

BY DONALD G. YERG**

Ionosphere Research Laboratory, The Pennsylvania State University, State College, Pennsylvania

(Received October 7, 1954)

ABSTRACT

The kinematic viscosity η/ρ approaches infinity as the density ρ approaches zero, since the results of kinetic theory show that the molecular viscosity η is independent of density. The elementary viscosity derivations use a linear velocity profile which implies near infinite streaming velocities as the density becomes small. The streaming velocities must be finite, and the velocity profile must have an upper and a lower limit in the atmosphere. It is shown that the viscous stress must approach zero with decreasing density when the velocity profile is bounded. Either the velocity gradients or the corrected viscosity coefficients become small in the higher atmosphere. The viscous effect depends on a length scale representative of the wind shear and is a maximum in the lower F-region for scales comparable to those representative of the air currents studied in synoptic meteorology.

I. INTRODUCTION

In the atmosphere, where the variation of the divergence term may be neglected, the x-component of the viscous force per unit mass F_x is given by

$$F_x = (1/\rho)\partial/\partial z(\eta\, \partial u/\partial z) = (\eta/\rho)(\partial^2 u/\partial z^2) \quad \ldots\ldots\ldots\ldots\ldots (1)$$

if η is independent of z. Here ρ is the mass density, η is the coefficient of molecular viscosity, u is the x-component of the streaming velocity, and z is the height above a reference level. The coefficient $\nu = \eta/\rho$ is called the kinematic viscosity. Kinetic theory indicates that

$$\eta = -1/3NmcL \quad \ldots\ldots\ldots\ldots\ldots\ldots\ldots\ldots (2)$$

where N is the number density, m is the molecular mass, c is the mean molecular velocity, and L is the mean free path. Since L is inversely proportional to N, it follows that η is independent of density. Also,

$$\nu = -1/3cL \ldots\ldots\ldots\ldots\ldots\ldots\ldots\ldots\ldots (3)$$

*The research reported in this paper has been sponsored by the Geophysics Research Division of the Air Force Cambridge Research Center, Air Research and Development Command, under Contract AF19(122)-44.

**Present affiliation is College of Agriculture and Mechanic Arts, University of Puerto Rico, Mayaguez, Puerto Rico.

since ρ equals Nm. Thus, as ρ approaches zero and L approaches infinity, ν approaches infinity.

Large values of ν are to be expected in the higher atmosphere, and equation (1) suggests that it may be necessary to treat the higher atmosphere as a viscous fluid.

A preliminary study of viscosity suggested that the relatively long travel times of molecules in the outer atmosphere may be a factor in the viscosity derivations leading to a dependence on density [see 1 of "References" at end of paper]. It was suggested that either the effective molecules be limited to a finite volume or that a weight factor limiting the importance of the distant molecules be introduced. These arguments are incorrect if it is assumed for purposes of the derivation that steady state conditions may be approximated. For steady state conditions, the molecules that cross the elemental area at the origin may have originated at any distance and time. However, the reasoning does indicate that the viscous term will require modification if the velocity profile may be expected to change within the period required for a molecule to travel 10 mean free-path lengths. In the upper F-region, this time may be the order of several minutes. For the study of turbulence in the higher atmosphere, such considerations may be important.

The study also shows that any process which limits the effect of molecules which have experienced the last collision at great distances from the elemental area must result in a dependency between the coefficient of molecular viscosity and density.

II. THE EFFECT OF A NON-LINEAR VELOCITY PROFILE

One such limiting process results from the physical necessity that the transfer of momentum is finite, since the streaming velocity must be finite. A convenient way of illustrating this effect is to represent the transfer of momentum per unit area per unit time as the product of the average number of molecules that cross a unit area in unit time and the average net value of momentum transferred by these molecules. Thus,

$$\tau = \overline{N}\ \overline{mu} \qquad (4)$$

where τ is the viscous force per unit area and u is the streaming velocity. If $\overline{mu}$ remains finite, τ must approach zero as the density and $\overline{N}$ approach zero.

Equation (4) may be written

$$\tau = (Nc/4)[-4/3(mL\ \partial u/\partial z)] \qquad (5)$$

if the linear velocity profile of the simple kinetic theory derivation is used [2]. That τ is found independent of density results from increasing the momentum to be transferred by increasing L an amount sufficient to counterbalance the effect of decreasing density. This derivation implies that the average amount of momentum to be transferred by a molecule is related to an average streaming velocity $u = L\partial u/\partial z$, which becomes infinite as the density decreases to zero.

Physical reasoning excludes the occurrence of infinite velocities in the atmosphere. Consequently, the absolute value of the velocity must be bounded, and

the velocity profile in the vicinity of a shearing zone may be regarded as possessing an upper and a lower limit. The distribution of streaming velocity above and below a reference level may be regarded as possessing a symmetry such that $u(-z) = -u(z)$ if the air currents are moving in opposite directions. If the air currents are in the same direction, a convenient approximation to the velocity profile above and below the reference plane is

$$\left.\begin{aligned} u(z) &= u_0 + F(z) \\ u(-z) &= u_0 - F(z) \end{aligned}\right\} \quad \ldots\ldots\ldots\ldots\ldots\ldots\ldots\ldots (6)$$

where $F(z)$ is some function of height. Then, the velocity profile may be expressed in terms of a Taylor's series involving derivatives evaluated at the reference level and appropriate regard being given to equation (6). If the resulting velocity profile is used to replace the linear velocity profile in the kinetic theory derivation of viscosity [3,4], there results

$$\tau = -Nmc[(L/3)(\partial u/\partial z) + (L^2/4)(\partial^2 u/\partial z^2) + (L^3/5)(\partial^3 u/\partial z^3) + \cdots] \ldots\ldots\ldots (7)$$

The first term on the right is the conventional expression for the viscous stress. It is evident that the higher order terms must be considered as the density approaches zero and the mean free path approaches infinity. The effect of the higher order terms will be governed by the magnitude of the derivatives.

III. EXAMPLE OF THE EFFECT OF A BOUNDED VELOCITY PROFILE

The effect of the velocity profile may be further illustrated by assuming a particular example limiting the streaming velocity to finite values. Let

$$\left.\begin{aligned} u &= U_m(1 - e^{-z/b}) \qquad \text{for } z \geq 0 \\ u &= U_m(-1 + e^{z/b}) \qquad \text{for } z \leq 0 \end{aligned}\right\} \quad \ldots\ldots\ldots\ldots\ldots\ldots\ldots\ldots (8)$$

where U_m is the limiting velocity and b is a dimensional constant. At $z = b$, $U = U_m(1 - e^{-1})$. Also, $b = U_m(\partial u/\partial z)^{-1}_{z=0}$, or $| b^2 | = U_m | (\partial^2 u/\partial z^2)^{-1}_{z=0} |$. Thus, b is a measure of the space variation of the velocity profile or wind shear. In this example, two currents are supposed moving in opposite directions in an infinitely long channel in a steady state.

If the assumed velocity profile is substituted in place of the linear velocity profile in the simple kinetic theory derivation for the viscous force per unit area [2,3], it is found that

$$\eta' = NmcL\{(b/L)[-1/2 + b/L - (b/L)^2 \log (1 + L/b)]\} \ldots\ldots\ldots (9)$$

where η' is an effective coefficient of molecular viscosity. If $b/L \to \infty$, then the quantity within the braces approaches $-1/3$, and comparison with (2) shows that $\eta' = \eta$. If $b/L \to 0$, then the quantity within the braces approaches zero and $\eta' \to 0$.

Since η' depends upon the velocity profile, it also depends upon height, and the first equality of (1) must be considered in obtaining an effective value of the

kinematic viscosity. If the variation of τ with height is regarded as the result of a shift in the datum level with the limiting velocity held constant, then $(\partial u/\partial z)_{z=0}$ can be treated as a variable $\partial u/\partial z$. This expresses the fact that the wind shear governs the scale factor b, so that a change in shear produces a change in η'. If (1) is then obtained in terms of η', an effective kinematic viscosity ν' may be found. Thus,

$$\nu' = cL\{(b/L)[2(b/L)^2 \log (1 + L/b) - (b/L)(2b/L + 1)(b/L + 1)^{-1}]\} \ldots . (10)$$

As $b/L \to \infty$, the quantity within the braces approaches $-1/3$, and comparison with (3) shows that $\nu' = \nu$. Also, it may be shown that $\nu' \to 0$ as $b/L \to 0$.

These results show that the viscosity coefficients depend upon the scale representative of the shearing zone. If the length scale is large compared to the mean free path, no corrections are required. If the mean free path is of the same order of magnitude as the length scale, corrections to the conventional expressions are necessary. Equations (9) and (10) indicate that the effect of limiting the value of the streaming velocity is to decrease the value of the viscosity coefficients. Also, for any fixed value of b, the coefficient ν' considered as a function of L will pass through a maximum as L increases. This is illustrated by the data presented in Table 1.

TABLE 1—*The density, mean free path, and kinematic viscosity of the atmosphere*

Height	N	L	ν	$\nu'(b = 1$ km)	$\nu'(b = 10$ km)
km	cm^{-3}	*km*	cm^2/sec	cm^2/sec	cm^2/sec
0	2.5×10^{19}	8.6×10^{-11}	1.7×10^{-1}	9.0×10^{-2}	9.0×10^{-2}
100	3.6×10^{13}	6.1×10^{-5}	1.2×10^{5}	6.1×10^{4}	6.1×10^{4}
160	3.7×10^{10}	7.0×10^{-2}	1.5×10^{8}	1.3×10^{8}	1.5×10^{8}
200	4.6×10^{9}	5.5×10^{-1}	1.6×10^{9}	8.3×10^{8}	1.3×10^{9}
240	1.1×10^{9}	2.2	7.9×10^{9}	1.2×10^{9}	5.8×10^{9}
300	2.6×10^{8}	9.5	4.1×10^{10}	8.2×10^{8}	1.4×10^{10}
350	1.1×10^{8}	2.3×10	1.1×10^{11}	4.7×10^{8}	1.6×10^{10}
400	5.1×10^{7}	4.9×10	2.5×10^{11}	2.8×10^{8}	1.4×10^{10}
450	1.7×10^{7}	1.5×10^{2}	8.2×10^{11}	3.7×10^{7}	7.6×10^{9}

The physical data required for these computations were obtained from the work of Nicolet and Mange [5]. It is seen that ν increases with increasing height, but ν' reaches a maximum at 240 km for $b = 1$ km and a maximum at 350 km for $b = 10$ km. Larger scales would show the maximum of ν' to be at greater heights, but ν' eventually would approach zero for any given scale.

It may be noted that the kinematic viscosity has been reported to be 8.3×10^3 cm^2 sec^{-1} at a height of 85 km [6]. This may be compared to a value of 8.6×10^3 cm^2 sec^{-1} reported for the eddy viscosity in the lower troposphere [7]. It would seem that the kinematic viscosity becomes important in the lower E-region, but may or may not be significant at much greater heights, depending on the length scale of the particular problem studied.

IV. THE IMPORTANCE OF VISCOSITY IN THE HIGH ATMOSPHERE

An estimate of the importance of the viscous term may be made by examining the equations of motion. If the coordinate axes are selected, so that initially the wind is moving parallel to the x-axis and in a plane parallel to the x, y-plane, the equations of motion become

$$\partial u/\partial t = -(1/\rho)\partial P/\partial x - \nu\partial^2 u/\partial z^2 \quad (11)$$

$$fu = -(1/\rho)\partial P/\partial y \quad (12)$$

where f is the Coriolis parameter and P is the pressure. If (11) is divided by (12), the relative importance of each term of (11) may be studied. If each ratio is small compared to unity, the wind is essentially geostrophic. In particular, the importance of the viscous term is given by the ratio

$$R = (\nu\partial^2 u/\partial z^2)(fu)^{-1} \quad (13)$$

The velocity profile given by (8) has a discontinuity in the second derivative evaluated at the origin. For the purposes of examining (13), this discontinuity may be avoided by assuming a second profile given by

$$u = (2U_m/\pi)\tan^{-1} z/b' \quad (14)$$

When $z = b'$, $u = U_m/2$. This may be compared with the comparable result for the dimensional constant b.

Substitution of (14) in (13) yields

$$R = (2/f)(\nu/b^2)[(z/b)(\tan^{-1} z/b)^{-1}(1 + z/b)^{-2}] \quad (15)$$

where the difference between b and b' has been neglected. The quantity within the brackets equals unity when $z = 0$, and approaches zero as $z \to \infty$. In particular, at $z = b$ and at 45° latitude, (15) becomes

$$|R| = |(1.22 \times 10^4)\nu/b^2| \quad (16)$$

If $b = nL$ and ν is given by (3), there results

$$|R| = (0.41 \times 10^4)(c/L)(1/n^2) \quad (17)$$

If $n \geq 1$, then R is proportional to c/L, the collisional frequency which approaches zero as the density approaches zero. The viscous term must become small in comparison to other terms if a length scale smaller than the mean free path is rejected as a possibility.

If values of b smaller than L are considered possible, the effective kinematic viscosity must be used in (16). The equivalent of (17) then becomes

$$|R| = |(1.22 \times 10^4)(c/L)[2n \log (1 + n^{-1}) - (1 + 2n)(1 + n)^{-1}]| \quad (18)$$

The term in the bracket approaches -1 as $n \to 0$ and approaches zero as $n \to \infty$. Since the absolute value of this term is between zero and unity for all possible values of n or the scale b, it follows that the ratio R is proportional to the collisional frequency and will approach zero with decreasing density, no matter what scale is considered appropriate.

The importance of the viscous term in the equations of motion depends upon density. If the length scale representative of the wind shear is larger than the mean free path, the kinematic viscosity increases without limit as the density decreases, but the shear given by the space derivatives of velocity decreases, so that the viscous term ultimately decreases in importance. If the length scale may be smaller than the mean free path, comparatively larger wind shears may result, but the coefficient of kinematic viscosity requires a correction which results in a decreasing importance of the viscous term as the density approaches a small value.

The maximum possible value of R for any given density is estimated from (17) by setting $n = 1$, since this represents the maximum possible shear, smallest value of b, which does not require a large correction to the kinematic viscosity. This maximum value of R is plotted in terms of height in Figure 1. Curves showing

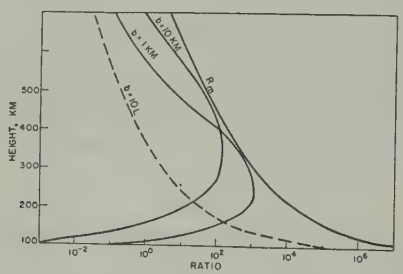

FIG. 1—The ratio of the viscous term to the Coriolis term

R for $b = 1$ km, $b = 10$ km, and $b = 10L$ also are presented. The maximum value of the ratio is at 250 km if $b = 1$ km, and is at 350 km if $b = 10$ km. If values of $b > 10$ km are used, the maximum would occur at heights greater than 350 km, but the maximum value decreases with increasing scale and is always smaller than the curve R_m .

If values of b less than 1 km are permissible, the maximum value of R for any given scale occurs at heights below 250 km. The value is quite large if molecular dimensions are approached in the lower atmosphere, indicating that transport of momentum by molecular action is important for small scale phenomena. Also, each level in the atmosphere would be associated with a maximum viscous effect for a particular length scale.

The above examples assume steady flow in an infinitely long channel. It may be considered that such a model can not be representative of conditions on a scale comparable to molecular dimensions. Since all but a small percentage of the viscous action is effected by molecules experiencing the last collision within $10L$ of the plane area selected for studying the transport of momentum [3], it may be regarded that $b \geq 10L$. The most pronounced shear in the troposphere occurs in the friction layer. Consequently, a value of $b = 1$ km may be selected as representative of the smallest possible value of b or the largest value of the shear.

If b is restricted to 1 km or $10L$, whichever is the larger, reference to Figure 1 shows that the ratio reaches a maximum value at 165 km. Thus, for all problems

comparable in scale to the air currents studied in synoptic meteorology, viscosity associated with molecular action must reach a maximum of importance in the vicinity of the lower F-region.

It may be noted that for $b = 1$ km the ratio equals unity at 110 km, indicating that viscous action becomes significant in the lower E-region. This is in accordance with the comparison of the kinematic viscosity and the eddy viscosity.

V. SUMMARY AND CONCLUSIONS

Rigorous corrections to the viscosity coefficients have not been attempted. However, it should be noted that Chapman and Cowling [8], in obtaining solutions to Boltzmann's equation by a series of functions, call attention to the increased importance of the higher order terms as the density decreases. Since the coefficient of viscosity may be obtained from these solutions, a density dependency of the viscosity coefficient is not unexpected. This problem would be further complicated by the variation of density and temperature over distances of several mean free-path lengths in the atmosphere. The correction to the kinematic viscosity for the higher atmosphere involves more than a simple consideration of the velocity profile.

Nevertheless, the effect of finite streaming velocities aids in understanding some of the limitations imposed on viscosity concepts in the higher atmosphere. That the assumed velocity profiles are not solutions to the equations of motion is not a serious objection to the conclusions. These profiles show that a length scale which is a measure of the wind shear may be used as a qualitative guide for the validity of the conventional values of the kinematic viscosity. If a mean free path of the same order of magnitude or smaller than this length scale is considered appropriate, corrections to the kinematic viscosity are required. The effects of these corrections are to decrease the viscosity coefficients.

Length scales smaller than a mean free path may be possible in the higher atmosphere. Hewish [9] reports a length of 5 km for irregularities in the F-region. The mean free path at these heights is probably greater than 50 km. A study of the applicability of the equations of motion in the higher atmosphere suggests that a volume with effectively constant mass may be selected from a cubical region with an edge smaller than a mean free-path length [4]. The resulting equations for the forces on such a unit mass would necessarily require corrections. The viscosity problem for small scales is somewhat comparable.

If length scales larger than 1 km are considered representative of the wind shear, the viscous term reaches a maximum relative value in the vicinity of the lower F-region. The viscous effect associated with molecular action should be sufficient at these levels to result in cross-isobar flow. This should be of considerable importance in the development of a general circulation in these regions [10].

The preceding discussion serves to illustrate that the viscous term in the equations of motion decreases in relative value above the F-region. Either the velocity gradients become small or an effective coefficient of kinematic viscosity which depends upon the velocity gradient becomes small. The maximum viscous action involving air currents comparable to those studied in synoptic meteorology probably occurs in the lower F-region.

VI. ACKNOWLEDGMENT

Portions of this paper were included in a thesis submitted in partial fulfilment of the requirements for the Ph.D. degree at the Pennsylvania State University. Sincere appreciation is extended to Dr. Hans H. Neuberger, of the Division of Meteorology, for his continued interest and encouragement during the development of this study.

The author is most grateful to Dr. A. H. Waynick and the staff of the Ionosphere Research Laboratory for the direct support of the laboratory and for the stimulating influence of the many conversations concerning meteorological aspects of ionospheric regions.

References

[1] D. G. Yerg, J. Geophys. Res., **57**, 217-220 (1952).
[2] D. G. Yerg, Sci. Rep. No. 45, Ionosphere Res. Lab., The Pennsylvania State University (April, 1953).
[3] L. B. Loeb, The kinetic theory of gases, New York, McGraw-Hill Book Co., Inc. (1934).
[4] D. G. Yerg, Sci. Rep. No. 49, Ionosphere Res. Lab., The Pennsylvania State University (Sept., 1953).
[5] M. Nicolet and P. Mange, Sci. Rep. No. 35, Ionosphere Res. Lab., The Pennsylvania State University (April, 1952).
[6] N. C. Gerson, Unsolved problems in physics of the high atmosphere, chapter in book "Advances in geophysics," Vol. I, edited by H. E. Landsberg, New York, Academic Press, Inc., pp. 155-242 (1952).
[7] O. G. Sutton, Micrometeorology, New York, McGraw-Hill Book Co., Inc. (1953).
[8] S. Chapman and T. G. Cowling, The mathematical theory of non-uniform gases, Cambridge, University Press (1939).
[9] A. Hewish, Proc. R. Soc. (London), A, **209**, 81-96 (1951).
[10] D. G. Yerg, J. Met., 8, 244-250 (1951).

MAGNETIC OBSERVATIONS DURING THE TOTAL SUN ECLIPSE OF 30TH JUNE 1954, AT THE MAGNETIC OBSERVATORY OF QUETTA

BY S. A. A. KAZMI AND K. A. WIENERT

Geophysical Observatory, Quetta, Pakistan

(Received November 4, 1954)

ABSTRACT

The following is a brief description of onsets observed on the magnetogram of the magnetic observatory, Quetta, during the total sun eclipse of 30 June 1954.

The total sun eclipse of 30th June 1954 offered the possibility to observe the behaviour of the magnetic elements at the magnetic observatory of Quetta (latitude 30° 11′.2 north, longitude 66° 57′.0 east). The observatory was within the zone of totality, about three miles south of the northern edge of the shadow. The total eclipse lasted for a few seconds.

In order to exploit the unique occasion, besides the Danish quick-running recording system (speed 180 mm/hour), the Ruska magnetograph (normal speed 20 mm/hour) was also set to operate at a higher speed of 80 mm/hour.

The sensitivity of the variometers was as follows:

	Ruska system	*Danish quick-running recording system*
Declination	0.51′/mm (4.9 γ/mm)	1.3′/mm (12.8 γ/mm)
Horizontal force	1.5 γ/mm	1.3γ/mm
Vertical force	4.2 γ/mm	3.0γ/mm

The time of totality was $13^h\ 54^m.8$ GMT. Hence the corpuscular eclipse was to be expected at $11^h\ 59^m$ GMT.

The following onsets were observed on the magnetogram in horizontal force (all times are in GMT).

The hours preceding the eclipse were magnetically quiet, except for a few groups of irregular pulsations of a period of 0.5 to 2 minutes. At $05^h\ 29^m.0$ and $08^h\ 07^m.5$, two minor onsets of pulsations were observed. Between $11^h\ 33^m.2$ and $11^h\ 34^m.9$, the horizontal force increased by 2.2γ. At $12^h\ 01^m.7$, a full oscillation of a period of $1^m.3$ and an amplitude of 0.8γ started to the positive side of H and was followed by minute irregular pulsations, which lasted until $12^h\ 47^m$. At $13^h\ 57^m.1$, a very slight onset started to the negative side of H and was followed by three full oscillations, which ended at $13^h\ 57^m.9$. The amplitude of these oscillations was about 0.2γ. The undamped horizontal force variometer of the quick-running La Cour recorder did not show this onset.

Two of the onsets are found in declination. Between $11^h\ 33^m.2$ and $11^h\ 34^m.9$, the declination decreased by 0.5γ. The full oscillation at $12^h\ 01^m.7$ is also visible

in declination. The onset starts to the negative side and its amplitude is 0′.1 or one gamma.

None of the above-mentioned onsets is visible in vertical force because of the low variometer sensitivity.

We would like to point out that the onsets of $12^h\ 01^m.7$ and $13^h\ 57^m.1$ follow the corpuscular eclipse and the optical eclipse after 2.7 and 2.3 minutes, respectively. We cannot, however, say with certainty whether the onsets are eclipse effects or whether the close coincidence with the eclipse times is merely accidental.

Another phenomenon of interest might be the rather sharp onset at $11^h\ 34^m.9$, which under the circumstances marks the beginning of the corpuscular eclipse.

The enclosed photograph (Fig. 1) shows the *D*- and *H*-traces of the Ruska

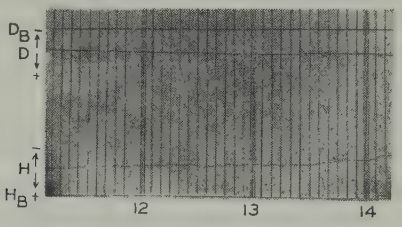

FIG. 1—Record of 30 June 1954, from $11^h\ 10^m$ to $14^h\ 15^m$ GMT; D_B = base-line for declination, D = trace of declination, H_B = base-line for horizontal force, and H = trace of horizontal force

magnetograph. The onset of $13^h\ 57^m.1$ has been enlarged eight times (Fig. 2). The time-marks are five minutes apart. The central lines of the groups of three time-marks give the full hour. The gap at $11^h\ 55^m$ was caused by the last inspection of the magnetograph. The missing time-marks are indicated by slight kicks in the

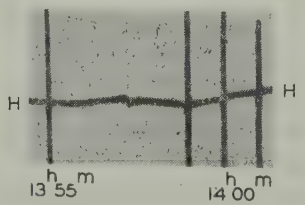

FIG. 2—Onset in horizontal force at $13^h\ 57^m.1$ (eight times enlarged)

trace, which are caused by the small magnetic field built up when the time-mark circuit is switched by the clock.

The clock was carefully compared with wireless signals. The make of the contact is two seconds early against correct GMT.

JOURNAL OF GEOPHYSICAL RESEARCH VOLUME 60, No. 1 MARCH, 1955

REFLECTION OF A TRANSIENT ELECTROMAGNETIC WAVE AT A CONDUCTING SURFACE

BY JAMES R. WAIT AND CHARLOTTE FROESE

Radio Physics Laboratory, Defence Research Board, Ottawa, Canada

(Received November 5, 1954)

ABSTRACT

A solution is given for the reflection of a transient electromagnetic plane wave at oblique incidence from the plane interface of a dissipative medium. The inversion of the Laplace transforms can only be carried out in closed form in special cases. Series solutions are developed for the general case and the numerical results are presented in graphical form. Brief mention is made of the possible application of this solution to the reflection of a radio atmospheric at a sharply bounded ionosphere.

Introduction

The reflection of a plane harmonic electromagnetic wave from a plane interface between two semi-infinite media has been treated theoretically on many occasions. When the media are both homogeneous, lossless, non-dispersive dielectrics, the reflection and transmission coefficients are dependent only on the dielectric constants, angle of incidence, and the polarization of the incident wave. In this case, the extension to a transient incident wave is trivial, since the spectral components are reflected in a uniform manner so the waveform of the reflected signal is preserved. A more complicated and a much more interesting case is when a transient wave is incident on a plane surface of a dissipative medium. The spectral components of the signal are then distorted in their relative amplitude and phase in the process of reflection and consequently the waveform of the reflected wave can be considerably modified. This case will be treated in this paper, and the application to the ionosphere is mentioned.

Statement of problem

A solution will now be derived for the reflection of a transient plane wave incident at angle θ at the plane interface between two semi-infinite media (see Fig. 1). The electric vector is contained in the plane of incidence. The lower medium

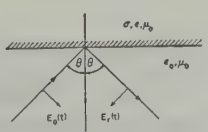

FIG. 1—The reflected and incident rays at the plane interface

is non-dissipative and has dielectric constant ϵ_0 and permeability μ_0, whereas the upper medium has a finite conductivity σ with a dielectric constant ϵ and permeability μ_0. Without subsequent loss of generality, the incident electric field $E_0(t)$ at the interface in the non-dissipative medium can be represented as [see 1 of "References" at end of paper]

$$E_0(t) = \frac{1}{2\pi i}\int_{c-i\infty}^{c+i\infty} \bar{E}_0(s)e^{st}\,ds \qquad (1)$$

or, symbolically, $E(t) \doteqdot \bar{E}_0(s)$, where $\bar{E}_0(s)$ is the Laplace transform of $E_0(t)$. The constant c is some small but finite real number which insures that the path of integration in the s plane passes to the right of any singularities of $\bar{E}_0(s)$ that may be on the imaginary axis.

Since $E_0(t)$ is a vector which is contained in the plane of incidence, the reflected electric field $E_r(t)$ is also in this plane and is represented by

$$E_r(t) = \frac{1}{2\pi i}\int_{c-i\infty}^{c+i\infty} \bar{E}_r(s)e^{st}\,ds \qquad (2)$$

or, symbolically, $E_r(t) \doteqdot \bar{E}_r(s)$, where $\bar{E}_r(s) = \bar{E}_0(s)R(s)$, and $R(s)$ is the Fresnel reflection coefficient and is of the same form as for an incident wave with harmonic time dependence $e^{i\omega t}$. It then follows that [2]

$$R(s) = \frac{\gamma_1^2 C - \gamma_0(\gamma_1^2 - \gamma_0^2 S^2)^{1/2}}{\gamma_1^2 C + \gamma_0(\gamma_1^2 - \gamma_0^2 S^2)^{1/2}} \qquad (3)$$

where $C = \cos\theta, S = \sin\theta, \gamma_1^2 = \mu_0 s(\sigma + s\epsilon)$, and $\gamma_0^2 = \mu_0 \epsilon s^2$. Formally, the reflected field is now specified in terms of the relative refractive index $(\epsilon/\epsilon_0)^{1/2}$, the ratio σ/ϵ, and the angle of incidence θ. The essential task is to evaluate the integral in equation (2) having specified $E_0(t)$. It will be shown that for special cases this can be done quite readily if we assume $E_0(t)$ to be in the form of a step-function. Again this does not constitute any loss of generality, since more complex forms of $E_0(t)$ can be treated by the principle of superposition.

Solution For Special Cases

When $E_0(t) = E_0 u(t)$, $u(t) = 1$ for $t > 0$ or 0 for $t < 0$, and $\epsilon = \epsilon_0$, it follows that

$$\bar{E}_0(s) = E_0/s \qquad (4)$$

and

$$R(s) = 1 - \frac{2C^2 - 2}{2C^2 - 1}\frac{s}{s+\beta} - \frac{2C^2}{(2C^2-1)}[(s^2 + \delta s)^{1/2} - s]\left[1 + \frac{\alpha - \beta}{s + \beta}\right] \qquad (5)$$

where

$$\alpha = \sigma/\epsilon, \qquad \beta = \frac{\alpha C^2}{2C^2 - 1},$$

and $\delta = \alpha/C^2$. The inversion of this transform can be carried out if use is made of the convolution theorem

$$\frac{f(s)}{s+\beta} \doteqdot \int_0^t e^{-\beta(t-x)} F(x)\, dx \qquad (6)$$

where

$$f(s) = \frac{(s^2 + \delta s)^{1/2}}{s} - 1 \doteqdot F(t) \qquad (7)$$

The function $F(t)$ is given in Campbell's and Foster's tables [3]:

$$F(t) = (\delta/2)e^{-\delta t/2}[I_1(\delta t/2) + I_0(\delta t/2)] \qquad (8)$$

It then follows that

$$E_r(t) = 1 - \frac{2C^2 - 2}{2C^2 - 1} e^{-\beta t} - \frac{2C^2}{\alpha(2C^2 - 1)} \left[F(t) + (\alpha - \beta) \int_0^t e^{-\beta(t-x)} F(x)\, dx \right] \qquad (9)$$

which is usable for $C^2 \neq 1$ or $1/2$. For the case of normal incidence ($C = 1$) for $\epsilon \neq \epsilon_0$, it easily follows from equation (3) that

$$\bar{E}_r(s) = \frac{E_0}{s} \frac{(s+\alpha)^{1/2} - s^{1/2}}{(s+\alpha)^{1/2} + s^{1/2}} \qquad (10)$$

and therefore [3]

$$E_r(t) = 1 - e^{-\alpha t/2}[I_1(\alpha t/2) + I_0(\alpha t/2)] \qquad (11)$$

This result can also be obtained from equation (9) if C is allowed to approach one. Another special case for $\epsilon = \epsilon_0$ is when $C^2 = 1/2$, whence

$$\bar{E}_r(s) = \frac{E_0}{s} \frac{(s+\alpha) - [s(s+2\alpha)]^{1/2}}{(s+\alpha) + [s(s+2\alpha)]^{1/2}} \qquad (12)$$

which can be rewritten

$$\bar{E}_r(s) = \frac{E_0}{s} \left[\frac{(s+2\alpha)^{1/2} - s^{1/2}}{(s+2\alpha)^{1/2} + s^{1/2}} \right]^2 \qquad (13)$$

The inverse transform of the square bracket term is known [3], so it follows that

$$E_r(t) = 2E_0 \int_0^t e^{-\alpha x} \frac{I_2(\alpha x)}{x}\, dx \qquad (14)$$

The general case

Apparently, for values of $\epsilon > \epsilon_0$ and $C \neq 1$, it is not possible to obtain formulas in closed form for $E_r(t)$; however, series formulas can be obtained for both large and small values of t.

For the general case, the inverse Laplace transform of the reflected field is

$$\frac{\bar{E}_r(s)}{E_0} = \frac{1}{s} \frac{(s+\alpha) - \eta(s^2 + \delta_1 s)^{1/2}}{(s+\alpha) + \eta(s^2 + \delta_1 s)^{1/2}} = A(s) \qquad (15)$$

where $\eta = (1/NC)[1 - (S^2/N^2)]^{1/2}$, $\delta_1 = \alpha N^2(N^2 - S^2)^{-1}$, $N^2 = \epsilon/\epsilon_0$. It is now assumed that $A(s)$ can be represented in the form

$$A(s) = \frac{a_1}{s} + \frac{a_2}{s^2} + \frac{a_3}{s^3} + \cdots \qquad (16)$$

with

$$a_n = \lim_{s\to\infty} s^n\left[A(s) - \frac{a_1}{s} - \frac{a_2}{s^2} \cdots - \frac{a_{n-1}}{s^{n-1}}\right] \quad \ldots\ldots\ldots\ldots(17)$$

and then the transient response is given by

$$E_r(t) = E_0\left[a_1 + a_2 t + \frac{a_3 t^2}{2!} \cdots + \frac{a_{n+1} t^n}{n!} \cdots\right] u(t) \quad \ldots\ldots\ldots(18)$$

The coefficients of this series are quite complicated and need not be written out in full here. Retaining the first two terms only, the series is given by

$$E_r(t) = E_0 \frac{N^2C - (N^2 - S^2)^{1/2}}{N^2C + (N^2 - S^2)^{1/2}}\left\{1 + \left[\frac{2C(N^2 - S^2)^{1/2} - N^2(N^2 - S^2)^{-1/2}}{N^4C^2 - (N^2 - S^2)}\right] N^2\alpha t + \cdots\right\} u(t) \quad \ldots\ldots(19)$$

which for normal incidence reduces to

$$E_r(t) = E_0 \frac{N-1}{N+1}\left[1 + \frac{N}{N^2-1}\alpha t + \cdots\right] u(t) \quad \ldots\ldots\ldots(20)$$

The asymptotic behaviour of $E_r(t)$ for large t is determined by the singularities of $\bar{E}_r(s)$ at the branch points $s = 0$, $s = -\delta$, and a pole which lies on the real axis, at $s = -\gamma$ where $\alpha < \gamma < \delta_1$, since α, η, and δ_1 are real and positive. Since the contributions from the branch point at $s = -\delta$ is of the order $e^{-\delta t}$ and the residue of the pole is of the order $e^{-\gamma t}$, the only singularity that need be considered is the branch point at $s = 0$ [4].

Near $s = 0$, $\bar{E}_r(s)$ can be represented in the form

$$\frac{s\bar{E}_r(s)}{E_0} = 1 + A_1 s^{1/2} + A_2 s^{3/2} \cdots + A_n s^{n-1/2} + B_1 s + B_2 s^2 + \cdots B_n s^n + \cdots \quad (21)$$

Then [4]

$$\frac{E_r(t)}{E_0} \sim 1 + \frac{1}{(\pi t)^{1/2}}\left[A_1 - \frac{A_2}{2t} + \frac{1\cdot 3\ A_3}{(2t)^2} - \frac{1\cdot 3\cdot 5\ A_4}{(2t)^3} \cdots \cdots (-1)^{n-1}(1\cdot 3 \cdots 2n-3)\frac{A_n}{(2t)^{n-1}}\right] \quad \ldots\ldots(22)$$

The coefficients are found in the usual manner. Retaining only the first two terms, the transient response for large times is given by

$$\frac{E_r(t)}{E_0} \sim 1 - \frac{2}{NC(\pi\alpha t)^{1/2}} + \text{terms containing } t^{-3/2}, t^{-5/2}$$

etc., which for the case $N = 1.0$ agree with equations (9) and (11) in the asymptotic sense.

Presentation of results

Employing the formulas developed in the previous section, the transient response $E_r(t)/E_0$ is plotted as a function of αt for various values of N in Figures 2 to 5. The curves in Figure 2 correspond to $N^2 = 1$ and for the case $\theta° = 0$ ($C = 1$) the response can be plotted from equation (11), employing the tabulated

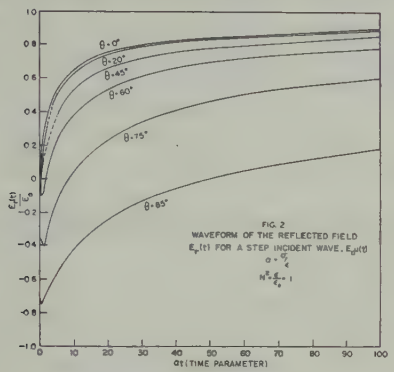

FIG. 2
WAVEFORM OF THE REFLECTED FIELD
$E_r(t)$ FOR A STEP INCIDENT WAVE. $E_{inc}(t)$
$\alpha = \frac{\sigma}{\epsilon}$
$N^2 = \frac{\epsilon_r}{\epsilon_0} = 1$

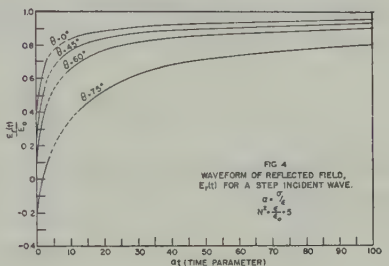

FIG. 4
WAVEFORM OF REFLECTED FIELD,
$E_r(t)$ FOR A STEP INCIDENT WAVE.
$\alpha = \frac{\sigma}{\epsilon}$
$N^2 = \frac{\epsilon_r}{\epsilon_0} = 5$

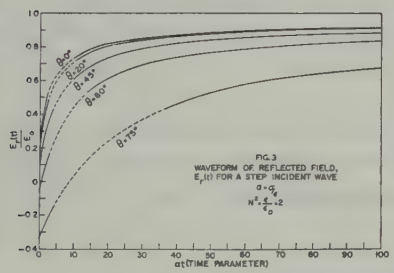

FIG. 3
WAVEFORM OF REFLECTED FIELD,
$E_r(t)$ FOR A STEP INCIDENT WAVE
$\alpha = \sigma_{\epsilon}$
$N^2 = \frac{\epsilon_r}{\epsilon_0} = 2$

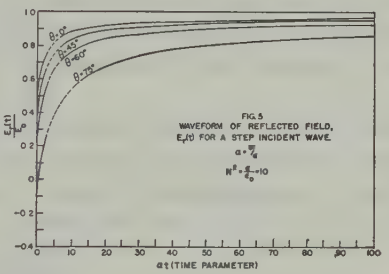

FIG. 5
WAVEFORM OF REFLECTED FIELD,
$E_r(t)$ FOR A STEP INCIDENT WAVE.
$\alpha = \frac{\sigma}{\epsilon}$
$N^2 = \frac{\epsilon_r}{\epsilon_0} = 10$

values of the Bessel functions. The curves for the cases $\theta = 20°$ and $\theta = 45°$ were drawn by using the power series for small times and the asymptotic series for large times. The intermediate region where neither of these series is satisfactory can be filled in by interpolation and is shown by the dashed portion of the curves. For the cases $\theta = 60°$, 75°, and 85°, the convergence of the power series is very poor, so numerical integrations of equation (9) were performed for αt in the range from 0 to 50. The remaining portions of the curves were drawn in by using the asymptotic series for large αt.

The curves in Figures 3, 4, and 5 for $N^2 = 2$, 5, and 10, respectively, were all computed by the power series for small t and the asymptotic series for large t. Again the intermediate regions were filled in by employing interpolation and are indicated by the dashed portions on the curves.

The shape of these transient response curves is rather interesting. The value of the ordinate at $t = 0$ is equal to the Fresnel reflection coefficient at the plane interface of a lossless homogeneous medium whose relative dielectric constant is N^2. As αt increases, the effect of the finite conductivity of the medium becomes noticeable, and in the limiting case as αt approaches infinity the reflection coefficient approaches unity. It should be noted, however, that the departure of the reflection

coefficient from unity is still quite significant for values of αt as large as 100, particularly for large angles of incidence.

An application

An interesting application of these results is to the study of the waveform of a short pulse of electromagnetic energy incident obliquely on a sharply bounded dissipative medium. Again, it is assumed that the electric vector is in the plane of incidence and, for convenience, the incident electric field $E_0(t)$ is considered to be rectangular in shape, so that

$$E_0(t) = \frac{E_0}{\alpha t_0} [u(t) - u(t - t_0)] \quad \ldots\ldots (24)$$

where t_0 is the pulse length. It should be noted here that in the limiting case where t_0 approaches zero

$$E_0(t) = \frac{E_0}{\alpha} \delta(t) \quad \ldots\ldots (25)$$

where $\delta(t)$ is the unit impulse or "Dirac" function. The transient response $E_r(t)$, for a source as specified by equation (24), is then obtained from the step function response by employing the principle of superposition. The response for the impulsive source is obtained by differentiation with respect to time of the step function response.

The transient response function $E_r(t)$ for $\theta = 45°$ is then plotted in Figure 6 for pulse lengths t_0 of $0.1/\alpha$, $0.3/\alpha$, $1/\alpha$, $3/\alpha$, and $10/\alpha$. The impulse response is also shown for comparison. It is not surprising that the shape of the waveform of the reflected field is almost independent of pulse length for t_0 less than about $1/\alpha$.

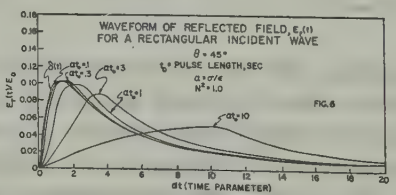

If the source of the incident wave is a lightning channel then, as a first approximation, we could regard the ionosphere as a sharply bounded conducting medium whose height is about 70 km [5]. For an angle of incidence of 45°, the point of reflection is of the order of 100 km from the source, and it can be expected that the wavefront of the incident wave is almost plane. Furthermore, the electric field vector is essentially in the plane of incidence, and the pulse is usually of a double exponential form and could be roughly approximated by a rectangular form with a width of about 50 microseconds [6]. For the ionosphere, the dielectric constant and conductivity are in general tensors, but if the effect of the earth's magnetic field can be neglected the medium can be regarded as isotropic for long waves [7]. If ω is the angular frequency of a spectral component of the exciting field, then it can be further assumed that $\omega \ll \nu$, where ν is the collision frequency, which itself is of the order of 10^7 sec^{-1}. This latter assumption is probably well

justified with reference to the transient responses for times greater than a microsecond following the trailing edge of the source pulse. With these approximations, it follows that the complex dielectric constant of the ionosphere at the point of reflection for long waves [7] is given by

$$\frac{\epsilon}{\epsilon_0}\left(1 - i\frac{\sigma}{\epsilon\omega}\right) \simeq 1 - i\frac{\omega_r}{\omega}$$

where $\omega_r \simeq 4\pi N_0 e^2 m\nu$, with e = charge on the electron, m = mass of the electron, and N_0 = number of electrons per cc. Therefore, it can be seen that $\alpha = \omega_r$ and $N = 1$ in the earlier notation. A typical value of ω_r (or α) is 6×10^3 sec^{-1}. Furthermore, the waveforms in Figure 6 for $\alpha t_0 = 0.3$ then correspond to a pulse length of 50 microseconds, which, as mentioned, is typical of the duration of the electric field of the lightning channel.

The transient curves for values of N greater than one also have a possible significance in connection with lightning discharges, since they would correspond to the ionospherically reflected wave incident on a homogeneous conducting ground. In this case, the appropriate value of α would be of the order of 10^8 for a typical soil with N^2 of the order of 5 or 10.

The analysis of many successive reflections between the ground and the ionosphere could be treated by the superposition of the individual responses at each reflection, but the procedure would soon become very complicated. It is more convenient to regard the propagation in this case in terms of the wave-guide modes, as discussed in detail by Budden [7].

It is possible that the results given in this paper also would have application to the reflection of transients at junctions in transmission lines and wave guides.

Acknowledgment

We would like to thank Lorne Campbell, who checked the equations in this paper.

References

[1] R. V. Churchill, Operational mathematics in engineering, New York, McGraw-Hill Book Co., Inc. (1944).

[2] J. A. Stratton, Electromagnetic theory, New York, McGraw-Hill Book Co., Inc., pp. 490 *et seq.* (1941).

[3] G. A. Campbell and R. M. Foster, Fourier integrals for practical application, New York, Van Nostrand Co., Inc. (1948).

[4] H. S. Carslaw and J. C. Jaeger, Operational methods in applied mathematics, London, Oxford University Press, Chap. 13 (1950).

[5] K. G. Budden, The propagation of low frequency waves to great distances, Phil. Mag., **44**, 504-513 (1953).

[6] R. B. Morrison, The variation with distance in the range 0-100 km of atmospheric waveforms, Phil. Mag., **44**, 980-986 (1953).

[7] K. G. Budden, The propagation of a radio atmospheric, Phil. Mag., **42**, 1-19 (1951).

INTERNATIONAL DATA ON MAGNETIC DISTURBANCES, THIRD QUARTER, 1954

This report continues the series which has appeared regularly in this JOURNAL since Vol. 54, No. 3, 295 (1949). Please refer to that first report for an explanation of the data given, and to Vol. 59, No. 3, 423 (1954) for the definition of Ap.

Preliminary Report on Sudden Commencements

S.c.'s given by five or more stations are in italics. Times given are mean values, with special weight on data from quick-run records.

Sudden commencements followed by a magnetic storm or a period of storminess (s.s.c.)

1954 July 17d 21h 08m: SJ Te.
1954 August: No s.s.c.
1954 September 29d 09h 42m: Ma SM Ci.

Sudden commencements of polar or pulsational disturbances (p.s.c.)

1954 July 03d 22h 40m: Tl Ta.—04d 23h 10: MB Bi.—05d 21h 31: Bi El.—06d 00h 18: Ta Te.—07d 21h 48: Ma CF.—10d 22h 48: CF Bi El.—*10d 23h 40:* six.—11d 22h 00: Tr Eb Bi.—*11d 23h 19:* six.—*12d 23h 07:* nineteen.—13d 23h 34: Eb Bi.—14d 02h 50: CF SM.—15d 01h 01: Ta Te.—15d 04h 00: CF Eb MB.—16d 12h 18: Ka To.—*17d 23h 40:* seven.—19d 18h 16: SM Ta.—19d 19h 42: CF Eb Tn Hr.—*24d 00h 24:* eight.—24d 00h 48: Ci Ta.—24d 18h 42: Ka Qu.—27d 11h 41: To Am.—27d 21h 37: CF Ta.—28d 16h 40: Ci Ta To Te.—30d 23h 16: Le Wn CF.—30d 23h 38: Le Bi.—31d 03h 40: SM Te.—31d 22h 03: Eb Ta Bi Hr.

1954 August *03d 20h 03m:* five.—04d 19h 49: Le CF.—05d 02h 01: MB Bi.—*05d 22h 41:* five.—*06d 20h 33:* ten.—06d 20h 47: SF Bi.—*09d 19h 34:* seven.—12d 00h 00: CF Bi.—13d 05h 22: SM Va.—*14d 00h 08:* six.—*14d 23h 16:* fifteen.—15d 18h 56: Do Fu.—*15d 19h 12:* five.—16d 22h 16: So Ta.—18d 13h 00: Ka To.—19d 00h 13: CF Eb Bi.—19d 23h 15: CF SM T1 SF.—19d 23h 46: MB Bi El.—21d 01h 08: MB Bi.—21d 04h 50: Ta MB.—21d 10h 16: To Am.—22d 00h 09: Do Wi Ma Ta.—*22d 01h 05:* sixteen.—22d 04h 51: Wn SM.—23d 00h 58: SM Ta.—24d 13h 18: Ka Am.—*24d 19h 44:* six.—*26d 04h 44:* five.—27d 00h 36: SM Ci Bi.—27d 23h 01: CF Ta.—*28d 23h 31:* fourteen.—28d 23h 48: Tr El.—29d 18h 19: So Qu.—30d 18h 00: Qu Tn.—31d 18h 05: So SM.

1954 September *01d 23h 35m:* six.—02d 06h 00: SM Ta.—02d 15h 44: Ka Qu.—02d 22h 32: CF Ta.—03d 11h 01: Ka Ap Am.—*03d 23h 18:* eleven.—05d 00h 36: SM Ci.—05d 18h 26: So Ta.—06d 00h 18: CF Ta Bi.—*06d 19h 00:* seven.—*07d 20h 33:* fourteen.—*09d 21h 10:* eight.—11d 07h 08: Ap Am.—*12d 19h 35:* five.—

12d 22h 29: CF Tl Bi.—13d 21h 55: Le Wn CF Bi.—*13d 22h 20:* thirteen.— *14d 22h 09:* nineteen.—15d 17h 42: Wn Qu.—*16d 00h 48:* five.—17d 01h 00: Ta Bi.—17d 19h 39: So Wn CF Qu.—17d 23h 21: Ma Ta.—*18d 00h 37:* seven.—*18d 21h*

TABLE 1—*Geomagnetic planetary three-hour-range indices Kp, preliminary magnetic character-figures C, average amplitudes Ap (unit 2_γ), and final selected days, July to September, 1954*

July 1954

E	1	2	3	4	5	6	7	8	Sum
1	4 −	4 −	3 +	2 −	2 +	1o	1o	1 −	17 +
2	0o	1 +	1o	0o	2o	1 −	1 +	2 −	8o
3	1 −	2 −	1 +	0 +	1 −	1 −	0 +	2 −	7 +
4	1 −	1 −	1 −	1 −	2 −	0 +	0 +	0 +	5 +
5	0 +	1o	1 +	1o	1 +	2o	2 −	1 +	10o
6	2 −	2o	3o	2 +	2o	2o	2 +	3 −	18o
7	2 +	1o	1 +	3 +	1 +	1o	1o	1 +	13 −
8	1o	1 −	1 −	2o	2 −	1 +	2o	1o	10 +
9	2o	1o	1 −	0 +	1 −	0 +	1 −	1o	7 −
10	1o	1o	2 −	1o	1o	1o	1 −	2 −	9o
11	1 +	2o	2 −	1o	1 −	1 −	1 −	1o	9o
12	2o	1 +	1 +	1 +	2 +	3o	2 −	3 +	16 +
13	2 −	1o	1 +	2 −	1 +	1o	1o	2 −	11 −
14	2o	4 −	3o	3 −	3 −	1 +	2o	2o	20o
15	1o	1 +	3 +	4 −	3 +	2o	1o	1o	17 −
16	1o	1 −	1 +	2 −	2o	2o	4 −	2 +	15 −
17	1 +	3o	3 +	1o	0 +	0 +	1 −	4 −	14 −
18	5 −	3 +	2o	1o	1 +	1 +	1 +	2 −	17 −
19	2 +	1 +	1o	2 −	2 +	3 −	4 −	2o	17o
20	3 −	3 −	3 −	2o	1 +	1 +	0 +	1 −	14 −
21	1o	2 −	2o	1o	1 +	3 −	2 +	2 +	14 +
22	1 +	1 −	2o	1 +	2 −	1 −	1o	0 +	9o
23	0o	1 +	1 +	3 −	1 +	1 +	1 +	1 +	11 −
24	3 +	3o	2 +	2 −	2o	1 −	1 +	1o	15 +
25	2 +	3o	4 −	3 +	3 −	2o	1 +	2 −	20o
26	2 −	2 −	2 +	2 +	3 +	2o	1o	2 −	16o
27	3o	3 +	2 −	2o	2 +	2o	2o	3o	19 +
28	2o	4o	2 +	4 −	4o	4o	2 +	2 +	25 −
29	3o	3 −	3 −	3o	2 +	2 −	2o	1 −	18o
30	3o	1 −	1 −	2 −	2o	2o	1 −	2 −	12 +
31	1 +	2 −	3o	2 −	3 −	1 +	2 −	2 +	16 −

August 1954

1	2	3	4	5	6	7	8	Sum
1 +	1 +	2 −	4 −	3 +	2 +	2o	1 +	17o
2 +	3 +	2o	2 +	1 −	1 +	2 −	1 −	14 +
1 −	1o	1 −	3 −	1o	1 −	2o	2 −	10 +
1o	2 −	3o	1 −	2o	1 +	2o	1 −	12 +
2 −	2 −	1 −	1 −	1 +	2 −	2o	3 −	12 +
2 +	3 −	4 −	2 +	3o	2 −	4 +	4o	24o
3 −	0 +	1 +	3o	3o	3 +	3o	2 +	19o
2o	1o	2o	2 +	2o	1 +	0 +	1o	12o
2 −	1o	2 +	1 −	4 −	3 −	2o	3 −	17 −
3 −	1 +	3 −	1o	1 −	2o	1o	2o	13 +
3o	2o	2 +	2 −	1 +	2 −	1 +	1o	14 +
3 −	2o	2o	2 +	1 +	1 −	1 +	1 +	14 −
0 +	2 −	2o	2o	2 −	2 +	2 −	1o	13 −
3o	1 +	2 +	2o	1o	1o	2 −	2 +	15 −
2 +	1 −	1 +	1o	1o	1o	3 +	3 −	13 +
1 +	2 −	3o	3 +	4 −	2 +	2 −	2o	19o
2 −	2o	3 +	3o	2o	1 +	2 −	1 +	16 +
2 −	2 +	2 +	3o	3 −	2o	2 +	2 −	18o
4 −	2 +	2o	1 +	1 +	2 −	2o	3 −	17o
2 +	3 −	2o	1o	2 −	2o	1o	1o	14 −
1 +	3o	4o	4 +	2 +	1 +	2 −	1 +	19 +
4 +	5o	3 +	2 −	2 −	1 +	1o	3o	21 +
3 −	1o	0 +	2 −	2 −	2 −	3o	3 −	15 −
3 +	3 −	4 −	3o	5o	3o	3 +	3 +	27 +
4 −	2o	2 +	2 −	1o	1o	1o	1 +	14o
1 +	5 −	4 +	2 +	2 +	2 +	3 −	3 −	23 −
5o	2 +	2 +	3o	1o	2 −	3 −	3 −	21 −
3o	4o	2o	3 −	3o	2 +	2 −	4 −	22 +
3 +	4 −	4 −	4 −	2 +	2 −	3 −	2 +	23 +
3 −	2o	3 −	2o	3 −	3 −	2o	1 +	18o
2o	2o	2o	1o	1 +	2 +	3o	3o	17 −

September 1954

E	1	2	3	4	5	6	7	8	Sum
1	3 −	3o	2 +	3 +	5 −	4o	4 +	6 −	30o
2	5 +	4 +	4o	4 −	1o	3 −	2 +	3 +	27 −
3	2o	2 +	3o	4 +	4o	4 +	4 +	5 −	29o
4	4 −	3 +	3o	3 +	3 +	4o	1o	2o	24 −
5	3o	3o	3o	3 +	3 −	2 −	2o	1 +	20o
6	3 −	2 +	2 +	1 +	2 −	4 +	6 −	4o	24 +
7	3o	4 −	4 −	3o	2 +	3 +	3 +	3o	25 +
8	3o	2o	1 −	1 +	2o	3 −	3o	1o	16 −
9	1 +	4o	4 −	2 −	3 +	3o	1 +	3 −	21o
10	2 −	3 +	3o	3 −	2 +	2o	1 +	2o	18 +
11	2 −	3 −	3o	3 +	3o	3 +	2 −	2o	21 −
12	0 +	1 −	2 −	3 −	2 −	1 +	1 +	2o	12 −
13	2o	1 −	2 −	2 −	1o	1 −	1o	4 +	13o
14	4 −	6 −	4 +	3 +	5o	3 +	2o	4 +	32 −
15	2 +	2 +	3 +	4o	4 −	3o	2 −	2 +	23 −
16	4 +	4o	3 +	4 −	4o	3o	3o	2 +	28 −
17	4o	3 −	2 −	2o	0 +	1 −	2 +	3 −	16 +
18	4o	2 +	3 +	3 +	1o	3 −	3 −	3o	22 +
19	2 +	3 −	3o	1 +	2 −	2o	2 +	2 +	18 −
20	4 −	4o	4o	3o	5 −	6o	7 −	5 −	37 −
21	4o	4 +	4 −	4o	4 −	4 +	4 +	3 −	31o
22	2 +	2 +	2 +	3 −	4 −	2 +	2 +	2 −	20 −
23	2 −	1o	3o	3 +	2o	1 +	1o	1o	14 +
24	2o	2o	2 −	2 −	1 +	3 −	2o	4o	17 +
25	3 −	3 +	4 −	3 −	3o	3o	4 +	2 +	25o
26	3o	3 −	3o	2o	2 +	2 −	2 +	2 −	19 −
27	2 −	2o	2 −	2o	2 −	3o	4o	3 +	19 +
28	5o	4 −	3 +	3 −	3o	2o	1 +	2 +	23 +
29	4o	4o	3 −	4 −	3 −	5 −	5o	5 +	32o
30	2 −	4o	4 −	4 −	2 +	2 +	4 −	4o	25 +
31									

Preliminary *C*, 1954		
July	Aug.	Sep.
0.7	0.6	1.2
0.2	0.3	1.0
0.1	0.2	1.2
0.1	0.4	1.0
0.3	0.3	0.8
0.8	1.1	1.3
0.4	0.8	1.0
0.3	0.2	0.5
0.1	0.8	0.8
0.1	0.4	0.5
0.2	0.3	0.8
0.7	0.3	0.2
0.3	0.4	0.7
0.8	0.5	1.4
0.7	0.6	0.9
0.6	0.8	1.0
0.7	0.4	0.7
1.0	0.6	0.9
0.7	0.6	0.5
0.4	0.3	1.6
0.4	0.9	1.3
0.2	1.0	0.7
0.3	0.6	0.3
0.6	1.2	0.6
0.8	0.3	1.0
0.6	0.8	0.5
0.8	0.9	0.8
1.1	0.9	0.9
0.7	1.0	1.4
0.4	0.8	1.0
0.6	0.6	

Average amplitude *Ap*		
July	Aug.	Sep.
11	10	27
4	8	22
4	5	24
3	6	16
5	6	12
9	16	21
7	11	17
5	6	8
4	9	14
4	7	10
4	7	12
9	7	6
5	6	8
12	7	30
10	7	14
8	11	21
9	9	10
11	9	14
9	9	9
7	7	45
7	13	26
4	17	11
5	8	8
8	21	10
12	8	17
8	16	10
10	14	12
17	14	17
10	15	30
6	9	18
8	9	

TABLE 1 (Concluded)—*Final selected days, July to September, 1954*

Month	Five quiet days	Ten quiet days	Five disturbed days
July	2 3 4 9 10	2 3 4 5 8 9 10 11 13 22	1 14 25 27 28
August	3 4 5 8 13	3 4 5 8 10 11 12 13 15 20	6 22 24 26 29
September	8 12 13 19 23	8 10 12 13 17 19 22 23 24 26	1 14 20 21 29

52: five.—*20d 02h 19:* eight.—20d 19h 48: Ta Bi.—21d 23h 10: SM Ta.—24d 21h 16: Tr So Fu.—*24d 21h 59:* eight.—*27d 18h 20:* eight.—28d 01h 35: Wn CF Tl SM.—30d 10h 00: Ka Am.—30d 18h 59: Do SM Qu.—*30d 23h 29:* sixteen.

Sudden impulses found in the magnetograms (s.i.)

1954 July 16d 19h 58m: SM Ci Te Bi.—17d 23h 08: Do SM Ta Bi.—18d 00h 00: Ta Tn Hr.—*18d 01h 56:* seven.—18d 04h 48: Do Ka.—18d 08h 15: Ta Te Hr.—*19d 14h 56:* seven.

1954 August 04d 04h 16m: Bi El.—09d 12h 16: SM Hu Hr.—16d 08h 04: Ta Hr.—27d 11h 29: Tr Le Wi Te.

1954 September 03d 19h 09m: Ka Qu Hr.—*14d 14h 12:* seven.—*29d 19h 53:* seven.

Preliminary Report on Solar-flare Effects

Effects confirmed by ionospheric or solar observations are in italics.

1954 July 06d 17h 43m–17h 53m: Te.—07d 13h 35–13h 40: Te.—10d 21h 31–21h 42: Te.—11d 13h 08–13h 19: Te.—13d 13h 30–13h 36: Te.—14d 14h 16–14h 27: Te.—14d 22h 35–22h 53: Te.—19d 13h 00–13h 06: SM.—20d 14h 36–14h 44: Te.—21d 13h 45–13h 54: Te.—22d 13h 33–13h 42: Te.—24d 13h 30–13h 40: Te.—26d 13h 40–13h 47: Te.—26d 16h 42–16h 48: Te.—28d 17h 34-17h 45: Te.—28d 18h 07–18h 13: Te.—30d 14h 38–14h 43: Te.

1954 August 02d 08h 08m–08h 13m: SM.—03d 09h 20: El.—06d 20h 14–22h 08: Ch.—07d 20h 18–20h 27: Ch.—07d 22h 53–23h 01: Ch.—09d 12h 00: Bi.—17d 14h 18–15h 07: Ch.—18d 12h 26–12h 45: Ch.—28d 08h 59: Bi.—28d 16h 47–16h 53: Ch.—30d 19h 11–19h 19: Ch SJ.—31d 09h 43–09h 50: SM.

1954 September 02d 12h 50m–12h 55m: SM.—08d 14h 53–14h 58: Ch.—12d 10h 24: Bi.—19d 16h 10–16h 37: Ch.

Ionospheric or solar disturbances without clear geomagnetic effect

None.

Minor disturbances reported by one station only are listed in the De Bilt quarterly circular, but omitted here.

COMMITTEE ON CHARACTERIZATION OF MAGNETIC DISTURBANCES

J. BARTELS, *Chairman*
University
Göttingen, Germany

J. VELDKAMP
Kon. Nederlandsch Meteorologisch Instituut
De Bilt, Holland

PROVISIONAL SUNSPOT-NUMBERS FOR OCTOBER TO DECEMBER, 1954

(Dependent on observations at Zurich Observatory and its station at Locarno and Arosa)

Day	Oct.	Nov.	Dec.
1	0	0	0
2	7	0	0
3	14	0	0
4	8	0	0
5	7	0	0
6	0	7	0
7	0	8	0
8	0	7	0
9	0	24	0
10	0	36	0
11	0	44	0
12	7	38	0
13	7	37	0
14	15	23	0
15	17	9	11
16	24	7	18
17	22	7	17
18	7	7	14
19	8	7	19
20	14	0	19
21	8	0	14
22	8	0	7
23	14	0	7
24	8	0	15
25	8	0	10
26	7	0	7
27	0	0	0
28	0	0	0
29	0	0	13
30	0	0	29
31	0		25
Means.....	6.8	8.7	7.3
No. days.....	31	30	31

Mean for quarter: 7.6 (92 days)
Mean for year 1954: 4.2 (365 days)

M. WALDMEIER

SWISS FEDERAL OBSERVATORY
Zurich, Switzerland

CHELTENHAM THREE-HOUR-RANGE INDICES *K* FOR OCTOBER TO DECEMBER, 1954

[$K9 = 500\gamma$; scale-values of variometers in γ/mm: $D = 5.4$; $H = 2.4$; $Z = 4.3$]

Gr. day	October 1954		November 1954		December 1954	
	Values *K*	Sum	Values *K*	Sum	Values *K*	Sum
1	5753 2432	31	4433 4444	30	2321 0112	12
2	3320 0113	13	5423 3233	25	2122 2113	14
3	5432 2334	26	4443 2221	22	2122 0112	11
4	5423 2322	23	2312 1112	13	0012 1021	7
5	1312 0232	14	3333 1110	15	2111 1111	9
6	2343 4322	23	2222 1121	13	2112 0122	11
7	2322 3222	18	2211 0111	9	3232 1212	16
8	3331 3223	20	2001 1111	7	2311 1001	9
9	1320 0112	10	1221 1221	12	2232 2021	14
10	2322 1021	13	2111 0000	5	1221 1020	9
11	2232 1100	11	2212 2111	12	1000 0110	3
12	0000 0000	0	2412 2121	15	0231 1223	14
13	1011 0012	6	2210 1221	11	2211 1121	11
14	1112 1121	10	2311 1122	13	2000 0110	4
15	2123 1011	11	1000 0010	2	0001 0000	1
16	1021 2321	12	0000 0000	0	0100 0010	2
17	2221 1123	14	0121 1111	8	1243 3323	21
18	4455 4413	30	1112 1223	13	4412 1113	17
19	3433 3223	23	2421 1223	17	2221 2212	14
20	4234 3213	22	3233 3222	20	1333 3223	20
21	2033 1110	11	3223 2113	17	2111 2222	13
22	1232 2233	18	3342 1111	16	3111 0010	7
23	4233 3334	25	2412 2432	20	1212 1101	9
24	5454 3444	33	2232 0120	12	1110 0121	7
25	4533 3212	23	2232 1113	15	1021 1211	9
26	3232 1232	18	2221 2112	13	1110 1012	7
27	1335 3321	21	1322 1221	14	4213 5122	20
28	3211 1211	12	2111 2113	12	2313 1222	16
29	1112 0013	9	1112 3323	16	1222 1111	11
30	5521 2213	21	3521 2223	20	1222 1112	12
31	1223 2234	19			1111 1111	8

J. B. CAMPBELL
Observer-in-Charge

CHELTENHAM MAGNETIC OBSERVATORY
Cheltenham, Maryland, U.S.A.

PRINCIPAL MAGNETIC STORMS

(Advance knowledge of the character of the records at some observatories as regards disturbances)

Observatory (Observer-in-Charge)	Greenwich date	Storm-time		Sudden commencement				C-figure, degree of activity[4]	Maximal activity on K-scale 0 to 9			Ranges		
		GMT of begin.	GMT of ending[1]	Type[2]	Amplitudes[3]				Gr. day	Gr. 3-hr. period	K-index	D	H	Z
					D	H	Z							
(1)	(2)	(3)	(4)	(5)	(6)	(7)	(8)	(9)	(10)	(11)	(12)	(13)	(14)	(15)
	1954	*h m*	*d h*		′	γ	γ					′	γ	γ
llege	Oct. 1	02 ..	1 20	.....	....	....	....	ms	1	2,3	6	120	1150	700
C. J. Beers)	Oct. 18	01 ..	18 23	.....	....	....	....	ms	18	4,5	7	320	1450	810
	Oct. 23	07 36	25 17	.....	....	....	....	ms	24	4	6	200	1390	1130
	Nov.	None												
	Dec.	None												
tka	Oct. 1	02 30	2 07	.....	....	....	....	ms	1	2	7	68	648	459
C.L.Skillman)	Oct. 18	00 30	18 23	.....	....	....	....	ms	18	3	7	68	470	571
	Oct. 23	07 23	25 16	.....	....	....	....	ms	24	4	7	105	678	583
									25	2	7			
	Nov.	None												
	Dec. 17	06 15	18 11	.....	....	....	....	ms	17	5	6	46	215	388
Vitteveen	July	None												
D.van Sabben)	Aug.	None												
	Sep. 1	10 00	4 24	.....	....	....	....	m	1	5,8	5	20	130	105
									2	1	5			
									3	6,7,8	5			
									4	6	5			
	Sep. 6	15 00	7 24	.....	....	....	....	ms	6	7	7	35	250	55
	Sep. 13	21 00	17 03	.....	....	....	....	ms	14	2	6	20	180	55
	Sep. 20	12 00	21 24	.....	....	....	....	ms	20	7	7	40	215	125
	Sep. 29	09 00	1 22	.....	....	....	....	ms	29	6,8	6	40	185	80
									30	6	6			
	Oct. 2	20 00	4 07	.....	....	....	....	ms	3	8	6	25	155	100
									4	1	6			
	Oct. 6	07 00	6 24	.....	....	....	....	ms	6	6	6	30	170	50
	Oct. 17	21 00	20 09	.....	....	....	....	ms	18	6	6	35	160	75
	Oct. 22	13 00	25 24	.....	....	....	....	ms	24	6	7	45	160	110
	Nov. 1	14 00	2 24	.....	....	....	....	ms	1	7	6	40	180	75
									2	1	6			
	Dec.	None												
heltenham	Oct. 17	21 ..	20 16	.....	....	....	....	m	18	3,4	5	29	111	42
J.B.Campbell)	Oct. 23	17 ..	25 13	.....	....	....	....	m	24	1,3	5	26	105	107
	Oct. 27	07 47	27 19	s.c.*	−1	+15	+2	m	27	4	5	18	85	33
	Nov. 1	14 ..	3 21	.....	....	....	....	m	2	1	5	22	109	48
	Dec. 17	06 18	18 06	s.c.	−1	+3	0	..	17	3	4	19	82	39
									18	1,2	4			
ucson	Sep. 30	19 00	1 19	.....	....	....	....	ms	1	2	6	17	105	15
M.L.Cleven)	Oct. 18	01 00	18 18	.....	....	....	....	m	18	3,4,5,6	5	15	112	14
	Oct. 23	07 00	25 13	.....	....	....	....	m	24	2,3,6	5	16	136	23
									25	1,2,3	5			
	Oct. 31	21 00	2 06	.....	....	....	....	ms	2	1	6	15	80	18
	Dec. 17	03 00	18 06	.....	....	....	....	m	17	3	5	13	92	9
an Juan	Oct.	None												
P. G. Ledig)	Nov.	None												
	Dec.	None												

[1]Approximate time of ending of storm construed as the time of cessation of reasonably marked disturbance movements in the aces; more specifically, when the *K*-index measure diminished to 2 or less for a reasonable period.

[2]s.c. = sudden commencement; s.c.* = small initial impulse followed by main impulse (the amplitude in this case is that of the *ain impulse only*, neglecting the initial brief pulse); . . . = gradual commencement.

[3]Signs of amplitudes of *D* and *Z* taken algebraically; *D* reckoned positive if towards the east and *Z* reckoned positive if verti-lly downwards.

[4]Storm described by three degrees of activity: *m* for moderate (when *K*-index as great as 5); *ms* for moderately severe (when = 6 or 7); *s* for severe (when *K* = 8 or 9).

PRINCIPAL MAGNETIC STORMS—Continued

Observatory (Observer-in-Charge)	Greenwich date	Storm-time GMT of begin.	Storm-time GMT of ending[1]	Sudden commencement Type[2]	Amplitudes[3] D	H	Z	C-figure, degree of activity[4]	Maximal activity on K-scale 0 to 9 Gr. day	Gr. 3-hr. period	K-index	Ranges D	H
(1)	(2)	(3)	(4)	(5)	(6)	(7)	(8)	(9)	(10)	(11)	(12)	(13)	(14)
	1954	*h m*	*d h*		′	γ	γ					′	γ
Instituto	Oct. 1	01 40	1 23	.....	....	....	....	m	1	6	5	7	175
Geofisco de	Oct. 17	22 59	18 19	.....	....	....	....	m	18	6,7	5	6	155
Huancayo	Oct. 22	18 49	25 06	.....	....	....	....	m	24	5,6	5	6	221
(A.A.Giesecke)	Nov. 23	05 03	23 22	.....	....	....	....	ms	23	6	6	4	219
	Dec. 17	00 08	18 05	.....	....	....	....	m	17	6	5	7	204
Vassouras	July	None											
(Lelio I. Gama)	Aug.	None											
	Sep.	None											
Hermanus	Oct. 17	21 ..	18 18	.....	....	....	....	m	18	4,5	5	16	94
(A.M.van Wijk)	Oct. 23	07 22	25 15	s.c.	0	+1	+1	m	24	6	5	20	104
	(*Note*: Small s.c. at $07^h\ 22^m$ followed by stronger movements at $07^h\ 24^m$)												
	Nov. 1	14 30	2 07	.....	....	....	....	m	1	7	5	15	75
	Nov. 23	11 45	23 22	s.c.	+1	+11	+11	m	23	6	5	7	72
	Dec.	None											
Watheroo	Oct. 18	03 ..	18 18	.....	....	....	....	m	18	4,5,6	5	16	87
(A. F. Tillott)	Oct. 23	07 22	25 16	s.c.*	....	+17	....	m	23	4,6,7,8	5	14	101
									24	4,5,6	5		
	Oct. 27	07 47	.. ..	s.c.	....	+14	....	(Minor activity only)					
	Nov.	None											
	Dec.	None											
Amberley	Oct. 1	02 ..	1 21	.....	....	....	....	m	1	2	5	16	72
(A.L.	Oct. 18	04 ..	18 18	.....	....	....	....	m	18	4,5	5	21	87
Cullington)	Oct. 23	07 23	25 15	s.c.	0	+24	0	m	23	4	5	20	147
									25	2	5		
	Oct. 27	07 46	27 18	s.c.*	0	+19	−1	m	27	4	5	15	62
	(*Note*: No *K*-index greater than 4 in November)												
	Dec. 17	03 ..	18 06	.....	....	....	....	m	17	3	5	17	100
	(*Note*: No record on December 13)												
	1953												
Heard Island	Jan. 5	05 30	7 03	.....	....	....	....	ms	5	4,5,8	7	125	1075
(J. A. Brooks)	Jan. 18	10 00	20 16	.....	....	....	....	m	20	1	5	39	307
	Jan. 24	08 00	24 24	.....	....	....	....	m	24	7	5	28	207
	Jan. 25	04 00	31 15	.....	....	....	....	ms	26	5,6,7	7	94	1154
									27	6,7	7		
									28	8	7		
									29	7	7		
	Feb. 22	15 00	28 24	.....	....	....	....	s	22	7,8	8	123	1308
									24	7	8		
	Mar. 1	20 04	4 04	s.c.	....	....	....	s	2	6	8	151	1066
	Mar. 8	13 20	11 04	.....	....	....	....	s	8	8	8	145	1191
									9	1,8	8		
	Mar. 19	00 00	20 03	.....	....	....	....	ms	19	8	6	68	516
	Mar. 20	18 08	29 03	s.c.	....	....	....	s	24	8	9	137	1417
	Apr. 3	15 00	4 24	.....	....	....	....	ms	3	8	6	69	575
									4	1,7	6		
	Apr. 16	01 00	17 04	.....	....	....	....	s	16	8	8	66	1004
	Apr. 18	18 30	24 01	.....	....	....	....	ms	21	1	6	57	505
	May 4	20 50	10 01	s.c.	....	....	....	ms	6	8	7	88	783
	May 14	20 00	21 02	.....	....	....	....	s	16	7	9	228	1830
	June 1	17 22	6 22	s.c.	....	....	....	ms	2	5,7,8	6	66	701
									3	1,7	6		
	June 29	07 30	3 01	.....	....	....	....	ms	29	6,8	7	145	1005
									30	1	7		
	July 23	08 09	24 23	s.c.	+1	−3	−1	s	23	8	8	117	1290
	July 25	16 32	31 16	s.c.	....	....	....	ms	27	7	6	38	365
	Aug. 10	07 00	14 06	.....	(*Note*: Periods of record missing)							.....	.....
	Aug. 23	00 24	26 03	s.c.	+1	−1	−1	s	24	8	8	125	1123
	Aug. 26	13 00	1 03	.....	....	....	....	ms	27	7	7	73	659

PRINCIPAL MAGNETIC STORMS—Concluded

Observatory (Observer-in-Charge)	Greenwich date	Storm-time GMT of begin.	Storm-time GMT of ending[1]	Sudden commencement Type[2]	Amplitudes[3] D	H	Z	C-figure, degree of activity[4]	Maximal activity on K-scale 0 to 9 Gr. day	Gr. 3-hr. period	K-index	Ranges D	H	Z
(1)	(2)	(3)	(4)	(5)	(6)	(7)	(8)	(9)	(10)	(11)	(12)	(13)	(14)	(15)
	1953	*h m*	*d h*		′	γ	γ					′	γ	γ
Heard Island	Sep. 2	01 00	5 10	.....	.....	.....	.....	s	3	8	9	197	1349	817
—*Continued*	Sep. 15	03 00	18 03	.....	.....	.....	.....	ms	15	7	7	93	571	281
(J. A. Brooks)		(*Note:* Suspected s.s.c., September 15, approximately 02h 59m, but no record, as trace was changed at this time)												
	Sep. 18	15 30	26 00	.....	.....	.....	.....	s	19	6	8	129	1197	484
	Oct. 15	08 45	21 16	s.c.	+2	+4	−3	s	15	6	8	171	1190	649
	Oct. 26	18 17	28 03	s.c.	.....	.....	.....	ms	27	7	7	39	452	185
	Nov. 12	09 00	21 14	.....	.....	.....	.....	ms	14	7	7	90	953	469
									19	7	7			
		(*Note:* On November 13, 15 hours of record missing, from 12h on)												
	Nov. 23	06 00	24 12	.....	.....	.....	.....	ms	23	7,8	7	88	709	528
	Dec. 10	20 50	13 03	.....	.....	.....	.....	ms	11	7	7	121	788	322
	1954			*Reports added in proof:*										
Honolulu	Oct.	None												
(R. F. White)	Nov.	None												
	Dec. 17	03 00	18 11	.....	.....	.....	.....	m	17	3	5	2	97	15
Lisabethville	Oct. 23	07 23	24 24	s.c.	−1	+19	−2	m	23	3,7,8	...	8	161	20
(A. Alexandre)	Oct. 27	07 46	27 24	s.c.	0	+18	....	m	27	4,5	...	5	106	25
	Nov. 23	11 45	24 06	s.c.	....	+14	....	m	23	5,6	...	9	126	21
	Dec.	None												
Apia	Oct. 2	21 ..	4 15	.....	.....	.....	.....	m	3	8	5	5	87	20
(F. J. Gill)	Oct. 23	06 42	25 18	s.c.	0	+7	−2	m	23	7	5	5	108	30
									25	1,2	5			
	Nov.	None												
	Dec. 17	03 ..	18 15	.....	.....	.....	.....	m	17	3	5	Recording incomplete		
Tsinza	July	None												
(J. Leroy)	Aug.	None												
	Sep.	None												
	Oct.	None												
	Nov. 23	11 47	23 22	s.c.	0	+14	−1	m	23	6	...	1	139	26
	Dec.	None												
Watheroo	Sep. 30	22 35	2 07	.....	.....	.....	.....	m	1	4	5	16	99	48
(E. A. Brooks)	Oct. 5	20 30	6 21	.....	.....	.....	.....	m	6	5,6	5	14	87	29
	Oct. 17	21 30	19 16	.....	.....	.....	.....	m	18	4,5,6	5	22	111	44
									19	4	5			
	Oct. 23	07 23	25 16	s.c.	.....	.....	.....	m	23	4,5	5	21	129	72
									24	4,5,6	5			
	Oct. 31	05 ..	3 20	.....	.....	.....	.....	m	1	5,6	5	18	130	35
		[*Note:* Record incomplete on October 30]												
	Dec.	None												

LETTERS TO EDITOR

THE FREQUENCY DISTRIBUTION OF THE INTENSITY OF AURORAE AND THE NIGHT AIRGLOW FOR 5577[OI]

The question of whether the aurora and nightglow are two manifestations of the same phenomenon will probably not be settled until a satisfactory definition of either or both is proposed. This should, of course, be based upon a carefully reasoned study resulting from a knowledge of the characteristics of both forms of nocturnal illumination. The working hypothesis has been adopted by some observers that the presence of the bands of N_2^+ in the spectrum differentiate the aurora and the airglow. This, however, is arbitrary. Is the difference merely one of brightness? Does it have to do with excitation potential? Is the nightglow produced by a different process than that which produces the aurora polaris? Does the fact that the aurora appears to be largely confined to the polar regions and to only a narrow, toroidal section of the polar regions differentiate it from the nightglow which is presumably omnipresent? A method that holds the promise of an approach to this problem is suggested below.

St. Amand and Pettit[1] have given a histogram of the intensity of the 5577 nightglow for Cactus Peak, California, based upon the mean intensity for whole nights for a four-year period. A similar histogram has been published by Dufay and Mao-Lin Tcheng.[2] The two histograms are similar in appearance, and although the latter is not based upon an absolute scale, it appears as if in the latitudes of Southern France and California the nightglow does not vary markedly in intensity. The observations are fitted well by a unimodal normal distribution. There is a finite probability of zero intensity indicated, but values above 10^{-6} erg/cm^2 sec square degree are rare indeed. Some data on the frequency distribution of the maximum intensity of auroral arcs and bands have been given by Ashburn.[3] The two curves are combined in Figure 1 in order to show the nature of the range in intensity.

A direct comparison of the two sets of data cannot be made because they were taken under entirely different conditions in different places and for different periods of time. There are, however, some questions suggested by the two histograms. If strictly comparable data were obtained for aurora and for nightglow at the same location, say histograms for hourly mean intensities, would the histograms have two distinct modes—one in the region of nightglow intensities and one in the

[1]P. St. Amand and H. B. Pettit, A comment on a four-year study of the OI 5577A in the nightglow, J. Atmos. Terr. Phys. (in press).

[2]J. Dufay and M.-L. Tcheng, Recherches spectrophotométriques sur la lumière du ciel nocturne dans la région visible, Partie 2, Ann. Géophys., **3**, No. 2, 153-184 (1947).

[3]E. V. Ashburn, Measurements of the specific intensities of the auroral green line at College, Alaska, J. Atmos. Terr. Phys. **6**, 57-60 (1955).

region of auroral intensities? Or would the histogram have one mode? If there were two modes, would it indicate a different genesis for the two phenomena?

Basing predictions upon the histogram for Cactus Peak, it would appear that the nightglow would be of the same brightness as a weak aurora (about 5 times

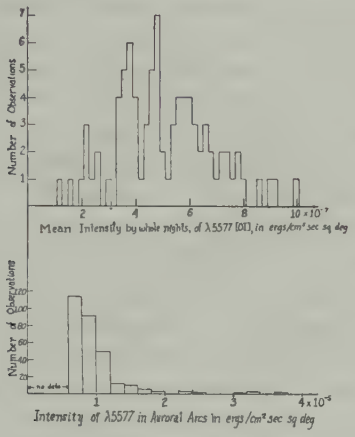

FIG. 1—Frequency distribution of airglow and auroral intensities

the mean nightglow brightness) only once or twice in geologic time. Fritz's chart of auroral frequencies[4] shows that aurora has been seen oftener than this. It must be remembered, however, that Fritz's auroral map indicates aurora seen anywhere in the sky, and for Southern California the aurora seen may well have been as far north as Oregon. Therefore, the chart really shouldn't be used to assess the occurrence of zenith aurora in the vicinity of Cactus Peak.

A second question suggested by the histogram concerns the nature of the complete histogram for the aurora. Are there aurorae whose maximum intensity is approximately that of the airglow? If so, what is the frequency of their occurrence? Is there a brightness threshold below which there is no aurora?

It appears that an analysis of continuous records taken at a station near or in the auroral zone would answer these questions and perhaps present a new approach to the development of a theory of aurora and the nightglow.

PIERRE ST. AMAND AND E. V. ASHBURN*

MICHELSON LABORATORY,
U.S. NAVAL ORDNANCE TEST STATION,
Inyokern, China Lake, California, September 14, 1954
(Received September 18, 1954)

[4]H. Fritz, Das Polarlicht, Leipzig, Brockhaus (1881).

*Also of the Geophysical Institute, University of Alaska, College, Alaska.

LE MOMENT MAGNÉTIQUE DE LA TERRE A COMMENCÉ À CROÎTRE

Dans un numéro récent du Journal of Geophysical Research, Vol. 58, June 1953, p. 277, est paru un interessant article, "Is the earth's dipole moment increasing?," dans lequel E. C. Bullard arrive à la conclusion que le moment du champ magnétique du Globe, qui depuis plus de 100 ans diminue continuellement, a commencé à croître depuis 1932. On y signale encore que C. G. Puertas de Madrid est arrivé en 1951 à des conclusions similaires.

Le but de cette lettre est de signaler que je suis arrivé en 1947 à des conclusions similaires par l'étude de la variation du champ magnétique terrestre à Iassy-Roumanie. Dans un travail, "Valeurs des éléments magnétiques et les variations séculaires à Iassy pendant 17 ans, de 1931 à 1947. Variation du magnétisme terrestre en Roumanie de 1772 à 1947," publié dans le Bulletin de l'École Polytechnique de Iassy, tome 2, fasc. 2, 1947, pp. 457-470, j'ai été conduit a la conclusion suivante: Par des observations de H and I, faites à Iassy, on peut déduire que l'intensité du champ magnétique, caractérisée par la quantité G, a diminué d'abord, a passé par un minimum, et à présent elle croît depuis 1932 à 1947.

L'intensité du magnétisme terrestre peut être représentée par la quantité G, introduite par L. A. Bauer et nommée "constante magnétique locale." Cette quantité intervient dans le moment magnétique M du Globe par la relation $M = G R^3$, où R est le rayon moyen du Globe. G est défini par l'expression

$$G = \sqrt{H^2 + \tfrac{1}{4}Z^2} = H\sqrt{1 + \tfrac{1}{4}tg^2 I}$$

La valeur de G décroît, d'après Bauer, en fonction du temps, la variation annuelle moyenne étant 1/1520 de sa valeur. Les valeurs de G, trouvées à Iassy, sont:

1898	*1932*	*1947*
$G = 0.29980$	$= 0.29800$	$= 0.30027$

On calcule pour l'intervalle 1932 à 1947 une variation positive annuelle de G d'environ 13 gammas, ou à peu près 1/2400 de la valeur de G, c'est-à-dire, du moment magnétique de la Terre. La variation annuelle de G peut être exprimée à Iassy par l'expression

$$dG = 1.39\, dH + 13.5\, dI$$

lorsque dH est donné en unités gammas et dI en minutes.

J'avais formulé en 1947 la conclusion: "La constatation que la quantité G, représentant le moment magnétique du Globe, pour certaines stations croît, après avoir diminué, et que cette variation positive est du même ordre de grandeur que la variation relative négative de l'ensemble du Globe, qui a régné depuis 100 ans, montrent que la quantité G subit des variations cycliques (p. 467).

Ces conclusions de 1947 correspondent aux conclusions récentes de E. C. Bullard: le moment magnétique de la Terre a commencé à croître depuis 1932.

Stefan Procopiu
(Professeur a l'Université
de Iassy, Roumanie)

Aleea Gr. Ghica-Vodă No. 10,
Iassy, Roumania, September 15, 1954,
(Received October 18, 1954)

GEOMAGNETIC CONTROL OF THE $F1$ REGION OF THE IONOSPHERE

It was shown earlier by Appleton[1] that for stations of widely differing longitudes but lying near the geomagnetic equator the latitudinal variations of the noon values of $f^{\circ}F2$ show much less scatter when plotted as a function of the magnetic dip or geomagnetic latitude than as a function of geographic latitude. According to Appleton, "it appears that for noon conditions, there is a belt of low values of $f^{\circ}F2$ circling the earth and centered roughly on the magnetic equator. For stations situated within this belt it is found that these low values are associated with marked bifurcation of the F layer into $F1$ and $F2$ strata. Such bifurcation is accompanied by the usual phenomena (for example, low noon value, evening

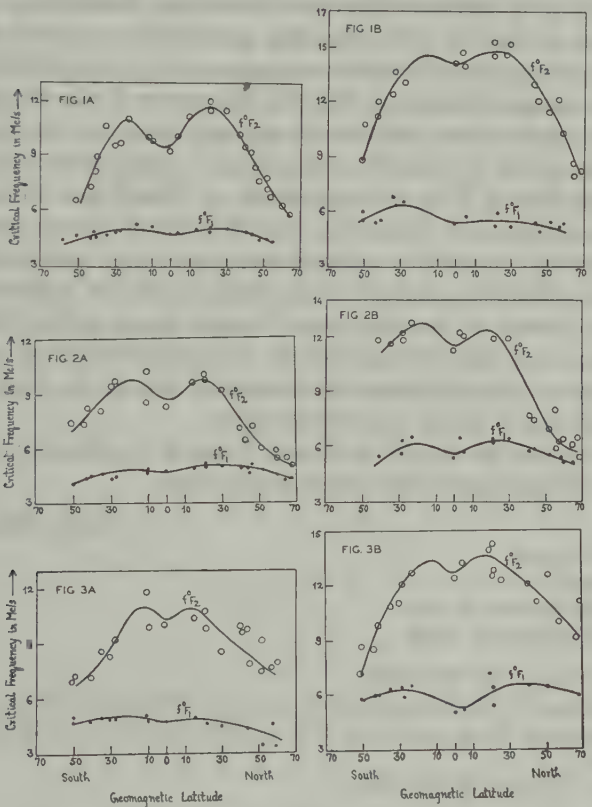

FIG. 1—Variation of the $F1$- and $F2$-region critical frequencies with geomagnetic latitude for the month of March: (A) for the year 1951 (low sunspot-activity), and (B) for the year 1947 (high sunspot-activity)

FIG. 2—Variation of the $F1$- and $F2$-region critical frequencies with geomagnetic latitude for the month of June: (A) for the year 1951 (low sunspot-activity), and (B) for the year 1947 (high sunspot-activity)

FIG. 3—Variation of the $F1$- and $F2$-region critical frequencies with geomagnetic latitude for the month of December: (A) for the year 1951 (low sunspot-activity), and (B) for the year 1947 (high sunspot-activity)

[1]E. V. Appleton, Nature, **157**, 691 (1946).

concentration of ionisation, slow electron disappearance after sunset, etc.) with which we are familiar under English summer conditions. In other words, the longitude effect and the geomagnetic control are exhibited not only in the noon values of $f^{\circ}F2$ but also in the whole diurnal behaviour."

It is to be noted that exactly the same type of geomagnetic control, though in a somewhat less degree, is exhibited by the $F1$-region critical frequencies, as shown in Figures 1, 2, and 3. Figures 1*A* and 1*B* show the noon values of the critical frequencies of the $F1$ and $F2$ regions plotted against the geomagnetic latitude for the month of March for the years 1951 and 1947, that is, for the years of low and high sunspot-activities, respectively. Figures 2*A* and 2*B* and Figures 3*A* and 3*B* show the same variations for the months of June and December, respectively. From the curves, it is observed that the latitudinal distribution of $f^{\circ}F1$ is completely analogous to that of $f^{\circ}F2$, showing geomagnetic control of the $F1$ region in all the seasons. The curves for higher sunspot-activity, however, show more prominent dips at the magnetic equator. The similar nature of the world distribution of the $F1$- and $F2$-region critical frequencies strongly supports the present hypothesis of the production of the $F1$ and $F2$ layers from a common bank of ionisation.

The Appleton dip of $f^{\circ}F2$ was explained by Mitra[2] and Menzel and Bailey[3] in terms of concentration of ionisation on both sides of the magnetic equator due to "distilling process" caused by solar photon absorption and thermal expansion, respectively. But it has been shown by Chatterjee[4] that the latitudinal distribution of the total ion content of the composite F region shows a single maximum at the magnetic equator, and hence there can be no concentration of ionisation on the sides of the equator. The Appleton dip is actually due to the large semi-thickness of the layers concerned in the equatorial region.

My thanks are due to Dr. B. N. Singh, Dean of the Faculty of Science, Patna University, for his guidance and interest in the work.

(Miss) Mrinmayee Ghosh

Patna Women's College,
Patna University,
Patna 3, India, November 3, 1954
(Received December 23, 1954)

[2]S. K. Mitra, Nature, **158**, 668 (1946).

[3]D. H. Menzel, and D. K. Bailey, Relations entre les Phénomènes Solaires et Géophysiques, Colloque International de Lyon, septembre 1947, Centre National de la Recherche Scientifique, pp. 163-166 (1949).

[4]B. Chatterjee, Nature, **173**, 263 (1954).

NOTES

(1) *New geophysical observatory, Tatuoca, Belem, Brazil*—The magnetic equipment of the new geophysical observatory at Tatuoca, Belem, Brazil (lat. 1° 12′ south; long. 48° 30′ west) was installed during December 1954. Ruska variometers are housed in sawdust-insulated building of non-magnetic construction, and the absolute observatory has two complete sets of piers designed for intercomparisons of field equipment. The installation was carried out by W. C. Parkinson (for many years a staff member of the Department of Terrestrial Magnetism, Carnegie Institution of Washington) under the Technical Assistance Program of UNESCO. He was assisted by Dr. Lelio I. Gama, Director of the Observatorio Nacional de Brasil, under whose auspices the Tatuoca Observatory will function. Unfortunately, the observatory will not operate on a continuous basis until power and water supplies have been installed; these facilities, it is hoped, will be available within the next few months. Provisional magnetic elements at Tatuoca (Dec. 1954) were found to be as follows: H, .28800 c.g.s.; D, 14° 49′ west; I, 18° 11′ north; Z, .09460 c.g.s.

(2) *Departure of the U.S. Navy icebreaker "Atka" for the Antarctic*—The U.S. Navy icebreaker "Atka" sailed for the Antarctic on December 5, 1954, on a reconnaissance trip for stations for the International Geophysical Year that is expected to take four or five months. Rear Admiral Richard E. Byrd, technical adviser to the "Atka" expedition, disclosed that a second and larger expedition as a follow-up of the one-ship expedition is being planned by the U.S. Defense Department. An objective of both expeditions is to explore an area in the Antarctic larger than the United States which it is believed no human has ever seen. The size, make-up, and time of departure of the second expedition will be based on the findings of the "Atka" group.

(3) *Published report of Cambridge conference on physics of the ionosphere*—The Physical Society, London, has published a report (around 400 pages) of the Conference on the Physics of the Ionosphere, which was held at the Cavendish Laboratory, Cambridge, England, September 6-9, 1954. The conference was devoted mainly to a discussion of four topics, an introductory paper being given by a well-known authority in each field who surveyed the existing state of knowledge. These authors have also contributed a summary of the conclusions as to future trends drawn from the discussions which took place at the conference. The subjects are as follows: Part 1—The lowest ionosphere, introductory paper by Prof. A. H. Waynick; Part 2—Irregularities and movements in the ionosphere, introductory paper by Mr. J. A. Ratcliffe; Part 3—The $F2$ layer, introductory paper by Dr. D. F. Martyn; and Part 4—The mathematics of wave propagation through the ionosphere, introductory paper by Dr. K. G. Budden. Each of the mentioned presentations is supported by a number of papers by authors from Belgium, France, Germany, the United States, and Great Britain. Copies of the publication may be obtained from the Secretary-Editor of the Physical Society, 1 Lowther Gardens, Prince Consort Road, London, S.W. 7, England, at £2 each,

plus 1 shilling postage (price to Fellows and Students of the Physical Society is 25 shillings, plus 1 shilling postage).

(4) *Symposium on scientific aspects of the International Geophysical Year, 1957-1958*—By invitation of the Committee on Arrangements for the Annual Meeting of the National Academy of Sciences, the following papers were read before the Academy on April 28, 1954, in connection with a symposium on scientific aspects of the International Geophysical Year, 1957–1958, and have been published in the Proceedings of the National Academy of Sciences (Vol. 40, No. 10, pp. 923-982, October 1954): Explanatory foreword, by L. V. Berkner; Introduction, by Sydney Chapman; The scientific program of the International Geophysical Year, by Joseph Kaplan; Morphology of ionospheric storms, by H. G. Booker; The morphology of the aurora, by A. B. Meinel; Diurnal and seasonal variation of the airglow, by F. E. Roach; Transport problems in the atmosphere, by H. Wexler; Evidence for winds in the outer atmosphere, by F. L. Whipple; Solar activity and terrestrial disturbances, by D. H. Menzel; and Geographic basis for antarctic scientific observations, by P. A. Siple.

(5) *French Bibliographical Digest in geology*—This third issue (October 1954) of the second series of the French Bibliographical Digest is devoted to geology (general, tectonics, tectonophysics, tectogenesis, applications of electricity and terrestrial magnetism, paleocology, etc.). Its companion volume, dealing with mineralogy, geophysics, and paleontology, is also under preparation and is expected to be published in the near future. A publication of 102 pages, in addition to the bibliography and in some instances abstracts, it contains a résumé of activities and trends in French geology between 1948 and 1954 by Prof. Louis Glangeaud and lists of French scientific periodicals and learned societies. The purpose of the bibliography, which is in English, is to provide a useful guide for other scientists wishing to keep informed of contributions to geology made by their French colleagues. The Digest is edited and published by the Cultural Division of the French Embassy, 972 Fifth Avenue, New York 21, N.Y., and is free of charge upon request.

(6) *Publication of scientific papers of Maria Sklodowska-Curie*—The Polish Academy of Sciences has announced the forthcoming publication of the complete original texts of the scientific papers of Maria Sklodowska-Curie, the great Polish scientist, who with her husband, Pierre, discovered radium in 1898. The papers are to be issued as part of Poland's nation-wide commemoration this year of the twentieth anniversary of Mme. Sklodowska-Curie's death. An introduction has been written by the scientist's daughter, Irene Joliot-Curie, an outstanding physicist.

(7) *Release of geophysical maps for public inspection*—The United States Geological Survey is releasing in open files for consultation in the Washington, D.C., and Minnesota offices (copies not available for distribution) the following total-intensity aeromagnetic maps of various parts of Minnesota: Western Polk county; western Red Lake and central Polk counties; central and western Kittson county; western Marshall and northwestern Polk counties; eastern Marshall and northwestern Beltrami counties; eastern Kittson and western Roseau counties; central Marshall and western Pennington counties; eastern Roseau

county; and eastern Pennington, northwestern Red Lake, west-central Beltrami, and northern Clearwater countries.

(8) *Geomagnetic activities of the United States Coast and Geodetic Survey*—Compilation of a new set of world magnetic charts for epoch 1955.0 has been completed. The magnetic elements constituting the charts are variation (or declination, D), inclination (or dip, I), horizontal intensity (H), vertical intensity (Z), and total intensity (F). Each chart portrays the isomagnetic lines as of January 1, 1955, and current annual rates of change. World coverage in each element is attained by the use of a Mercator projection and two polar projections. In addition to these, an Isogriv chart, on a north polar projection, shows the direction of magnetic north referred to a rectangular grid so chosen that grid north is parallel to the Greenwich meridian, with the same sense of direction (or parallel to the southward sense of the 180th meridian of longitude). The world magnetic charts were compiled by the U. S. Coast and Geodetic Survey; they are being published and distributed by the U.S. Navy Hydrographic Office, Washington 25, D.C.

A new set of magnetic charts for epoch 1955.0 of the United States and of of Alaska has been compiled and is being published by the U.S. Coast and Geodetic Survey in the five elements D, I, H, Z, and F. The isogonic charts are now being distributed, and it is expected that the other four of the series will be printed within the next few months. Like the world charts, each of the United States and Alaska charts carries isoporic lines (showing rates of annual change) as well as isomagnetic lines. Further information can be obtained from The Director, U.S. Coast and Geodetic Survey, Washington 25, D.C.

Mr. Abdul Patah of Indonesia, Mr. Syed J. Ahmed of Pakistan, and Lt. Rojana Hongprasith of Thailand continued their studies of the methods and procedures of the U.S. Coast and Geodetic Survey in office and field work in geomagnetism.

(9) *URSI Spring meeting*—The spring meeting of the URSI is scheduled to be held at the National Bureau of Standards, Washington, D.C., on May 3, 4, and 5, 1955. The co-sponsors this year will include the IRE Professional Group on Antennas and Propagation, and Microwave Theory and Techniques. One or two additional Professional Groups are considering acting as co-sponsors. A combined technical session of interest to all participants is scheduled for the morning of May 3, to be followed by one or more sessions in each of the following fields: Commission 1, on radio measurements and standards; Commission 2, on radio and troposphere; Commission 3, ionospheric radio; Commission 4, on radio noise of terrestrial origin; Commission 5, on radio astronomy; Commission 6, on radio waves and circuits; and Commission 7, on radio electronics. Symposia on the following subjects have been tentatively planned: (1) The forward scattering of radio waves; (2) the theoretical aspects of ferrites at microwaves; (3) the mechanisms and limitations of microwave noise sources; and (4) multi-mode microwave transmission systems.

(10) *Loss of the non-magnetic survey ship "Carnegie" 25 years ago*—The destruction of the "Carnegie" by explosion in Apia harbor, Samoa, November 29, 1929, is recalled, in which Captain James P. Ault unfortunately lost his life, depriving oceanography and terrestrial magnetism of an inspired leader.

(11) *Personalia*—Dr. *Gerhard Neumann* has been promoted from associate professor to the first full professorship of oceanography in New York University's College of Engineering. Formerly oceanographer at the University of Hamburg, Germany, Dr. Neumann joined the New York University faculty in 1951. The department of meteorology was redesignated "department of meteorology and oceanography" in 1952 with the introduction of full formal curricula in both subjects leading to master's and doctor's degrees. It was the first time an American university formally combined the subjects. Dr. Neumann is noted for his research in ocean-atmosphere interaction, wave forecasting, and the dynamics of the Gulf Stream system.

Dr. *Caryl P. Haskins*, president and director of research of Haskins Laboratories, New York City, has been elected president of the Carnegie Institution of Washington, to succeed Dr. Vannevar Bush upon his retirement on January 1, 1956.

It is with regret that we have learned of the death on November 26, 1954, of Mr. *Percy William Glover*, formerly of Christchurch Magnetic Observatory and Apia Observatory. Among his published papers were several on magnetic secular variation at Apia, Samoa, 1905-1929, and correlation between sunspot activity and daily ranges of terrestrial magnetic elements, which appeared in *Terr. Mag.* during the 1930's.

(12) *International Council of Scientific Unions, Mixed Commission on the Ionosphere*—A symposium under the general title "Solar eclipses and the ionosphere" will be held in the rooms of the Royal Society, Burlington House, London, on August 22-24, 1955. Topics to be discussed include the following: (*a*) Ionospheric and other geophysical eclipse phenomena; (*b*) Recent ionospheric eclipse results; (*c*) Ionospheric processes—ion production and recombination; (*d*) Sources of ionising radiation; and (*e*) Radio astronomical eclipse observations. Contributors include Prof. S. Chapman, Prof. H. S. W. Massey, Mr. J. A. Ratcliffe, Dr. M. Nicolet, Dr. J. Bartels, Mr. L. V. Berkner, Prof. D. R. Bates, Prof. J. Sayers, Dr. R. P. Lejay, Dr. K. Weekes, Prof. C. W. Allen, Mr. W. R. Piggott, and Mr. C. M. Minnis. The proceedings of the symposium will be published as a Special Report by the International Union of Scientific Radio (URSI). Those wishing to attend the symposium or to submit written contributions are invited to communicate with Dr. W. J. G. Beynon, Secretary, Mixed Commission on the Ionosphere, Department of Physics, University College, Swansea, U.K.

LIST OF RECENT PUBLICATIONS

BY W. E. SCOTT

Department of Terrestrial Magnetism
Carnegie Institution of Washington,
Washington 15, D.C.

(Received January 4, 1955)

A—*Terrestrial Magnetism*

ANGENHEISTER, G. Registrierungen erdmagnetischer Pulsationen, Göttingen 1952/53. Beitr. Geophysik, **64**, Heft 2, 108-132 (1954).

BARTELS, J., AND J. VELDKAMP. Geomagnetic indices *K* and *C*, 1953. Internat. Union Geod. Geophys., Assoc. Terr. Mag. Electr., Bull. No. 12h, 90 pp. (1954). 24 cm.

BARTELS, J., AND J. VELDKAMP. International data on magnetic disturbances, second quarter, 1954. J. Geophys. Res., **59**, No. 4, 543-545 (1954).

BELL, B., AND H. GLAZER. Geomagnetism and the emission-line corona. J. Geophys. Res., **59**, No. 4, 551-553 (1954). [Letter to Editor.]

BRUCKSHAW, J. M., AND S. A. VINCENZ. The permanent magnetism of the Mull lavas. Mon. Not. R. Astr. Soc., Geophys. Sup., **6**, No. 9, 579-589 (1954).

CAMPBELL, J. B. Cheltenham three-hour-range indices *K* for July to September, 1954. J. Geophys. Res., **59**, No. 4, 546 (1954).

CHERNOSKY, E. J., E. MAPLE, AND R. M. COON. Rapid geomagnetic fluctuations at Tucson, Arizona. Trans. Amer. Geophys. Union, **35**, No. 5, 711-721 (1954).

DUNGEY, J. W. The motion of magnetic fields. Mon. Not. R. Astr. Soc., **113**, No. 6, 679-682 (1954).

ELSASSER, W. M. Hydromagnetic dynamo theory, I. University of Utah, Dept. of Physics, Tech. Rep. No. 7, 58 pp., mim. (Aug. 1, 1954). 28 cm.

ELSASSER, W. M., AND H. TAKEUCHI. Non-uniform rotation of the earth and geomagnetic drift. University of Utah, Dept. of Physics, Tech. Rep. No. 11, 16 pp., mim. (1954).

FANSELAU, G. Ergebnisse der Beobachtungen am Adolf Schmidt-Observatorium für Erdmagnetismus in Niemegk in den Jahren 1939-1944. III. Teil: Zeichnerische Darstellung der typischen Variationen, Störungskurven und Tagesmittel der Komponenten. Berlin, Akad.-Verlag, 134 pp. (1954). 30 cm. [Published under the auspices of the Meteorologischer Dienst der Deutschen Demokratischen Republik, Erdmagn. Jahr. 1939-1944.]

GAIBAR-PUERTAS, C. Fluctuaciones experimentadas por la intensidad de la fuerza geomagnética durante el periodo 1885-1950 (Conclusión). Rev. Geofísica, Madrid, **13**, No. 49, 1-36 (1954).

GRENET, G., AND Y. KATO, J. OSSAKA, AND M. OKUDA. Pulsations in terrestrial magnetic field at the time of bay disturbance. Sci. Rep. Tôhoku Univ., Ser. 5, Geophysics, **6**, No. 1, 1-10 (1954).

MALURKAR, S. L. Geomagnetic variations and diurnal range of atmospheric ozone. Ann. Geofis. Roma, **7**, No. 2, 209-213 (1954).

NAGATA, T. An intuitive description of the Chapman-Ferraro theory of the initial phase of a magnetic storm. J. Geophys. Res., **59**, No. 4, 467-470 (1954).

PECKER, J.-C., AND W. O. ROBERTS. Detection of *M*-regions in geomagnetic data. Science, **120**, 721-722 (Oct. 29, 1954).

RICHARD, M., UND H. WIESE (Ed.). Die Neubestimmung der absoluten erdmagnetischen Feldgrössen am Adolf-Schmidt-Observatorium für Erdmagnetismus in Niemegk. Berlin, Geophys. Inst. Potsdam, Abh. No. 13, 70 pp. (1954). 30 cm.

TAKEUCHI, H., AND Y. SHIMAZU. The instability of a rotating fluid sphere heated from within. University of Utah, Dept. of Physics, Tech. Rep. No. 8, 25 pp., mim. (Aug. 15, 1954). 28 cm.

TROMSÖ, Auroral Observatory. Observations 1952. Bergen, Norske Inst. Kosmisk, No. 35, 31

pp. (1954). 30 cm. [Contains report of spectrographic work on aurora and twilight, and results of ozone and magnetic observations at Tromsö and Bear Island, 1952.]

Vincenz, S. A. The magnetic properties of some Tertiary intrusives on the Isle of Mull. Mon. Not. R. Astr. Soc., Geophys. Sup., 6, No. 9, 590-603 (1954).

Wohlfarth, E. P. Recent developments in magnetism. Research, 7, No. 9, 360-367 (1954). [A review of recent books and surveys on ferromagnetism.]

B—*Terrestrial Electricity*

Barlow, J. S., G. W. Frey, Jr., and J. B. Newman. Very low frequency noise power from the lightning discharge. J. Frank. Inst., 258, No. 3, 187-203 (1954).

Gunn, R. Electric-field regeneration in thunderstorms. J. Met., 11, No. 2, 130-138 (1954).

Gunn, R. Electric field meters. Rev. Sci. Instr., 25, No. 5, 432-437 (1954).

Hacking, C. A. Observations on the negatively-charged column in thunderclouds. J. Geophys. Res., 59, No. 4, 449-453 (1954).

Jones, R. F. Radar echoes from lightning. Q. J. R. Met. Soc., 80, No. 346, 579-582 (1954).

Sagalyn, R. C., and G. A. Faucher. Aircraft investigation of the large ion content and conductivity of the atmosphere and their relation to meteorological factors. J. Atmos. Terr. Phys., 5, Nos. 5/6, 253-272 (1954).

San Miguel (Argentina), Observatorio de Física Cósmica. Electricidad atmosférica en San Miguel análisis de los registros efectuados durante las años 1946 a 1951. Acta Scientifica, Cuaderno No. 3, 22 pp. (1954). 24 cm.

Schonland, B. F. J., and D. J. Malan. Upward stepped leaders from the Empire State Building. J. Frank. Inst., 258, No. 4, 271-275 (1954).

C—*Cosmic Rays*

Cranshaw, T. E., and W. Galbraith. Time variations of extensive air showers and the origin of cosmic rays. Phil. Mag., 45, No. 370, 1109-1117 (1954).

Dauvillier, A. Les rayons cosmiques, dans leurs rapports avec l'électricité atmosphérique la météorologie, le géomagnétisme et l'astronomie. Paris, Dunod, Tome I, xi + 247 + 116 figs., and Tome II, xi + 317 + 137 figs. (1954). 24 cm. [These may be purchased from Dunod, Editeur, 92 rue Bonaparte, Paris, 6ème, France; Vol. I for 1.750 fr., Vol. II for 2.600 fr., or the two in a single volume for 4.700 fr.]

Farley, F. J. M., and J. R. Storey. The sidereal correlation of extensive air showers. Proc. Phys. Soc., A, 67, No. 419, 996-1004 (1954).

Forbush, S. E. World-wide cosmic-ray variations, 1937-1952. J. Geophys. Res., 59, No. 4, 525-542 (1954).

Lovati, A., A. Mura, C. Succi, and G. Tagliaferri. A cloud chamber analysis of cosmic radiation at 3500 m. Part B: Results on the hard and soft components. Nuovo Cimento, 12, No. 4, 526-538 (1954).

Moroney, J. R., and J. K. Parry. Momentum distribution and charge ratio of μ-mesons at zenith angles in the east-west plane. Aust. J. Phys., 7, No. 3, 423-438 (1954).

Officer, V. C., and P. J. Eccles. The residual range of delayed particles in extensive air showers. Aust. J. Phys., 7, No. 3, 410-422 (1954).

Quercia, I. F., and B. Rispoli. Geomagnetic effects of the μ meson component of cosmic radiation at sea level. Nuovo Cimento, 12, No. 4, 490-518 (1954).

Sarabhai, V., U. D. Desai, and D. Venkatesan. Cycle of world-wide changes in the daily variation of meson intensity. Phys. Rev., 96, No. 2, 469–470 (1954).

Seymour, D. W., and W. F. G. Swann. A determination of μ-mesotron rest lifetime and a verification of the relativistic expression for variation of lifetime with momentum. J. Frank. Inst., 258, No. 4, 277-286 (1954).

Swann, W. F. G. Acceleration to cosmic ray energies by electromagnetic inductive action. J. Frank. Inst., 258, No. 3, 205-212 (1954).

Symposium on Cosmic Rays. Discussions on the time variations of cosmic-ray intensity, morning

session, September 11, 1953. Tokyo, Scientific Research Institute, Ltd., pp. 57-93 (rec'd Dec. 13, 1954). 26 cm. [Repr., Proc. Internat. Conf. on Theoretical Physics, Kyoto and Tokyo, September 1953.]

D—*Upper Air Research*

Agy, V. Geographic and temporal distribution of polar blackouts. J. Geophys. Res., **59**, No. 4, 499-512 (1954).

Allcock, G. McK. Ionospheric absorption at vertical and oblique incidence. Proc. Inst. Elec. Eng., **101**, Pt. 3, No. 74, 360-367 (1954). [A discussion of paper follows.]

Appleton, E. V. The anomalous equatorial belt in the F_2-layer. J. Atmos. Terr. Phys., **5**, Nos. 5/6, 348-351 (1954). [Research note.]

Barber, D. R. Note on the seasonal variation of sodium *D*-line emission in twilight. J. Atmos. Terr. Phys., **5**, Nos. 5/6, 347-348 (1954). [Research note.]

Bates, D. R., and A. Dalgarno. Theoretical considerations regarding the dayglow. J. Atmos. Terr. Phys., **5**, Nos. 5/6, 329-344 (1954).

Bennett, W. H., and E. O. Hulburt. Magnetic self-focussed solar ion streams as the cause of aurorae. J. Atmos. Terr. Phys., **5**, No. 4, 211-218 (1954).

Beynon, W. J. G., and K. Davies. Simultaneous ionospheric absorption measurements at widely separated stations. J. Atmos. Terr. Phys., **5**, Nos. 5/6, 273-289 (1954).

Bok, B. J. Radio studies of interstellar hydrogen. Sky and Telescope, **13**, No. 12, 408-412 (1954).

Bowles, K. L. Doppler shifted radio echoes from aurora. J. Geophys. Res., **59**, No. 4, 553-555 (1954). [Letter to Editor.]

Buchholz, H. Der vollkommen leitende Ring unter dem Einfluss von hochfrequenten Strömen und Magnetfeldern. Archiv Elektr. Uebertrage., 8, Heft 10, 427-435 (1954).

Budden, K. G. A reciprocity theorem on the propagation of radio waves via the ionosphere. Proc. Cambridge Phil. Soc., **50**, No. 4, 604-613 (1954).

Bullough, K., and T. R. Kaiser. Radio reflections from aurorae. J. Atmos. Terr. Phys., **5**, No. 4, 189-200 (1954).

Chaffee, D. D., Jr. Statistical analysis of "150-km" echo. J. Geophys. Res., **59**, No. 4, 549-550 (1954). [Letter to Editor.]

Chamberlain, J. W. On the production of auroral arcs by incident protons. Astroph. J., **120**, No. 3, 566-571 (1954).

Chamberlain, J. W., C. Y. Fan, and A. B. Meinel. A new O_2 band in the infrared auroral spectrum. Astroph. J., **120**, No. 3, 560-562 (1954).

Chandrasekhar, S., and D. D. Elbert. The illumination and polarization of the sunlit sky on Raleigh scattering. Trans. Amer. Phil. Soc., **44**, Pt. 6, 643-654 + 12 tables (1954).

Chapman, S. A monochromatically ionized layer in a non-uniformly recombinant atmosphere; with applications to the *D* and *E* ionospheric regions. Proc. Phys. Soc., B, **67**, No. 417, 717-727 (1954).

Davies, R. D. An analysis of bursts of solar radio emission and their association with solar and terrestrial phenomena. Mon. Not. R. Astr. Soc., **114**, No. 1, 74-92 (1954).

Dufay, M. Les émissions radioélectriques d'origine galactique ou extragalactique. J. Physique Rad., **15**, 30-37 (Jan. 1954). [Pub. de l'Observatoire de Lyon, **5**, No. 24.]

Dufay, M. Le spectredu ciel nocturne de 3380 á 4200 Å. Paris, C.-R. Acad. sci., **239**, No. 7, 533-535 (1954).

Dungey, J. W. Electrodynamics of the outer atmosphere. Pennsylvania State University, Ionosphere Res. Lab., Sci. Rep. No. 69, 52 pp., mim. (Sept. 15, 1954). 28 cm.

Evans, S. Scale heights and pressures in the upper atmosphere from radio-echo observations of meteors. Mon. Not. R. Astr. Soc., **114**, No. 1, 63-73 (1954).

Gardner, F. F. Ionospheric thermal radiation at radio frequencies. II. Further observations. J. Atmos. Terr. Phys., **5**, Nos. 5/6, 298-315 (1954).

Hagen, J. P., and E. F. McClain. Galactic absorption of radio waves. Astroph. J., **120**, No. 2, 368-370 (1954). [Note.]

Higgins, C. S., and C. A. Shain. Observations of cosmic noise at 9.15 Mc/s. Aust. J. Phys., **7**, No. 3, 460-470 (1954).

Jacka, F. Variations of intensity of the aurora at Macquarie Island. Aust. J. Phys., 7, No. 3, 477-484 (1954).

Kaiser, T. R. Theory of the meteor height distribution obtained from radio-echo observations—I. Shower meteors, and II. Sporadic meteors. Mon. Not. R. Astr. Soc., **114**, No. 1, 39-51 and 52-62 (1954).

King, G. A. M. Electron distribution in the ionosphere. J. Atmos. Terr. Phys., 5, No. 4, 245-246 (1954). [Research note.]

Little, C. G. High latitude ionospheric observations using extra-terrestrial radio waves. Proc. Inst. Radio Eng., **42**, No. 11, 1700-1701 (1954). [Correspondence.]

Major, G. The association of pulsating and flaming auroras with complete ionospheric absorption at Macquarie Island. Aust. J. Phys., 7, No. 3, 471-476 (1954).

Martyn, D. F. The morphology of ionospheric disturbances in the F_2 region. Rep. Ionosphere Res. Japan, 8, No. 1, 11-16 (1954).

Mitra, A. P. Atomic nitrogen as a constituent for region F_1 . Indian J. Phys., 28, No. 6, and Proc. Indian Assoc. Cultivation Science, **37**, No. 6, 269-284 (1954).

Mitra, S. K., and M. R. Kundu. Thunderstorms and sporadic E ionization of the ionosphere. Nature, **174**, 798-799 (Oct. 23, 1954).

Nagata, T. Ionospheric storms in high latitudes. Rep. Ionosphere Res. Japan, 8, No. 1, 39-44 (1954).

Nakata, Y. Short period variations in the ionosphere. J. Radio Res. Labs., Japan, **1**, No. 2, 1-82 (1954).

Obayashi, T. On the development of ionospheric storm. Rep. Ionosphere Res. Japan, 8, No. 1, 19-27 (1954).

Omholt, A. Electron density in the E-layer during auroral displays deduced from measurements of absolute brightness of the auroral luminosity. J. Atmos. Terr. Phys., 5, No. 4, 243-244 (1954). [Research note.]

Piggott, W. R. On the interpretation of the apparent ionization distribution in the ionosphere. J. Atmos. Terr. Phys., 5, No. 4, 201-210 (1954).

Pillow, M. E. Intensity distribution among nitrogen bands in the auroral spectrum. Proc. Phys. Soc., A, **67**, No. 417, 780-788 (1954).

Pressman, J. The latitudinal and seasonal variations of the absorption of solar radiation by ozone. J. Geophys. Res., **59**, No. 4, 485-498 (1954).

Ratcliffe, J. A. The physics of the ionosphere. Proc. Inst. Elec. Eng., **101**, Pt. 1, No. 132, 339-346 (1954). [The 45th Kelvin Lecture, April 29, 1954.]

Reber, G. Spread F over Washington. J. Geophys. Res., **59**, No. 4, 445-448 (1954).

Roberts, J. A. Radio astronomy. Research, 7, No. 10, 388-399 (1954).

Schrag, R. L. Extended range ionospheric observations at 150 kc/s. Pennsylvania State University, Ionosphere Res. Lab., Sci. Rep. No. 66, 137 pp., mim. (July 15, 1954). 28 cm. [Contract No. AF19(122)-44.]

Seddon, J. C. Electron densities in the ionosphere. J. Geophys. Res., **59**, No. 4, 463-466 (1954).

Seddon, J. C., A. D. Pickar, and J. E. Jackson. Continuous electron density measurements up to 200 km. J. Geophys. Res., **59**, No. 4, 513-524 (1954).

Shain, C. A., and A. P. Mitra. Effects of solar flares on the absorption of 18.3 Mc/s cosmic noise. J. Atmos. Terr. Phys., 5, Nos. 5/6, 316-328 (1954).

Shakeshaft, J. R. The isotropic component of cosmic radio-frequency radiation. Phil. Mag., 45, No. 370, 1136-1144 (1954).

Skinner, N. J., and R. W. Wright. F_2-layer regularities at Ibadan. J. Atmos. Terr. Phys., 5, Nos. 5/6, 290-297 (1954).

Stanley, C. R. A new method for the production of active nitrogen and its application to the study of collision effects in the nitrogen molecular spectrum. Proc. Phys. Soc., A, **67**, No. 417, 821-827 (1954).

Struve, O. Cosmic dust. Sky and Telescope, **13**, No. 12, 415-418 (1954).

Uyeda, H. Ionospheric storms in middle and low latitudes. Rep. Ionosphere Res. Japan, 8, No. 1, 3-10 (1954).

Warwick, C. S. Some characteristics of solar flares. Astroph. J., **120**, No. 2, 237-244 (1954).

[Study of solar flares and limb events in relation to radio noise at 200 Mc/sec and to sudden ionospheric disturbances.]

Wild, J. P., J. D. Murray, and W. C. Rowe. Harmonics in the spectra of solar radio disturbances. Aust. J. Phys., **7**, No. 3, 439-459 (1954).

Wulf, O. R., and J. E. Zimmerman. A method for the measurement of atmospheric ozone using the absorption of ozone in the visible spectrum. Washington, D.C., Smithsonian Misc. Coll., **123**, No. 3, Pub. No. 4177, 14 pp. (Oct. 27, 1954).

Yonezawa, T. A consideration of the electron disappearance in the *F*2 layer of the ionosphere—Parts 1 and 2. J. Radio Res. Labs., Japan, **1**, No. 3, 1-62, and **1**, No. 4, 63-111 (1954).

E—*Earth's Crust and Interior*

Bartels, J. Erdmagnetisch erschliessbare lokale Inhomogenitäten der elektrischen Leitfähigkeit im Untergrund. Akad. d. Wiss., Göttingen, Phys.-Math. Kl. Abt. IIa, No. 5, 95-100 (1954).

Båth, M. A study of *T* phases recorded at the Kiruna seismograph station. Tellus, **6**, No. 1, 63-72 (1954).

Birch, F. The present state of geothermal investigations. Geophysics, **19**, No. 4, 645-659 (1954).

Bullen, K. E. Composition of the earth's outer core. Nature, **174**, 505 (Sept. 11, 1954). [Letter to Editor.]

Drake, C. L., J. L. Worzel, and W. C. Beckmann. Geophysical investigations in the emerged and submerged Atlantic Coastal Plain: Part IX, Gulf of Maine. Bull. Geol. Soc. Amer., **65**, No. 10, 957-970 (1954).

Howell, B. F., Jr., and E. K. Kaukonen. Attenuation of seismic waves near an explosion. Bull. Seis. Soc. Amer., **44**, No. 3, 481-491 (1954).

Kertz, W. Modelle für erdmagnetisch induzierte elektrische Ströme im Untergrund. Akad. d. Wiss., Göttingen, Phys.-Math. Kl. Abt. IIa, No. 5, 101-110 (1954).

Knopoff, L., and R. J. Uffen. The densities of compounds at high pressures and the state of the earth's interior. J. Geophys. Res., **59**, No. 4, 471-484 (1954).

National Research Council, Division of Earth Sciences. Report of the Committee on the measurement of geologic time, 1952-1953. Washington, D.C., Nation. Acad. Sci., Pub. No. 319, 187 pp., mim. (1954).

Research Group for Explosion Seismology. The fourth explosion-seismic observations in north-eastern Japan. Bull. Earthquake Res. Inst., Tokyo Univ., **32**, Pt. 1, 79-86 (1954).

Ritsema, A. R. A statistical study of the seismicity of the earth: I. Tangential stresses in the earth's crust and below; II. Discontinuities and the distribution of earthquake foci in depth; III. Earthquake strain releases during the period 1904-1953. Meteorological and Geophysical Service, Djakarta, Bull. No. 19, 36 pp. (Sept. 1954).

F—*Miscellaneous*

Anderson, C. N. Notes on the sunspot cycle. J. Geophys. Res., **59**, No. 4, 455-461 (1954).

Chandrasekhar, S. Problems of stability in hydrodynamics and hydromagnetics. Mon. Not. R. Astr. Soc., **113**, No. 6, 667-678 (1954). [George Darwin Lecture of Nov. 13, 1953.]

Chernosky, E. J. A relationship between the length and activity of sunspot cycles. Pub. Astr. Soc. Pacific, **66**, No. 392, 241-247 (1954).

Greenwich Observatory. Results of measures made at the Royal Observatory, Greenwich, of photographs of the sun, taken at Greenwich, the Cape, and Kodaikanal in the year 1944. London, H. M. Stationery Office, vii + 68 pp. (1954). 30 cm.

McNish, A. G., and J. V. Lincoln. Prediction of the present sunspot cycle. Trans. Amer. Geophys. Union, **35**, No. 5, 709-710 (1954).

Parker, E. N. A theory of the solar magnetic field. University of Utah, Dept. of Physics, Tech. Rep. No. 6, 32 pp., mim. (Aug. 1, 1954). 28 cm.

Parker, E. N. The formation of sunspots from the solar toroidal field. University of Utah, Dept. of Physics, Tech. Rep. No. 9, 36 pp. + 4 figs., mim. (Sept. 15, 1954). 28 cm.

Pierce, J. A., H. T. Mitchell, and L. Essen. World-wide frequency and time comparisons by means of radio transmissions. Nature, **174**, 922 (Nov. 13, 1954). [Letter to Editor.]

Ter Haar, D. On Kuiper's theory of the origin of the solar system. Proc. R. Soc. Edinburgh, A, **64**, Pt. I, 1-8 (1953-54).

Waldmeier, M. Provisional sunspot-numbers for July to September, 1954. J. Geophys. Res., **59**, No. 4, 546 (1954).

Whittle, P. A statistical investigation of sunspot observations with special reference to H. Alfvén's sunspot model. Astroph. J., **120**, No. 2, 251-260 (1954).

NOTICE

When available, single unbound volumes can be supplied at $6 each and single numbers at $2 each, postpaid.

Charges for reprints and covers

Reprints can be supplied, but prices have increased considerably and costs depend on the number of articles per issue for which reprints are requested. It is no longer possible to publish a schedule of reprint charges, but if reprints are requested approximate estimates will be given when galley proofs are sent to authors. Reprints without covers are least expensive; standard covers (with title and author) can be supplied at an additional charge. Special printing on covers can also be supplied at further additional charge.

Fifty reprints, without covers, will be given to institutions paying the publication charge of $8 per page.

Alterations

Major alterations made by authors in proof will be charged at cost. Authors are requested, therefore, to make final revisions on their typewritten manuscripts.

Orders for back issues and reprints should be sent to Editorial Office, 5241 Broad Branch Road, N.W., Washington 15, D.C., U.S.A.

Subscriptions are handled by The Editorial Office, 5241 Broad Branch Road, N.W., Washington 15, D.C., U.S.A.

CONTENTS—Concluded

JOURNAL OF GEOPHYSICAL RESEARCH